TECHNICAL UNIVERSITY IN ZVOLEN

FACULTY OF TECHNOLOGY

XXIII. INTERNATIONAL SCIENTIFIC CONFERENCE OF YOUNG SCIENTISTS

XXIII. Medzinárodná vedecká konferencia mladých

Book of Extended Abstracts

June 22, 2021, Zvolen, Slovakia

TECHNICAL UNIVERSITY IN ZVOLEN

FACULTY OF TECHNOLOGY

XXIII. INTERNATIONAL SCIENTIFIC CONFERENCE OF YOUNG SCIENTISTS

XXIII. Medzinárodná vedecká konferencia mladých

Book of Extended Abstracts

June 22, 2021

Zvolen, Slovakia

Title:	XXIII. International Scientific Conference of Young Scientists
Edited by:	Peter Koleda
Cover design:	Peter Koleda
Published by:	Technical University in Zvolen

ISBN 978-80-228-3270-0

Committee Members

Scientific conference committee members

Beňo Pavel	Technical University in Zvolen	Slovakia
Dado Miroslav	Technical University in Zvolen	Slovakia
Gálik Roman	Slovak University of Agriculture in Nitra	Slovakia
Herák David	Czech University of Life Sciences Prague	Czech Republic
Chotěborský Rostislav	Czech University of Life Sciences Prague	Czech Republic
Kováč Ján	Technical University in Zvolen	Slovakia
Krilek Jozef	Technical University in Zvolen	Slovakia
Kučera Marián	Technical University in Zvolen	Slovakia
Mašek Jiří	Czech University of Life Sciences Prague	Czech Republic
Pivarčiová Elena	Technical University in Zvolen	Slovakia
Tkáč Zdenko	Slovak University of Agriculture in Nitra	Slovakia
Vozárová Vlasta	Slovak University of Agriculture in Nitra	Slovakia

Reviewers

Barcík Štefan	Kučera Marián	Dado Miroslav
Beňo Pavel	Pivarčiová Elena	Krilek Jozef

Technical University in Zvolen Slovakia

Organizing conference committee members

Koleda Peter	Vargová Monika	Lipnický Lukáš
Kováč Ján	Hudec Lukáš	Hortobágyi Áron
Melicherčík Ján		

Technical University in Zvolen Slovakia

Table of Contents

DIGITAL TWINS AS A TOOL FOR REMOTE MONITORING OF KEY PERFORMANCE INDICATORS

Roman Bambura, Erika Sujová, Miroslav Dado

Department of Manufacturing Technology and Quality Management, Faculty of Technology, Technical University in Zvolen, Študentská 26, 960 01 Zvolen

Engineers cannot be everywhere at once which is one of the major reasons why remote monitoring is expected to define the future. Key performance indicators (KPIs) unfold their full potential if they are seamlessly integrated into the Digital Twin (DT) for data analytics. KPIs are important for monitoring the performance of production systems in industry. KPIs can be used to identify poor performance and provide options for the potential identification of weaknesses, the elimination of which improves the performance of the manufacturing system. KPIs can be defined for individual devices, sub-processes, but also for entire plants.

Key words: digital twin, KPIs, manufacturing

INTRODUCTION

DT integrates data into virtual models and combines historical, real-time, and predicted data. DTs remote monitoring refers to the ability to monitor and observe specific processes and operations within a production without physical presence in production. DTs remote monitoring is used to present current manufacturing data of a physical object. Remote monitoring involves observing the parameters of physical production through a computers screen in a virtual world. (Zipper et al., 2018; Redelinghuys et al. 2019; Tao et al. 2019; Schleich et al. 2017). Providing a real-time bridge between the physical and digital world, DT enables remote monitoring and control of manufacturing processes. Making use of such data requires a substantial and valid data basis. Data collection is no longer a particular challenge due to increasingly improved and cheaper sensor technology. Data evaluation contributes to improvement of the specific process. Another important aspect is the processing time required to evaluate collected data. Therefore, DT enables an extensive exchange, monitoring and analysis of collected data (Furmann et al., 2017).

MATERIAL AND METHODS

The DTs implementation framework consists of physical, virtual and information processing layer. Physical layer includes physical devices and sensors to enable data exchanged with the local server. Virtual layer contains a digital model used to describe the physical world from various perspectives, including geometric dimensions, physical properties, and behaviour. The digital model is created in the Tecnomatix Plant Simulation software (TPS). Information processing is used to collect, transmission and archive data collected by sensors and represents a "bridge" that connects physical and virtual world. 51 collection points were selected to collect data from physical world. Transmission Control Protocol / Internet Protocol (TCP / IP) was used as the transport protocol and Siemens S7 as the application protocol. TPS has an Open Database Conectivity (ODBC) interface that can retrieve data from the physical layer through a SQL database.

RESULTS

The KPIs of the production line, which can be obtained from the DT, are displayed as graphs in TPS software. KPIs allows to monitor production line parameters such as:

- LeadTime- latency between the initiation and completion of a process,
- CNC cycle time,

- Throughput- amount of a production within a specified time period,
- CNC machining time histogram,
- Manipulation time,
- Total production,
- Gantt chart.

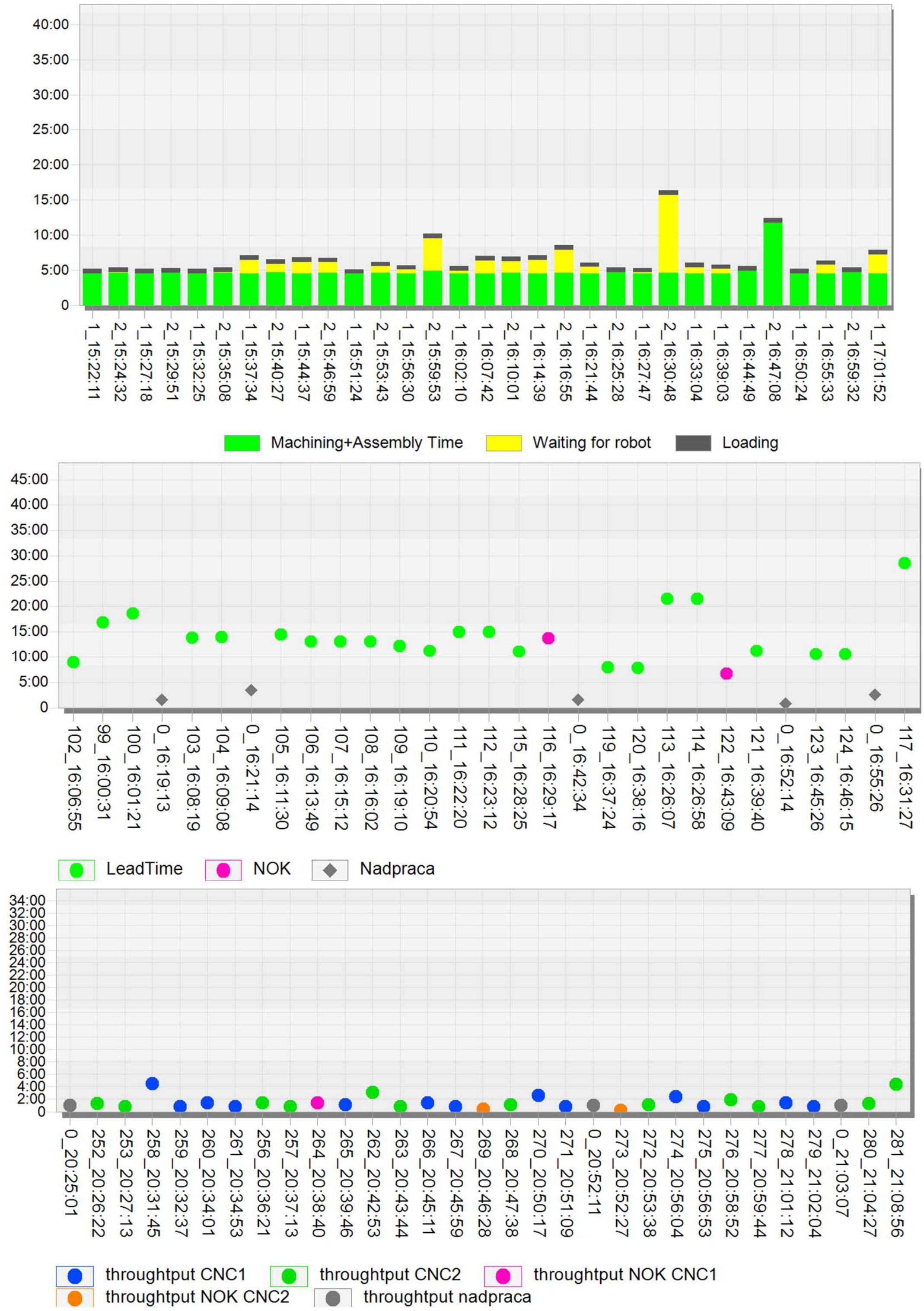

Fig. 1 KPIs monitoring with DT (Cycle Time, LeadTime, Throughput)

CONCLUSION

DT represents the digital counterpart of a real manufacturing line and faithfully displays and analyses the production processes. Remote monitoring involves observing the parameters of physical production through a screen in a virtual world. DT visualisation and remote monitoring of KPIs of the manufacturing processes in real time provides an ability to predict the performance of the manufacturing system.

LITERATURE

FURMANN, R. FURMANNOVÁ, B., WIĘCEK, D., 2017. Interactive design of reconfigurable logistics systems. In *Procedia Engineering*, 192, pp. 2017 - 212. https://doi.org/10.1016/j.proeng.2017.06.036

ZIPPER, H., AURIS, F., STRAHILOV, A., PAUL, M., 2018. Keeping the digital twin up-to-date—Process monitoring to identify changes in a plant. In *2018 IEEE International Conference on Industrial Technology*. 20-22 February 2018, Lyon, France, pp. 1592-1597, ISBN 978-1-5090-5950-8

REDELINGHUYS, A. J. H., BASSON, A. H., KRUGER, K., 2019. A six-layer architecture for the digital twin: a manufacturing case study implementation. In *Journal of Intelligent Manufacturing*. pp. 1-20, ISSN 15728145

TAO, F., SUI, F., LIU, A., QI, Q., ZHANG, M., SONG, B., NEE, A. Y. C., 2019. Digital twin-driven product design framework. In *International Journal of Production Research*. Vol. 57(12), pp. 3935-3953, ISSN 0020-7543

SCHLEICH, B., ANWER, N., MATHIEU, L., WARTZACK, S., 2017. Shaping the digital twin for design and production engineering. In *CIRP Annals*. Vol. 66(1), pp. 141-144, ISSN 0007-8506

Corresponding author:
Roman Bambura, bambura.r@gmail.com

CYCLIC STRESS RESEARCH FOR HYBRID SANDWICH SKI STRUCTURE

Božák, Hanušová, Tichý, Kolář, Müller

Department of Material Science and Manufacturing Technology, Faculty of Engineering, Czech University of Life Sciences Prague. Kamýcká 129, 165 00 Prague 6-Suchdol. Czech Republic.

The paper deals with the research of low-cyclic fatigue of a newly designed hybrid composite ski structure. The current consumer market is characterized by a demand for quality sports equipment, including skis of various types. The Czech Republic is one of the world's leading manufacturers of this segment of sports equipment. When used, skis are exposed to cyclic stress, which can have a major impact on durability and safety. The aim of the research is to determine the effect of repeated low-cycle loading of the hybrid sandwich construction of a newly manufactured ski, i.e. to simulate the course of changes that could occur during use. The results of the research did not show the effect of long-term cyclic stress on the change of mechanical properties, shape and delamination of individual layers of the hybrid structure in the newly designed and manufactured ski.
Key words: gluing, skiing, testing, low cycle fatigue

INTRODUCTION

An important segment of manufacturing companies that manufacture sports equipment are skis. Skis represent a complex set of technological operations in their production that affect their use. The construction of the skis is based on a composite hybrid sandwich construction using different materials, using gluing technology (Božák 2020).

The properties of the ski are determined by the type of individual layers and the sequence in which they are stacked. The resulting properties of the skis are determined mainly by the material used, the constructional arrangement and the quality of the created mutual connections inside the glued joint (Božák 2020). For a quality connection of materials it is necessary to have knowledge of their mechanical and chemical properties (Müller and Valášek 2013, Messler 2004).

There is no general methodology for testing the properties of individual skis. Ski manufacturers only test skis internally, so it is not possible to compare the properties of the products of individual brands (Božák, T., 2020).

Low cycle fatigue is used to determine the mechanical properties of a given sample (Šleger and Müller 2016, Zavrtálek and Müller 2016, Zavrtálek et al. 2016, Kolář et al. 2020, Tichý et al. 2020, Pothan et al. 2005, Kelly 2006). Its principle is to expose the material to a certain stress, which is repeated cyclically until its destruction. At low cycle fatigue, destruction of the sample should not occur within ten thousand repetitions (Hashim et al. 2019, Harik et al. 2002, Wang et al. 2020).

The aim of the research is to determine the effect of repeated low-cycle loading of a hybrid sandwich construction of a ski manufactured in cooperation with the company Bear-skis, i.e. to simulate the course of changes that could occur during the use of the product. This research has an impact on setting possible limits in the practical use of this product during the season.

MATERIAL AND METHODS

The aim was to make the skis light enough to simplify long climbs, but at the same time strong enough for everyday skiing on the piste.

The universal test machine LabTest 5.50ST with software enabling low-cyclic fatigue testing was used for the research. In order to be able to perform the bending test of the skis, it was necessary to use special jigs for clamping the skis to the bending machine. The spacing of the supports was set to the value of the length of the effective edge of the ski in our case. Other parts were mounted on a movable crossbar. These parts were two thorns, which was to simulate the pressure on the ski in the same places as it would be in the case of a skier.

The average skier tilts the ski in a carving curve most often to a value of 70° compared to the ground. This value has been increased by 10 % to 77° for our calculations. According to this angle and depth of cut of the test sample 13.5 mm, the displacement of the cross member of the test device to 60 mm was calculated according to the formula $X = 13.5/\cos(77°)$. This determined the main measurement parameter. The number of ski bends was determined as another parameter. We set it at a minimum value of 10,000 load cycles. This amount was reached only after a total of ten partial fatigue measurements.

RESULTS AND DISCUSSION

The results of the research are shown in Table 1.

Table 1. The results of partial cycles of low-cycle fatigue test of composite hybrid ski construction

Indication of the completed fatigue test cycle	**Arithmetic mean and standard deviation of the loading force after cyclic loading**	**Coefficient of variation of load force after cyclic loading**
	(N)	**(%)**
A	516.90 ± 2.22	0.43
B	512.40 ± 1.45	0.28
C	514.99 ± 2.25	0.44
D	517.38 ± 1.18	0.23
E	516.76 ± 2.02	0.39
F	516.62 ± 1.41	0.27
G	516.04 ± 1.57	0.3
H	514.18 ± 1.80	0.35
I	512.76 ± 2.02	0.39
J	515.72 ± 1.67	0.32

CONCLUSION

The research results based on long-term cyclic experimental tests exceeding 10 thousand. The average value of the measured force, which was needed to achieve the required deflection of the ski in the individual series, differed only minimally and had no increasing or decreasing character between the individual measurements, i.e. the cycles marked A to J. The differences in the measured values are minimal and do not affect the mechanical properties of the ski. The skis do not change, they show the same stiffness all year round.

ACKNOWLEDGMENT

Supported by the Internal grant agency of Faculty of Engineering no. 2021:31140/1312/3108 "Experimental research of hybrid adhesive bonds with multilayer sandwich construction, Czech University of Life Sciences Prague".

LITERATURE

BOŽÁK, T., 2020. Výzkum mechanických vlastností konstrukce lyží. Prague. Magister thesis. Czech University of Life Sciences Prague. Thesis supervisor prof. Ing. Miroslav Müller, Ph.D.

BROUGHTON, W.R., MERA, R.D., HINOPOULOS, G., 1999. Project PAJ3 - Combined Cyclic Loading and Hostile Environments 1996-1999, Cyclic Fatigue Testing of Adhesive Joints Test Method Assessment. Environments.

HAFIZ, T.A., ABDEL WAHAB, M.M., CROCOMBE, A.D., SMITH, P.A., 2010. Mixed-mode fracture of adhesively bonded metallic joints under quasi-static loading. Eng. Fract. Mech. 77, 3434–3445.

HARIK, V. M., KLINGER, J. R., & BOGETTI, T. A., 2002. Low-cycle fatigue of unidirectional composites: Bi-linear S-N curves. *International Journal of Fatigue*, 24(2–4), 455–462.

HASHIM, N., MAJID, D. L. A., MAHDI, E. S., ZAHARI, R., & YIDRIS, N., 2019. Effect of fiber loading directions on the low cycle fatigue of intraply carbon-Kevlar reinforced epoxy hybrid composites. *Composite Structures*, 212, 476–483.

CHOCHOLOUŠ, P., 2014. Vybrané technické parametry a marketingová studie sendvičových materiálů. Prague. Magister thesis. Czech University of Life Sciences Prague. Thesis supervisor prof. Ing. Miroslav Müller, Ph.D.

KELLY, G., 2006. Quasi-static strength and fatigue life of hybrid (bonded/bolted) composite single-lap joints. *Compos. Struct*. 72, 119–129.

KOLÁŘ, V., MÜLLER, M., MISHRA, R., RUDAWSKA, A., ŠLEGER, V., TICHÝ, M., HROMASOVÁ, M., VALÁŠEK, P., 2020. Quasi-Static Tests of Hybrid Adhesive Bonds Based on Biological Reinforcement in the Form of Eggshell Microparticles. *Polymers,* roč. 12, č. 6, s. 0-0.

MESSLER, R. W., 2004. Joining of Materials and Structures: From Pragmatic Process to Enabling Technology. Joining of Materials and Structures: From Pragmatic Process to Enabling Technology (pp. 1–790). *Elsevier Inc*

MÜLLER, M., & VALÁŠEK, P., 2013. Assessment of bonding quality for several commercially available adhesives. *Agronomy Research,* 11(1), 155–162.

MÜLLER, M., VALÁŠEK, P., KOLÁŘ, V., ŠLEGER, V., KAGAN GÜRDIL, G.A., HROMASOVÁ, M., HLOCH, S., MORAVEC, J., PEXA, M., 2019. Material utilization of cotton post-harvest line residues in polymeric composites. *Polymers (Basel)*., 11, 1106.

NAN, C. W., SHEN, Y., & MA, J., 2010. Physical properties of composites near percolation. Annual Review of Materials Research, 40, 131–151.

POTHAN, L.A., POTSCHKE, P., HABLER, R., THOMAS, S., 2005 The static and dynamic mechanical properties of banana and glass fiber woven fabric-reinforced polyester composite. *J. Compos*. Mater, 39, 1007–1025

SADASIVUNI, K. K., SAHA, P., ADHIKARI, J., DESHMUKH, K., AHAMED, M. B., & CABIBIHAN, J. J., 2020. Recent advances in mechanical properties of biopolymer composites: a review. *Polymer Composites*. John Wiley and Sons Inc.

ŠLEGER, V.; MÜLLER, M., 2016. Low-cyclic fatigue of adhesive bonds. Manuf. Technol. 16, 1151–1157.

TICHÝ, M., KOLÁŘ, V., MÜLLER, M., MISHRA, R., ŠLEGER, V., HROMASOVÁ, M., 2020. Quasi-Static Shear Test of Hybrid Adhesive Bonds Based on Treated Cotton-Epoxy Resin Layer. *Polymers,* roč. 12, č. 12, s. 2945-2959.

WANG, X., ZHAO, X., CHEN, S., & WU, Z., 2020. Static and fatigue behavior of basalt fiber-reinforced thermoplastic epoxy composites. *Journal of Composite Materials*, 54(18), 2389–2398

ZAVRTÁLEK, J., MÜLLER, M., 2016. Low-cyclic fatigue test of adhesive bond reinforced with biodegradable fabrics. *Manufacturing Technology*, roč. 16, č. 5, s. 1205-1211.

ZAVRTÁLEK, J., MÜLLER, M., ŠLEGER, V., 2016 Low-cyclic fatigue test of adhesive bond reinforced with glass fibre fabric. *Agronomy Research,* roč. 14, č., s. 1138-1146.

Corresponding author:
Ing. Tomáš Božák, bozak@tf.czu.cz

DEPENDABILITY ANALYSIS OF CRITICAL COMPONENTS OF AN AGRICULTURAL TRACTOR

David Fabiánek

Department for Quality and Dependability of Machines, Faculty of Engineering, Czech University of Life Sciences Prague, Kamýcká 129, 165 21, Prague, Czech Republic, fabianekd@tf.czu.cz

One of the possibilities of increasing the profitability of machine operation is to optimize its maintenance program. To optimize it, it is important to know dependability of each machine part. This article analysis a vast database containing operation data of 166 agricultural tractors John Deer 7530. Using critical quantification, 10 critical components were selected. Furthermore, the method of calculation of dependability indicators is described by parametric statistical methods according to ČSN EN 61649:2009 and mean time to operating failure.

Key words: dependability, weibull distribution, agriculture, tractor

INTRODUCTION

This paper demonstrates on 10 critical components of a John Deere 7530 tractor the dependability quantification results obtained using the parameters of the Weibull distribution function which can be an important element in optimizing the tractor maintenance program. The analyzed data are complete in cases in case of complete failure and incomplete in cases where a part did not fail.

Significant help in building optimal maintenance programs is the knowledge of dependability indicators. Dependability indicators are:

- Density function of operating time to failure *f(t)*,
- Probability of failure *F(t)*,
- Reliability function *R(t)*,
- Failure rate *λ(t)* (Legat 2013, Legat et al. 2002, Sherif 1982).

Weibull is very often used to determine dependability approximation. It is very flexible and it can be applied for data modeling without regards to failure tendencies (rising, falling or constant). It is essential to keep track of time of failing, cycles, shipping distance, mechanical stress or similar continuous or discrete parameters (Nassar et al. 2017, Teringl et al. 2015).

MATERIAL AND METHODS

For calculate indicators of dependability was used a database contain a records of 166 machines of the tractor John Deere 7530.

1. Objects with the number of occurrences of failures <10 were removed from the database.The criticality was quantified using the equation 1. Critical components were selected.

$$K = n_F \cdot C, \tag{1}$$

Where:
K……criticaly
n_F…... number of failures in a given time period [1]
C…… average prices of the components for the period [EUR/ given time]

2. The data were processed using the Weibull analysis with the support of an Excel spreadsheet. The analysis procedure was in accordance with the standard ČSN EN 61649:2009.
3. Dependability indicators were calculated.

RESULTS

Dependability indicators of selected components are in tables Table 1. Dependability characteristics *F(t), f(t), R(t), λ(t)* for calculated Weibull distribution for RE535729 Exhaust gas cooler are in Fig. 1

Table 1 Weibull distribution parameters, indicators of dependability

Machines component		*α* shape parameter	*β* scale parameter	*E(t)* [EH]
RE535729	Exhaust gas cooler	1,47	13601	12313
SE502330	Turbocharger	1,43	35137	31936
RE537578	Torsional vibration damper	3,28	11683	10477
RE43738	Tensile force sensor	0,86	36663	39585
SE501227	Water pump	2,86	14739	13136
AL160250	Three-way brake valve	0,71	113460	141273
AL168483	Fuel pump	2,58	22919	20351
RE543308	ERG valve	1,06	57135	55784
RE523318	Turbo actuator	2,00	23413	20749
RE167207	Engine oil pressure sensor	2,03	21374	18937

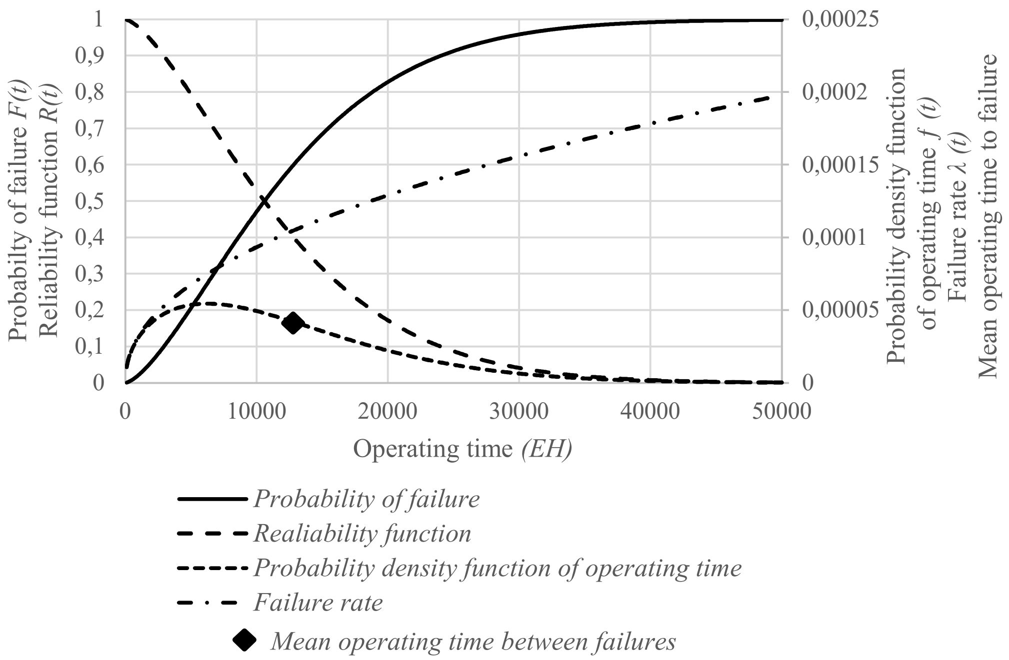

Fig. 1 Dependability characteristics *F(t), f(t), R(t), λ(t)* for calculated Weibull distribution for RE535729 Exhaust gas cooler

CONCLUSION

One of the ways to increase the profitability of machine operation is to optimize its maintenance program. Therefore, to optimize the program, it is necessary to know the dependability data of individual machine components. In this paper, an extensive database containing data on the operation of 166 agricultural tractors of the same model was analyzed. Using critical quantification, 10 critical components were selected. The calculated dependability indicators for the collected operating data of selected tractor components indicate that further research into the application of statistical methods to optimize the maintenance program of selfpropelled production equipment makes sense. Among the critical components of the tractor, there are those in which the results of the failure characteristics indicate that the increase in failure intensity is not accidental in nature. However, this hypothesis needs to be confirmed by further research.

LITERATURE

CSN EN 61649 (010653). (2009). Weibull analysis (In Czech).

LEGAT, V., 2013. *Management and maintenance engineering*. Professional Publishing.

LEGAT, V., MOSNA, F., CERVENKA, V., JURCA, V., 2002. Optimization of preventive maintenance and information system. *Eksploatacja i Niezawodność*., 4(16), pp 24–29.

NASSAR, M. A., ALZAATREH, M., ABO-KASEM, O., 2017. Alpha power Weibull distribution. *Communications in Statistics - Theory and Methods*, pp 1–17.

SHERIF, Y., 1982. Optimal maintenance schedules of systems subject to stochastic failure. *Microelectronics Reliability* 22(1), pp 15–29. DOI:10.1016/0026-2714(82)90047-6.

TERINGL, A., ALEŠ, Z., LEGÁT, V., 2015. Dependability characteristics - indicators for maintenance performance measurement of manufacturing technology. *Manufacturing Technology* 15(3), pp 456–461. DOI:10.21062/ujep/x.2015/a/1213-2489/mt/15/3/456.

Corresponding author:
David Fabiánek, tel. 605133898, e-mail: fabianekd@tf.czu.cz

DESIGN OF MEASUREMENTS METHODOLOGY IN CHIPLESS WOOD FELLING AREA

Pavol Harvánek, Ján Kováč, Ján Melicherčík, Jozef Krilek, Tomáš Kuvik

Katedra environmentálnej a lesníckej techniky, Fakulta techniky, Technická univerzita vo Zvolene, T.G.Masaryka 24, 960 53 Zvolen, E- mail: xharvanek@is.tuzvo.sk jan.kovac@is.tuzvo.sk , xmelichercikj@is.tuzvo.sk

The task of the article is to describe in detail the chosen measurement methodology that will be used for research in the dissertation. The measurement methodology is based on laboratory measurements. The proposed methodology is based on theoretical and practical knowledge in the field of wood cutting. These are implemented on the experimental equipment of the KELT department, which corresponds to the input and output parameters of the machine used in forestry. Based on the established methodology, laboratory measurements of chipless wood cutting will be performed using single-acting flat shading knives.

Key words: chipless cutting, chipless cutting head, methodology of wood cutting.

INTRODUCTION

There is a very rapid development of science and especially technology in the world, which is also related to the development of production, which results in an increasingly intensive extraction of natural resources. In order to ensure the rational management of forests, it is necessary to use more and more modern modern logging techniques, which would bring with them less and less waste generation when trees are cutting. One of the possible solutions is the use of chipless wood cutting in the actual harvesting of fast-growing wood but in overruns (Kováč et al., 2017).

Chipless wood cutting in the forestry process is mainly used in machines intended for machine delimbing of trees. Increasingly, however, chipless wood cutting is used in the form of chipless cutting heads in single-operating machines. The author (Hatton et al., 2015; Hatton et al., 2017) discussed the construction, advantages of use and modeling of cutting processes using shading heads.

MATERIAL AND METHODS

The entire course of laboratory measurements will be carried out on the hydraulic stand of the KELT department in the TUZVO workshop, as many marginal assignments will be used from the available stocks of the Faculty of Technology of the Technical University in Zvolen (Barcík et al., 2016). Cutting knives with different thicknesses and geometric parameters will be gradually attached to the stand. As these are laboratory conditions, the size of the cutting knives will be smaller compared to the cutting knives without chipless cutting heads (Marko 1996).

The process of chip-free division of woods in the direction perpendicular to the growth of fibers will provide a rectilinear hydraulic motor (3), which is placed on the beam (4) and will be driven by the pressure of the liquid from the hydrogenerator (6). The direction of movement of the piston rod of the linear hydraulic motor is secured from the control panel (7). To ensure the correct shading kinematics, the rectilinear hydraulic motor will push the wood (1) into the shading knife (2). The entire chipless cutting process will be recorded using the QUANTUM MX840 (8). During the chipless splitting process, the force will be monitored depending on the piston rod path. The force will be recorded indirectly due to the deformations of the piston of the rectilinear hydraulic motor by means of a resistance force sensor (5), to control the measured force a pressure sensor (11) will be included in the hydraulic system, thanks to which it will be possible to compare two values. Thanks to the path sensor (10), it will be possible to monitor the course of the measured force depending on the depth of penetration of the shading knife into the wood. The whole experimental measurement will be evaluated in PC (9).

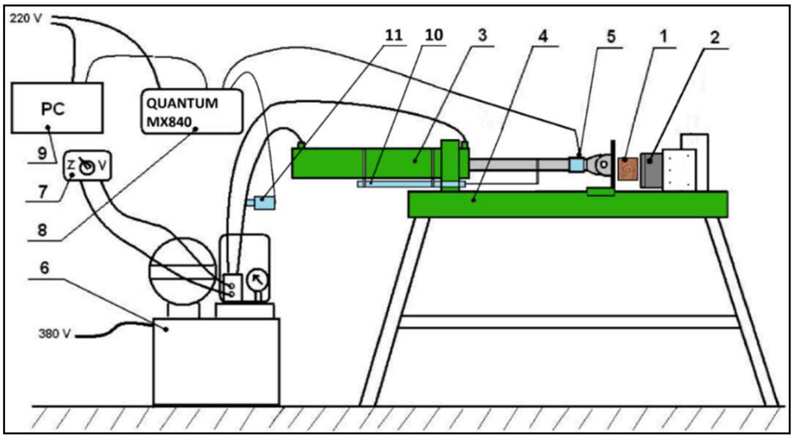

Fig. 1 Schematic of measurements (Krilek *et al., 2018*)

Tab. 1 Technical parameters of chipless cutting knives

Nr.	**Thickness s (mm)**	**Surface**	**Cutting edge shape**
1	6	polished	linear
2	8	ribbed	saw shape
3	10	roughened by sandblasting	sinusoidal

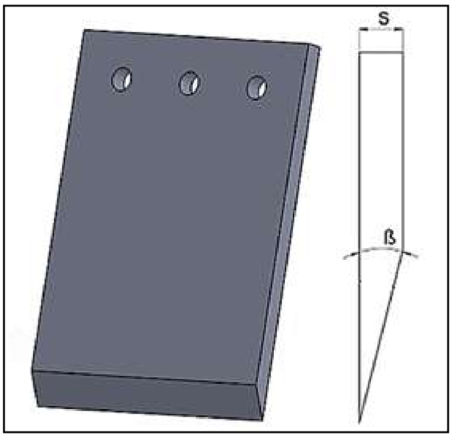

Fig. 2 Model and geometry of a single-acting flat shading knife (author): s- knife thickness, β- cutting wedge angle

RESULTS AND DISCUSSION

The proposed methodology for measuring chipless wood division is based on various studies that address similar issues in the field of wood processing technology in forestry (Hatton et al., 2015, Pathak et al., 2017, Melicherčík et al., 2020). The measurement methodology consists of several chipless shading knives and woods used, which have different effects on the resulting size of the shading force.

Based on a study in the process of chipless branching, it was found that the thickness of the cutting tool has the greatest influence on the size of the branching force (Mikleš, M., 2011, Mikleš, J., 2013). However, in the chipless separation process, this factor may have a different effect than in the branching process.

Due to the need to adhere to the required shielding kinematics, an experimental device for testing chipless shielding knives will be used. This hydraulic device will be used to test various shading knives in order to ultimately determine the most advantageous shape and geometry of the cutting tool. Subsequently, the most optimal technical parameters of shading knives will be selected, which will be used in the next experiment (Krilek et.al., 2018).

CONCLUSION

At the present time, when there is a high demand for low waste in sawing and wood processing, chipless shading heads are increasingly coming to the fore. Their construction is becoming better and easier for the operator and the operation itself.

In the end, this work determines the methodology of solving the dissertation with a description of laboratory measurements on experimental equipment. Based on research and theoretical knowledge, the cutting force and cutting speed in the process of chipless wood cutting on the proposed experimental equipment will be evaluated. Single-acting shading knives of different geometries and different materials will be used for these measurements.

REFERENCES

BARCÍK, Š.,NEUPAUEROVÁ, A.,KOLEDA, P.,SUJOVÁ, E.,MINÁRIK, M.,2016. Katalóg zariadení. Technická univerzita vo Zvolene. ISBN 978-80-228-2869-7

CAVALLI, R., GRIGOLATO, S., SGARBOSSA, A., 2014. Productivity and quality performance of an innovative firewood processor. *Journal of agricultural engineering*, pp. 32-36. 2014.

HATTON, B., BOUZGARROU, J., FAUROUX, V., GAGNOL, V., GOGU, G., 2017: An approach for modelling harvester head mechanism in the harvesting process of hardwood stands. Springer International Publishing AG, pp 133-141. 2017.

HATTON, B., POT, G., BOUZGARROU, B., GAGNOL, V., GOGU, G., 2015: Experimental determination of delimbing forces and deformations in hardwood harvesting. *Croatian journal of forest engineering*. pp 43-53. ISSN: 1845-5719. 2015.

JOHANSSON, J., 1996. Case studies on farm tractors as base machines for single-grip thinnings harvester heads. *Forestry*, pp 229-244. ISSN: 0015-752X. 1996.

KOVÁČ, J., KRILEK, J., KUČERA, M., AND BARCÍK, S. 2014. The impact of design parameters of a horizontal wood splitter on splitting force. *Drvna Industrija* 65(4), pp 263-271. DOI: 10.5552/drind.2014.1335

KOVÁČ,J., KRILEK, J.,JOBBÁGY, J., DVOŘÁK, J., 2017. Technika a mechanizácia v lesníctve, Technická univerzita vo Zvolene, 2017. ISBN 978-80-228-3021-8

KRILEK, J., KOVÁČ. J., DVOŘÁK, J., MIKLEŠ, J.,2018. Výskum rezných mechanizmov v lesníctve. Zvolen : Vedecká monografia. Technická univerzita vo Zvolene.ISBN 978-80-228-3056-0

MARKO, J. 1996. Problematika hodnotenia rezných mechanizmov pre výchovné zásahy. 1. vyd. Zvolen: Technická Univerzita vo Zvolene, 1996. 49s. ISBN 80-228-0586-8.

MARKO, J., HOLIK, J. 2000. Teória delenia dreva. 1. vyd. Zvolen: Technická Univerzita vo Zvolene, 2000. 66s. ISBN 80-228-0891-1.

MELICHERČÍK, J., KRILEK, J., HARVÁNEK, P., 2020. Simulation of stress and strain analysis on a delimbing knife with replaceable cutting edge. *BioResources* 2020(2), pp 3799--3808. ISSN 1930-2126 .VEGA 1/0609/20. CCC, WOS, SCOPUS.

MIKLES, J., 2011. Research into the geometry of the delimbing head of cutting knives. 4. medzinárodná vedecká konferencia o drevospracujúcich technikách, Praha, Česká republika.. pp 193-201. 2011.

MIKLES, J., 2013. Research in Agricultural Engineering. Research into the geometry of the delimbing head of cutting knives. pp 193-201. 2013.

MIKLEŠ, M., 2009. Štúdium geometrie nožov odvetvovacej hlavice. *Acta Facultatis Technicae*, XIV , 2009 (2) pp 121 – 129, ISSN 1136 – 4472

PATHAK, A.D., WARHANE, R.S.,DEOKAR, S.U.; 2017. Optimization of cutting parameters in Dry Turning of AISI A2 Tool Steel using Carbide Tool by Taguchi Based Fuzzy Logics. ScienceDirect- Material Today: Proceedings 5 (2018) ISSN 5082- 5090

SUCHOMEL, C., SPINELLI, R., MAGAGNOTTI, N., 2012. Productivity of processing hardwood from coppice forests. *Croatian journal of forest engineering*, pp 39-47. ISSN: 1845-5719. 2012.

Contribution has been prepared within the solving of scientific grant project VEGA no. 1/0609/2020 „Research of the cutting tools at the dendromass processing in agricultural and forestry production

Corresponding author:

Ján Kováč, tel. +421 45 5206 517, e- mail: jan.kovac@ituzvo.sk

EVALUATION OF HEAT LOAD IN CATTLE

Ana Hauliková, Jana Lendelová, Peter Kuchar

Department of Building Equipment and Technology Safety, Faculty of Engineering, Slovak University of Agriculture in Nitra, Trieda Andreja Hlinku 2, 949 76 Nitra, Slovak Republic, xhaulikova@uniag.sk

Monitoring of the indoor microclimate in the stable for dairy cows in summer is required because during this period there is a decrease in milk yield, and this causes large economic losses. In our paper, we focused on the assessment of microclimatic indicators as air temperature, relative humidity, and air velocity in three objects with natural ventilation and additional forced ventilation in the summer. All examined objects have the same floor plan but with different ventilation devices in each object. In Object 1 there were basket fans, in Object 2 and Object 3 there were panel fans with different performance. Based on the obtained microclimatic parameters, we calculated the values of environmental quality indices THI (Heat - humidity index) and HLI (Heat load index). Using the THI and HLI indices, we evaluated the indoor climate in three objects, and compared the obtained data between objects as well as in relation to the recommended values.

Key words: cows, environment, cooling

INTRODUCTION

During the summer months, hot weather causes heat stress of dairy cows, and affects health (Brown – Brandl, et al., 2006; Wheelock et al., 2010), quality and quantity of milk (Brouček et al., 2006; Bernabucci et al., 2014), reproduction (Moghaddam et al., 2009), behavior (Lendelová et al., 2012; Herbut & Angrecka, 2018), welfare (Lees et al., 2019) and causes great economic losses (St. Pierre et al., 2003). Heat load occurs in areas with high temperatures but also in regions with mild climates (Armstrong, 1994). Microclimatic parameters such as air temperature, relative humidity or solar radiation have a significant effect on changes in milk composition, including protein, fat, and lactose mineral content (Sharma et al., 1983). The Thermal-Humidity Index (THI) is commonly used, to estimate the heat load in cattle (Berman, 2005). THI from 72 to 79 is considered as mild stress, THI values from 79 to 89 as moderate stress and THI above 89 as severe stress (Akyuz et al., 2010). Ravagnolo et al. (2000) report, when the THI exceeded 72, changes in milk composition were observed, the decrease in protein was on average 0,009 kg per unit of THI and a decrease in fat on average 0,012 kg per unit of THI as well as reduced milk yield, on average 0,2 kg per THI unit. THI index is the most used index for estimating heat load, but this index does not consider other microclimatic parameters, such as air velocity and solar radiation (Berman, 2005). The index which in its equation includes of solar radiation and air velocity is the Heat Load Index, HLI. Values of 70 <HLI <77, are considered as a warm environment area, 77 <HLI <86, as a hot environment area and HLI values> 86 as a very hot environment area (Gaughan et al., 2008). Berman (2005) states, that by increasing the air flow rate in combination with moisture and soaking the animals, it appears to be an effective method to alleviate heat load. Many studies have confirmed that cooling dairy cows has shown improvements in the health, behavior (Frazzi et al., 2000; Honig et al., 2012) as well as in the composition or amount of milk (Correa-Calderon et al., 2004; Brouček et al., 2018).

The aim of our work was to test the state of the microclimate during extremely hot summer days in the conditions of Slovakia, carried out in three identical barns with different ventilation intensities.

MATERIAL AND METHODS

This study presents the results of research carried out during the summer season in three experimental objects for dairy cows. The investigated objects are situated at the same locality in Southern Slovakia, with an altitude of 220 m above sea level.

All objects have the same floor plan, with dimensions of 26,6 m × 62,1 m. There are four groups of animals in each object, with 32 dairy cows in each group. The average annual milk yield per animal is 9 500 kg. year^{-1}. The objects are ventilated naturally by built holes in the walls and a continuous ridge in the roof with additional motor ventilation in the summer. In all objects, a partial reconstruction of the roof was carried out, where a ridge slot with a deflector with dimensions of 55 m × 1,2 m was installed.

Object 1 - there are four rows of lying cubicles with two feed corridors and four manure corridors. In this stable, basket fans are installed at feed corridors with 7 fans on each side. The fans are mounted on the ceiling structure at 2,8 m above the floor. The distance of the fans from the longitudinal axis of the building is 3,5 m. The output of one fan is 15 600 $m^3.h^{-1}$, the total output of all fans is 218 400 $m^3.h^{-1}$.

Object 2 has the same layout as Object 1. All fans in Object 2 are mounted in the middle of the longitudinal axis of the building, installed on steel columns. The total number of fans is 12, of which 4 fans with a capacity of 36 530 $m^3.h^{-1}$ and 8 fans, with a capacity of 17 900 $m^3.h^{-1}$ with total fans performance of 289 320 $m^3.h^{-1}$.

Object 3 has a different layout. In this building there are three rows of lying cubicles, on the right and one row of lying cubicles the left side with one asymmetrically placed feed corridor and three manure corridors. There are 12 panel fans installed, each with a capacity of 37 965 $m^3.h^{-1}$ total fans performance in Object 3 is 455 580 $m^3.h^{-1}$.

Ambulant measurements were performed on selected days when the outdoor air temperature reached at least 30 ° C and the air flow rate was not higher than 2 $m.s^{-1}$. The measurement methodology was the same in all three objects, from each day, the sample contained of 576 data for each object.

For ambulant measurements, we used an Almemo 2490 – 1L instrument with a thermoanemometric probe with a hot wire with a measuring range of air velocity of 0.08 ÷ 2 $m.s^{-1}$ and an omnidirectional probe with a measuring range of air velocity of 0.05 ÷ 5 $m.s^{-1}$. For continuous measurements, we used COM S3121 instruments, which continuously recorded data on air temperature and relative humidity, both outdoors and indoors.

The calculation of selected heat indices THI and HLI was performed according to equation 1; equation 2.

$$THI = (1{,}8 \cdot Tdb + 32) - \big((0{,}55 - 0{,}0055 \cdot RH) \cdot (1{,}8 \cdot Tdb - 26{,}8)\big) \tag{1}$$

where *Tdb* is the dry bulb temperature, [°C],
RH is relative humidity, [%] , (Kelly & Bond, 1971)

$$HLI(if\ Tbg \geq 25) = 8{,}62 + (0{,}38 \cdot RH) + (1{,}55 \cdot Tbg) - (0{,}55 \cdot WS) + e^{2{,}4-WS} \tag{2}$$

where *Tbg* is black globe temperature, [°C],
RH is relative humidity, [%],
WS is wind speed, [$m.s^{-1}$] , (Gaughan et al., 2008)

RESULTS

The resulting values of microclimatic parameters indicate that in Object 1, the average air temperature was T_{avg} = 33,94 °C, while the maximum air temperature reached T_{max} = 34, 72 °C, which was also the highest measured temperature of all three examined objects. In Object 2, the average air temperature was T_{avg} = 32,89 °C, in Object 3, T_{avg} = 33,28 °C. We found that Object 3 has the average value of relative humidity significantly lower, RH_{avg} = 39,49 %, compared to Object 1, RH_{avg} = 48,41 % and Object 2, RH_{avg} = 47,87 %. The highest measured value of relative humidity was in Object 1, RH_{max} = 56,02 %, the lowest in Object 3, RH_{min} = 36,77 %. In Object 3, was measured the highest values of air flow v_{avg} = 0,50 $m.s^{-1}$, as well as the highest air flow of all three examined objects v_{max} = 0,85 $m.s^{-1}$. The average values of air flow were in Object 1, v_{avg} = 0,38 $m.s^{-1}$, in Object 2, v_{avg} = 0,31 $m.s^{-1}$.

Based on THI and HLI calculations (Tab. 1), it was found that the highest values of THI were found in Object 1, THI_{avg} = 83,35, the lowest values in Object 3, THI_{avg} = 80,88, but they all indicated the moderate heat load of the cows. Regarding the resulting HLI values, in Object 3, the average values were significantly lower HLI_{avg} = 80,53, compared to Object 1, HLI_{avg} = 85,88 and Object 2, HLI_{avg} = 84,48. Despite the results of HLI differences, in all three examined objects the HLI value was at a level called the hot environment area. At air flow of 0,15 $m.s^{-1}$, the average values of HLI ranged from HLI_{avg} = 83,36 (in Object 3), to HLI_{avg} = 87,88 (in Object 1), which is already classified as a dangerous heat load, in the category very hot environment for dairy cows.

Table 1 Results of the calculation Thermal – humidity index and Heat load index in all objects

	Object 1	Object 2	Object 3
THI			
AVG	83,35	81,91	80,88
max	84,51	83,26	81,69
min	82,54	81,10	80,09
STDEV	0,58	0,63	0,60
HLI			
AVG	85,88	84,48	80,53
max	88,39	86,93	83,27
min	83,51	81,99	77,52
STDEV	1,48	1,48	2,41

CONCLUSION

Our research focused on monitoring microclimatic parameters in three stables for dairy cows in the summer. The experimental objects had the same floor plan but with a different ventilation device. The average THI and HLI values in Object 1 were $THI_{avg} = 83{,}35$; $HLI_{avg} = 85{,}88$ and the average values for Object 2 were $THI_{avg} = 81{,}91$; $HLI_{avg} = 84{,}48$. The most significant changes in THI and HLI values were observed in Object 3, $THI_{avg} = 80{,}88$; $HLI_{avg} = 80{,}53$. Even though the value of HLI, in Object 3, was 3,51 % lower with the use of motor ventilation, compared to the situation without fans, $HLI_{avg} = 83{,}36$, the level of heat load in this object was high and represented a hot environment. In conclusion, we can state that the cooling effect in the examined objects was probably insufficient and this study requires a more detailed investigation of the issue and the search for future solutions.

ACKNOWLEDGEMENTS. This publication was supported by the Operational Programme Integrated Infrastructure within the project: Sustainable smart farming systems taking into account the future challenges 313011W112, cofinanced by the European Regional Development Fund.

LITERATURE

AKYUZ, A., BOYACI, S., CAYLI, A. 2010. Determination of critical period for dairy cows using temperature humidity index. In: *J Anim Vet Adv* vol. 9, no. 3, pp 1824–1827.

ARMSTRONG, D.V. 1994. Heat stress interaction with shed and cooling. In: *Journal of Dairy Science* [online], vol. 77, no. 7, pp. 2044-2050. Available on: <https://www.journalofdairyscience.org/article/S0022-0302(94)77149-6/pdf>.

BERMAN, A. 2005. Estimates of heat stress relief needs for Holstein dairy cows. In: *Journal of Animal Science* [online], vol. 83, no. 6, pp. 1377-1384. Available on: <https://www.researchgate.net/publication/7850173_Estimates_of_heat_stress_relief_needs_for_Holstein_dairy_cows>.

BERNABUCCI, U., BIFFANI, S., BUGGIOTI, L., VITALI, A., LACATERA, N., NARDONE, A. 2014. The effects of heat stress in Italian Holstein dairy cattle. In: *J. Dairy Sci*. [online], vol. 97, no. 1 pp 471–486, 2014. Available on: <https://www.sciencedirect.com/science/article/pii/S0022030213007467>.

BROUČEK, J., MIHINA, Š., RYBA, Š., TONGEL, P., KIŠAC, P., UHRINČAŤ, M., HANUS, A., 2006. Effects of high air temperatures on milk efficiency in dairy cows. In: *Czech Journalof Animal Science* vol. 3, no. 51, pp 93–101.

BROUČEK, J., *RYBA*, Š., DIANOVÁ, M., UHRINČAŤ, M., ŠOCH, M., HANUS, A., ZABRANSKÝ, L. 2018. Herd-level production impacts of evaporative cooling of dairy cows on milk production in Slovakian lowlands. In: *An ASABE*. International Livestock Environment Symposium. [online] Paper Number: ILES18-039. Available on: https://elibrary.asabe.org/abstract.asp?aid=49655&t=3&redir=&redirType=

BROWN-BRANDL, T. M., EIGENBERG, R.A., NIENABER, J.A., 2006. Heat stress risk factors of feedlot heifers. In: *Livestock Science*. vol. 105, pp 57–68. Available on: https://doi.org/10.1016/j.livsci.2006.04.025

CORREA-CALDERON, A., D. ARMSTRONG, D. RAY, S. DENISE, M. ENNS, HOWISON, C. 2004. Thermoregulatory responses of Holstein and Brown Swiss heat-stressed dairy cows to two different coolingsystems. In: *Int. J. Biometeorol*. vol. 48, pp 142–148.

FRAZZI, E., CALAMARI, L., CALEGARI, F., STEFANINI, L. 2000. Behavior of dairy cows in response to different barn cooling systems. In: *Trans ASAE* [online] vol. 43, no. 2, pp 387–394. Available on: https://www.researchgate.net/publication/270614121_Behavior_of_dairy_cows_in_response_to_different_barn_cooling_systems

GAUGHAN, J.B., MADER, T.L., HOLT, S., LISLE, A. 2008. A new heat load index for feedlot cattle. In: J. *Anim. Sci.* vol. 86 pp 226–234.

HERBUT, P. ANGRECKA, S. 2018. The effect of heat stress on time spent lying by cows in a housing system. In: *Ann. of Animal Science* [online], vol. 18, no. 3, pp. 825-833 ISSN: 2300-8733. Available on : <https://content.sciendo.com/view/journals/aoas/18/3/article-p825.xml?product=sciendo>.

HONIG, H., MIRON, J., LEHRER, H., JACKOBY, S., ZACHUT, M., ZINOU, A. PORTNICK, Y., MOALLEM, U. 2012. Performance and welfare of highyielding dairy cows subjected to 5 or 8 cooling sessions daily under hot and humid climate. In: J. *Dairy Sci.,* [online] vol. 95, pp 3736–3742. Available on: https://www.sciencedirect.com/science/article/pii/S0022030212003530

KELLY, C.F., BOND, T.E. 1971. Bioclimatic factors and their measrurments. National Research Council (Ed.), A guide to enviromenmental research on animals pp 7–92.

LEES, A. M., SEJIAN, V., WALLAGE, A., STEEL, C. C., MADER, T. L., LEES, J. C., GAUGAN, J. B. 2019. The impact of heat load on cattle. In: *Animals* 2019, [online] vol. 9, pp 322. Available on: https://pubmed.ncbi.nlm.nih.gov/31174286/

LENDELOVÁ, J., BOTTO, L., SZABOVÁ, T. 2012. Effect of different cooling systems on lying time of dairy cows in cubicles with separated manure solids bedding. In: *Journal of Central European Agriculture* [online] vol. 13, no.4, pp717-728. Available on : <DOI:10.5513/JCEA01/13.4.1118>

MOGHADDAM, A., KARIMI, I., POOYANMEHR, M., 2009. Effects of short-term cooling on pregnancy rate of dairy heifers under summer heat stress. In: Vet Res Commun. vol. 33, pp 567-575.

RAVAGNOLO, O., MISZTAL, I., HOOGENBOOM, G. 2000. Genetic component of heat stress in dairy cattle, development of heat index function. In: *J. Dairy Sci*. vol. 83 pp 2120–2125.

SHARMA A.K., RODRIGUEZ, L.A., MEKONNEN, G., WILCOX, C.J., BACHMAN, K.C., COLLIER R.J. 1983. Climatological and genetic effects on milk composition and yield. In: *Journal of Dairy Science* vol. 66, pp 119–126.

ST. PIERRE, N. R., COBANOV, B., SCHNITKEY, G. 2003. Economic losses from heat stress by US livestock industries. In: *Journal of Dairy Science* [online] vol. 86, pp 52-77. Available on: <https://www.sciencedirect.com/science/article/pii/S0022030203740405>

WHEELOCK, J. B., RHOADS, R. P., VANBAALE, M. J., SANDERS, S. R., BAUMGARD. L. H. 2010. Effects of heat stress on energetic metabolism in lactating Holstein cows. In: J. *Dairy Sci.* vol. 93, 644–655.

Corresponding author:

Ana Hauliková, +421 902 556 050, xhaulikova@uniag.sk

ON-GRID PHOTOVOLTAIC SYSTEM IN PRAGUE – 10 kW_P

Matouš Havrlík, Jana Šafránková, Vladislav Poulek, Martin Libra

Department of Physics, Faculty of Engineering, Czech University of Life Sciences Prague, Kamýcká 129, 16500 Prague 6, Czech Republic, e-mail: havrlik@tf.czu.cz

The on-grid photovoltaic system was installed at the Faculty of Engineering in 2015. The monitoring system developed in our laboratory monitors data and can also detect failure and type of failure. The evaluation of the data shows that the amount of electricity produced slightly exceeds the expected values predicted by the internationally used internet application PVGIS. Immediate output power is affected by multiple parameters. Higher temperatures reduce the efficiency of energy conversion, so in summer the instantaneous power may be lower even at higher radiation intensity and smaller angle of incidence.

Key words: solar energy, photovoltaic energy conversion, photovoltaic system, data monitoring

INTRODUCTION

The efficiency of a photovoltaic (PV) system depends on many parameters. In our previous article (Daneček et al., 2020), we compared PV systems with different constructions located in very different and distant locations in the Czech Republic in Central Europe and in Chile in South America. We compared mainly the amount of electricity produced.

At present, we are focusing on only one PV system located at the Faculty of Engineering, CULS Prague. We monitor the produced electricity amount and we compare measured values with expected values according Photovoltaic Geographical Information System (PVGIS). Influence of Roof Installation of PV Modules on the Microclimate Conditions was studied for example in the work (Bilčík et al., 2021).

MATERIAL AND METHODS

Fig. 1 shows the PV system installed at the Faculty of Engineering in Prague (50.13° north, 14.37° east). 40 PV panels (Renesola, GmbH, type JC 260M-24/Bb, nominal output power 260 W_p) based on polycrystalline silicon are divided into two independent sections. In each section, 20 PV panels are connected in a series and they are connected to the distribution network via inverters. PV panels are installed on a fixed stands, they are oriented nearly to the south with an inclination of 35°. The nominal output power is cca 10 kW_p. Solar conditions correspond to the temperate climate zone in Central Europe.

RESULTS

The evaluation of the data shows that the amount of electricity produced slightly exceeds the expected values predicted by the internationally used internet application (PVGIS), see Table 1. According to this application, the expected production of electricity is 1067.7 $kWh.kW_p^{-1}.year^{-1}$, the actual production in individual years is around 1100 $kWh.kW_p^{-1}.year^{-1}$. The highest value was reached in 2019, when it provided 1221 $kWh.kW_p^{-1}.year^{-1}$, as shown in Fig. 2. Not only sunny June contributed to this, but mainly sunny April, when the days were long enough and it was still cold. A lower temperature increases the efficiency of photovoltaic energy conversion.

Table 1 Estimated amount of electricity produced per year (PVGIS)

Month	Jan	Feb	Mar	Apr	Mar	Jun	Jul	Aug	Sep	Oct	Nov	Dec	**Total**
Electricity ($kWh.kW_p^{-1}.month^{-1}$)	37.4	54.9	90.8	122.2	128.8	128.4	130.4	121.4	105.2	72.6	39.3	36.3	**1067.7**

Fig. 1 On-grid PV system installed on the roof of the Faculty of Engineering in Prague

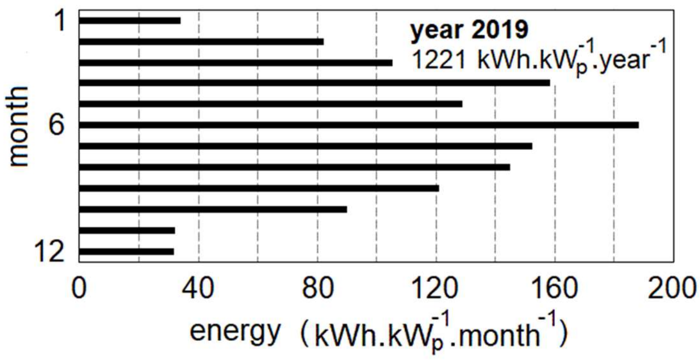

Fig. 2 Produced electricity amount during the year 2019

CONCLUSION

The PV system at the Faculty of Engineering has been operating without problems for almost 5 years and the amount of electricity produced is slightly higher than the expected value according to the internationally used PV GIS application. This indicates a good quality PV system.

The work was supported by the research project of the Faculty of Engineering IGA 2021.

LITERATURE

DANEČEK, M., HAVRLÍK, M., BERÁNEK, V., ŠAFRÁNKOVÁ, J., LIBRA, M., POULEK, V., SEDLÁČEK, J., BELZA, R. 2020. Design and data comparison of the photovoltaic power plants in the southern and northern hemispheres. *Agronomy Research*, 18(S1):755–761.

BILČÍK, M, BOŽIKOVÁ, M, ČIMO, J. 2021. Influence of Roof Installation of PV Modules on the Microclimate Conditions of Cattle Breeding Objects. *Applied Sciences*, 11:2140.

PVGIS (Photovoltaic Geographical Information System), [online] 2021. Available from: *https://re.jrc.ec.europa.eu/pvg_tools/en/tools.html*. Accessed 18.3.2021.

Corresponding author:
Matouš Havrlík, e-mail: havrlik@tf.czu.cz

HOLOGRAPHIC INTERFEROMETRY AS A METHOD FOR STUDY OF HEAT TRANSFER OF THERMALLY MODIFIED WOOD

Áron Hortobágyi, Elena Pivarčiová

Technical university in Zvolen, Faculty of technology, Department of manufacturing and automation technology, T. G. Masaryka 24, 960 01, Zvolen, Slovak republic, xhortobagyi@is.tuzvo.sk, elena.pivarciova@tuzvo.sk

The paper focuses on use of holographic interferometry as a method of heat transfer study. The method was used for observation of heat transfer from the wood surface to the surrounding air. In the experiment, spruce wood samples, thermally modified at 160 °C, 180 °C, 200 °C, 220 °C and an unmodified control sample were used. Results show that the thermal modification affected the heat transfer from the sample to the air. The value of the heat transfer coefficient α was lower in the modified samples than in the control samples and decreased also with the degree of thermal modification. Holographic interferometry shows a potential to be a suitable and helpful method in this field of the research.

Key words: Thermal modification, holographic interferometry, heat transfer, thermowood

INTRODUCTION

In this research, temperature fields over heated thermowood samples were observed. Main objective was to gain new information about properties of this material, mainly time dependencies, continual course of heat transfer and overall survey of temperature field.

Other objective was use of method of holographic interferometry in this field of study, with aim to gain results comparable to methods already in use.

Therefore, visualization of temperature fields was done by holographic interferometry. This enabled visualization of temperature fields and real-time tracking of events at boundary layer wood-ambient environment without affecting process by measuring devices. Multiple authors conducted research in field of heat conductivity of heat-treated beech wood (Czajkowski et al., 2020) wild cherry (Korkut et al., 2013), spruce (Olarescu et al., 2015), poplar (Pásztory et al., 2017) and untreated wood (Pivarčiová, 2019).

MATERIAL AND METHODS

Samples of spruce (*picea abies L.*) wood were used for the research. After drying, samples were heat treated by ThermoWood method, with final temperatures of 160, 180, 200 and 220 °C with final moisture content of 4–7 %. An untreated plank was cut into control samples. Samples were used also in other experiments, their preparation is further described by (Hrčková et al., 2018). After heat treatment, 40x40x10 mm samples were cut from planks, five for each final temperature, as well as five untreated control samples.

A holographic variant of the Mach-Zehdner interferometer was used, with setup as described by (Pivarčiová et al., 2019). This variant is one of the most used devices for visualization and measurement of two-dimensional transparent objects.

Dependence of temperature on the state variables of the environment, on the length of the model, wavelength of light and on the number of dark fringes between the object and the place of homogeneous environment can be determined according to (Černecký et al.,2012):

$$T(x, y) = T_\infty / [1 - 0.805 \cdot (T_\infty)/(l \cdot p_\infty) \cdot (s - ½)], \quad (1)$$

where $T(x, y)$ – temperature distribution, T_∞ – air temperature in the reference area, p_∞ – pressure in the given space, s – interference order, l – length of the object.

If it is necessary to determine the local value of the heat transfer coefficient, it can be done using the equation (Pivarčiová et al., 2019):

$$\alpha x = -\lambda v \cdot (\Delta T / \Delta y)x \cdot 1 / (Tx - T_{\infty}), \qquad (2)$$

where λ – coefficient of thermal conductivity of ambient air (for dry air at 20 °C, λ_v = 2,524 $W{\cdot}m^{-1}k^{-2}$), $(\Delta T / \Delta y)x$ – derivation of temperature at position x, Tx – body surface temperature at point x, T_{∞} – ambient temperature.

RESULTS

During the heating of the samples, heat transfer occurred, and a thermal boundary layer formed above the sample. Interference fringes formed in this layer. At low temperatures, there were few fringes, their number increased during the experiment.

Records from the range of heating time 12–25 min were suitable for evaluation. The temperature profile of the thermal boundary layer above the sample was obtained by analysis of interferograms using the Vibra program, with implemented formulas (1) for calculation of the temperature, and (2) for calculation of heat transfer coefficient.

In Figure 1. an example of the evaluation of the temperature profile above the sample is shown.

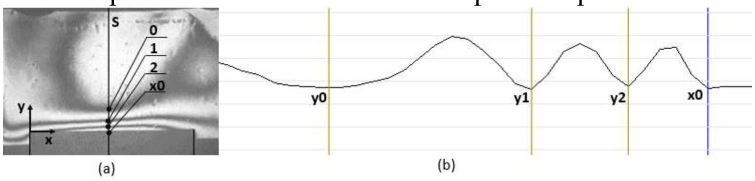

Fig. 1 Evaluation of the temperature profile above the sample (spruce treated at 200 °C, surface temperature 66.58 °C). (a) Evaluated interferogram indicating the section line (S), (b) Marking the position of the interference fringes (y0; y1; y2) and the surface of the heated sample (x0).

The dependences of the heat transfer coefficient on the heating time are summarized in Table 2 and graphically illustrated in Figure 6.

Table 2. Calculated values of the heat transfer coefficient α

	Final temperature of heat treatment [°C]				
Heating time [min]	**natural**	**160**	**180**	**200**	**220**
12	16.61	14.65	14.00	12.88	12.06
15	–	13.89	13.61	9.78	8.75
17	15.57	13.30	12.34	8.20	8.07
19	12.05	10.66	10.47	7.44	7.02
21	10.65	9.71	9.39	6.47	6.50
23	8.10	6.77	7.07	6.39	5.99
25	7.64	6.20	6.18	–	5.42

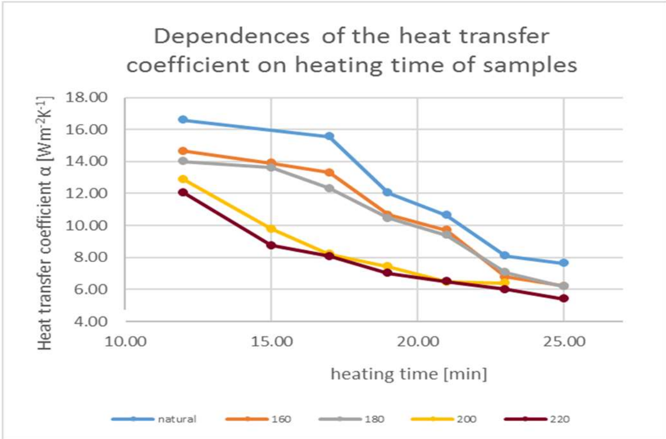

Figure 2. Dependences of the heat transfer coefficient on the heating time of the samples

DISCUSSION

In Figure 2, it is visible that the value of the heat transfer coefficient α for all samples of thermally modified wood was lower than the value corresponding to the control sample. In the observed range, it is observable that the value of the heat transfer coefficient decreases with increasing degree of thermal modification. The difference between the control sample and the sample modified at 160 °C is, according to Table 2, a decrease in the range of 9–19 %. The largest difference was between the samples modified at 180 °C and 200 °C, which ranged from 6 to 26 %. Minor, but still observable differences were between samples treated at 160 °C and 180 °C in the range of 0–6 % and between samples treated at 200 °C and 220 °C in the range of 0–5%. The differences according to Table 1 had a smaller range at the end of the experiment ($\alpha = 7.64 - 5.42$ Wm^{-2}K^{-1}) than at the beginning ($\alpha = 16.61 - 12.06$ Wm^{-2}K^{-1}). The largest difference was recorded in the 17th minute of heating ($\alpha = 15.57 - 8.07$ Wm^{-2}K^{-1}).

From the result, it can be concluded that the thermal modification has an effect on the heat transfer coefficient. The degree of wood treatment also has an effect – at higher temperatures of thermal modification, the heat transfer coefficient is significantly lower.

The heat transfer coefficient α also decreased with gradual heating of the sample. This decrease could be due to the higher air temperature in the boundary layer.

The method of holographic interferometry was used in the experiment, which allowed the visualization of the distribution of temperature fields over the heated sample.

In contrary to the hot and cold plate method used by (Pásztory et al., 2017) and (Czajkowski et al., 2020), holographic interferometry was used for data evaluation. Result leads to similar conclusion: thermal modification influences the heat transfer coefficient. Also, degree of wood treatment has an effect – at higher temperatures of thermal modification, the heat transfer coefficient is significantly lower.

CONCLUSION

The experiment showed that thermal modification of wood reduces the intensity of heat transfer. Compared to the control sample, the thermally modified samples achieved lower final values in the whole measurement range. The heat transfer coefficient α decreased with increasing degree of thermal modification.

The experiment shows that thermal modification has a positive effect on wood when used as a barrier to heat loss.

When compared to studies on thermal conductivity of thermally modified natural fir and beech wood (Czajkowski et al., 2020), and spruce and poplar wood (Pásztory et al., 2017), similar result was achieved. In this study focused on heat transfer coefficient, results are dispersed in larger range. Difference could occur due to multiple factors, such as type of wood, moisture content or variation in time intervals of heat treatment. In further experimentation, more samples should be used for testing.

ACKNOWLEDGMENT

This research was funded by VEGA 1/0086/18: Researching Temperature Fields in a Set of Shaped Heat Transfer Surfaces.

LITERATURE

KORKUT, D.; HIZIROGLU, S., AYTIN, A. 2013. Effect of Heat Treatment on Surface Characteristics of Wild Cherry Wood. BioResources, 2013, vol. 8, no. 2, pp. 1582-1590.

OLARESCU CM.; CAMPEAN M.; COSEREANU C. 2015. Thermal conductivity of solid wood panels made from heat-treated spruce and lime wood strips. PRO Ligno, 2015, vol. 11, no. 4, pp. 377–382

PÁSZTORY, Z., HORVÁTH, N., BÖRCSÖK, Z. 2017. Effect of heat treatment duration on the thermal conductivity of spruce and poplar wood. European Journal of Wood and Wood Products, 2017, vol. 75, pp. 843–845. Available on: https://doi.org/10.1007/s00107-017-1170-2

CZAJKOWSKI, Ł.; OLEK, W., WERES, J. 2020. Effects of heat treatment on thermal properties of European beech wood. European Journal of Wood and Wood Products, 2020, vol. 78, pp. 425–431. Available on: https://doi.org/10.1007/s00107-020-01525-w

PIVARČIOVÁ E.; BARCÍK Š.; ŠTEFKOVÁ J.; ŠKULTÉTY E. 2019. Investigation of Temperature Fields in the Air Environment above Wood Subjected to Thermal Degradation. Drvna Industrija 2019, vol. 70, no. 4, pp. 319-327 Available on: https://hrcak.srce.hr/index.php?show=clanak&id_clanak_jezik=334009

HRČKOVÁ, M.; KOLEDA, P.; KOLEDA, P.; BARCÍK, Š.; ŠTEFKOVÁ, J. 2018. Color Change of Selected Wood Spieces Affected by Thermal Treatment and Sanding. BioResources 2018, vol. 13, no. 4, pp. 8956–8975. Available on: https://bioresources.cnr.ncsu.edu/resources/color-change-of-selected-wood-species-affected-by-thermal-treatment-and-sanding/

PIVARČIOVÁ, E.; BOŽEK, P.; DOMNINA, K.; ŠKULTÉTY, E.; FEDOSOV, S. 2019. Interferometric measurement of heat transfer above new generation foam concrete. Measurement Science Review 2019, vol. 19, no. 4, pp. 153–160. Available on: https://doi.org/10.2478/msr-2019-0021

Possibilities and Prospects of Holography. Available online: http://www.holografia.wz.cz/holography/index.php (Accessed on 12. 10. 2020)

ČERNECKÝ, J.; KONIAR, J.; BRODNIANSKA, Z. 2012. Optimalizácia výmenníkov tepla s využitím experimentálnych metód a fyzikálneho modelovania. Technická univerzita vo Zvolene: Zvolen, Slovak republic 2012. ISBN 978-80-228-2325-8.

Corresponding author:
Áron Hortobágyi, tel.: +421917394179, e-mail: xhortobagyi@is.tuzvo.sk

DEFORMATION EVALUATION ON A FLOATING CALIPER BRAKE

Lukáš Hudec

Faculty of Technology, Technical University in Zvolen, T. G. Masaryka 24, 960 01 Zvolen, e-mail:xhudecl@is.tuzvo.sk

This paper aims to evaluate deformation on a floating caliper brake in response to the hydraulic pressure of the brake fluid. Specifically, the deformation in the piston chamber is being looked at as the change in volume can affect the pressure and could therefore pose a threat to the operation of the floating caliper brake. The resulting displacement of reference points between the brake caliper and the piston is then used to calculate the difference in volume after pressure is applied. Variants with different pressure values are compared. Furthermore, variants with different elements for mesh generation are used. A simplification of a brake pad in the form of a domed steel spacer is compared to a braking pad that has the compressibility behavior of a hyperfoamic material. The variants with different element types caused minimal differences in the displacement of the individual reference points and thus no significant difference in volume change. Changing the brake pads proved to be significant to the volume change. The volume change was smaller in the variant with the hyperfoam pads due to the higher compressibility of the pads. Uneven deformation could lead to uneven wear on the brake pads and their shorter lifespan.

Key words: brake caliper; deformation; element; fea

INTRODUCTION

The main uses of FEA today in vehicle manufacturing are crash simulations, brake modeling, tire modeling. When simulating models using FEA analysis, we look for results with the greatest accuracy, shortest computing time, and shortest meshing time. In general, computing time increases with the use of a mesh with smaller elements. On the other hand, using a mesh with larger elements can cause stress values to be less accurate. A courser mesh can be beneficial if we try to get a simplified model for an approximate and quick calculation of the effects of mesh density on the accuracy of the displacement and stress values. In a static simulation of a plate model, it was found that an adequate number of discretizations is about ten divisions for an approximate error under 1% (Liu 2013). The percentage of error is by far less for deflection as compared to von Mises stress. According to the Finite Element Analysis theory, stresses are not predicted as accurately as displacement (Dutt 2015). The situation gets complicated when we use different types of elements, different orders of elements, and solvers implemented in simulation software, as these have a profound impact on the results.

MATERIAL AND METHODS

An assembly of a floating caliper disc brake is used. The solver used for computation is Abaqus, and Abaqus Viewer is used for post-processing, while the mesh generation was handled using Altair HyperMesh. The assembly variant ΔV_1 consists of the housing (1), also known as the caliper bracket, which holds the cylinder piston (2). The inner and outer backplates (3,7) are connected to inner and outer pads (4,6) and the brake disc (5). The assembly variant ΔV_g represents a simplified alternative where the inner and outer pads (4,6) are replaced by a simplified inner and outer domed steel spacer (8,9).

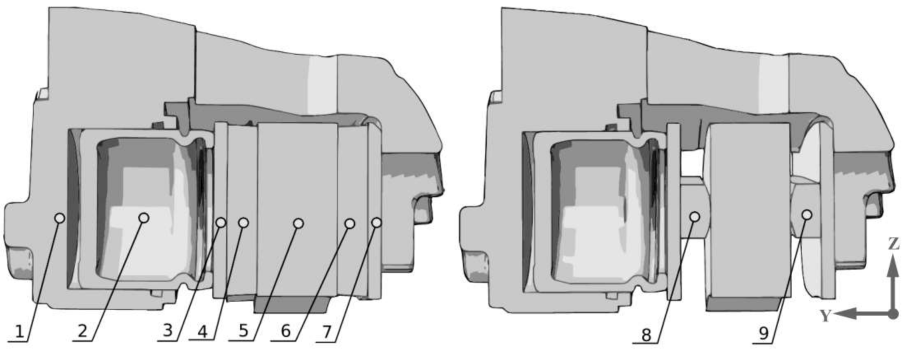

Fig. 1 Floating caliper disc brake assembly

The material definition for the pads is a compressible elastomeric foam modeled using the hyperfoam option in Abaqus. The quality criteria for the elements that the max allowed angle in a quad element is 130°. The minimum allowed angle in a quad element was 30° and 20° for a triangular one. The maximum allowed skew for an element was 60, and the aspect ratio between elements was kept, so it did not exceed 5. The displacement on the Y-axis is used to determine the change in volume ΔV. The average of the two reference values is used for determining the length of the cylindrical volume. To assess the deformation caused during the stress-strain analysis, the change in the volume in the chamber where the cylinder piston is located is measured. Displacement can also occur at the reference points; thus, the reference position of the caliper is then subtracted.

$$\Delta l_1 = \left(\frac{u_{c1}+u_{c1}}{2}\right) - u_{f1} \quad (1)$$

$$\Delta V = \Delta l_1 * \frac{{D_{piston}}^2 * \pi}{4} \quad (2)$$

The assembly is under load with a pressure of 100 and 160 bars. The pressure is distributed in the cylindrical space on the surfaces between the caliper and the plunger. Pressure is applied evenly in the direction perpendicular to the elements' surfaces, forming the space between the piston and the caliper.

RESULTS

The result of the stress-strain analysis is the deformation of the caliper brake. The displacement of the reference points is then used to calculate the change in deformation in the cylinder chamber. The figure shows the strain for the brake. The deformation is measured for both variants, the ΔV_g, and ΔV_1, respectively. Variants, where different types of elements were used, were also examined.

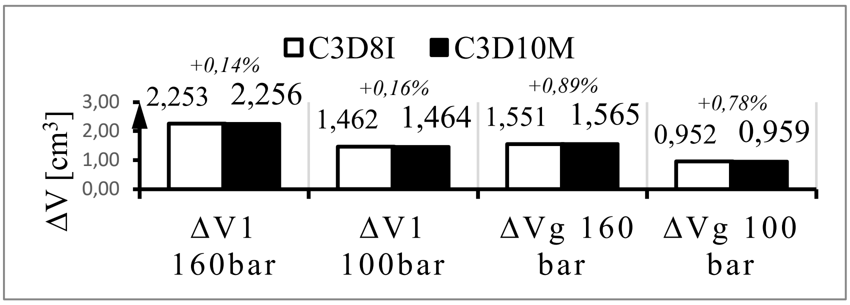

Fig. 4 Volume change results

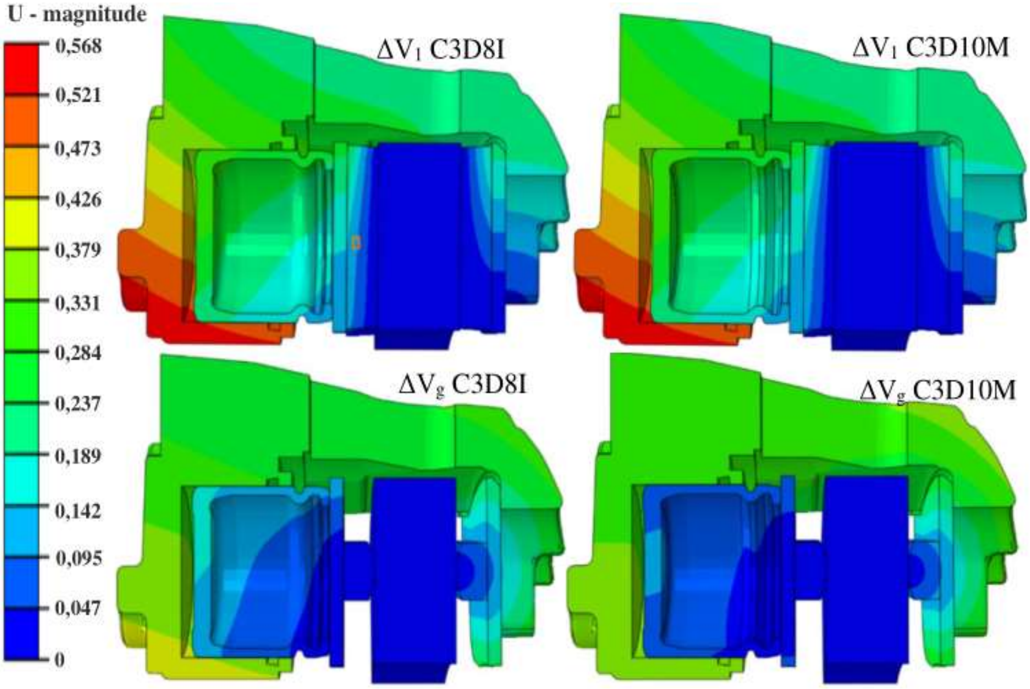

Fig. 3 Deformation magnitude

CONCLUSION

It is known that the compressibility of the brake pad is due to the combined physical effects of elastic and plastic deformations of the lining material. Compressibility describes the property of the pad, which depends on its material. It is, therefore, in accordance with the general knowledge that the variant with the brake pads has shown higher ΔV values compared to the variant with the steel spacers. For the evaluation of the reference points and volume change, we can see that the replacement of the elements caused minimal differences in the displacement of the individual reference points and thus in no significant difference of volume change. However, the change between the variant using steel spacers and the variant with the pads was significant. The volume change was smaller in the variant with the hyperfoam pads, which is most likely due to the higher compressibility of the pads. Uneven deformation could lead to uneven wear on the brake pads and their shorter lifespan.

REFERENCES

DUTT, A., 2015. Effect of Mesh Size on Finite Element Analysis of Beam. International Journal of Mechanical Engineering, roč. 2, č. 12, s. 8–10. ISSN 2348-8360. doi:10.14445/23488360/IJME-V2I12P102

LIU, Yucheng, 2013. Effects of Mesh Density on Finite Element Analysis SAE Technical Papers. roč. 2013,. doi:10.4271/2013-01-1375

Corresponding author:
Lukáš Hudec, e-mail: xhudecl@is.tuzvo.sk

ELEMENTAL ANALYSIS OF SPRUCE AND BARLEY

Lukáš Jeníček

Department of Mechanical Engineering, Faculty of Engineering, Czech University of Life Sciences Prague, Prague, Czech Republic

Tests performed in the laboratory at Czech University of Life Sciences were extended by torrefying the material at the operating temperature of 250°C and 280°C and pellet production on a small pellet press with a disk matrix. Elementary parameters were monitored in all material stages. Results of torrefaction and pellet production showed increase of calorific value in the material. Spruce wooden chips proofed to be a suitable material for domestic and industrial usage.

Key words: biomass, biofuel, greenhouse gas, calorific value, carbon footprint

INTRODUCTION

Fighting the greenhouse gas emissions is globally known problem, being discussed on many international and local forums. In Europe it has been enhanced by European Union (Regulation 2018/1999) which sets a target of reducing greenhouse gas emissions of 43 % compared to 2005 and increasing the share of Renewable Energy Sources (RES) in gross final consumption of energy at 32 % by 2030.

On a local level in Czech Republic the National Plan was introduced to reduce greenhouse gas emissions by 30 % by 2030 (compared to 2005) and to increase the share of RES in gross energy consumption to 22 %.

Biomass is a renewable material that is considered carbon neutral and therefore helping to counteract the greenhouse gas emissions (García et al., 2019).

Aim of this article is to evaluate and confirm the positive impact of torrefaction and pellet production on elemental and stochiometric analysis of biomass as a potential biofuel in households and industries.

MATERIAL AND METHODS

Material collected for analysis was Wood chip of Norway Spruce (Picea abies) and Barley (Hordeum vulgare).

- SAMPLE A - Wood spruce chips (66%) + Barley (33%)
- SAMPLE B - Wood spruce chips torrefied at 250 ° C (66%) + Barley (33%)
- SAMPLE C - Wood spruce chips torrefied at 280 ° C (66%) + Barley (33%)

Material was first grinded to a maximum particle size of 1mm, then torrefied in torrefaction unit and pelleted. Elemental analysis was performed in all the steps.

RESULTS

Torrefaction of the material increased the share of carbon in the material (Table 1), leading to the increase of combustion heat and calorific value of the material. This result is in line with evaluation of (Pimchuai et al., 2010, Rudolfsson et al., 2015), who analysed that pre-treatment of torrefaction increases the efficiency of biomass combustion processes.

Pellet production had a slightly negative effect on the elemental composition of the material (Table 1). Produced pellets had a lower carbon content and lower calorific value than pure non-pelleted material. The pellets also had a higher proportion of ash, water content and nitrogen.

On the other hand pellet burns better than the original material due to the lower moisture content and the higher concentration of energy value. As writes (LYČKA et al., 2011), the pellet also has lower demands on storage, transport, and handling Pellet production has a positive impact on the amount of air demand for perfect combustion and on carbon dioxide in dry flue gas for the torrefied material.

Table 2 Elemental analysis of Spruce wood chip and Barley samples

Sample	**Humidity (%)**	**Ash (%)**	**C (%)**	**H (inc. water; %)**	**H (in combustible part; %)**	**N (%)**	**S (%)**	**O (in combustible part; %)**	**Combustion heat ($MJ.kg^{-1}$)**	**Calorific value ($MJ.kg^{-1}$)**
Sample A - dried	7,01 (±0,05)	0,91 (±0,01)	45,79 (±0,12)	6,53 (±0,04)	5,74 (±0,04)	0,64 (±0,01)	0,03	39,86	17,99 (±0,08)	16,57
Sample B - dried	4,47 (±0,04)	1,31 (±0,01)	49,33 (±0,11)	6,24 (±0,05)	5,74 (±0,04)	0,62 (±0,01)	0,03	38,50	19,34 (±0,07)	17,99
Sample C - dried	4,98 (±0,05)	1,62 (±0,02)	53,13 (±0,17)	6,07 (±0,04)	5,52 (±0,03)	0,65 (±0,01)	0,03	34,07	20,82 (±0,08)	19,50
Sample A - pellets	8,86 (±0,07)	1,16 (±0,01)	44,24 (±0,12)	6,74 (±0,05)	5,75 (±0,05)	1,53 (±0,02)	0,00	38,47	17,38 (±0,11)	15,92
Sample B - pellets	7,83 (±0,06)	1,54 (±0,02)	45,63 (±0,13)	6,55 (±0,04)	5,67 (±0,04)	1,35 (±0,02)	0,00	37,97	17,90 (±0,10)	16,48
Sample C - pellets	7,67 (±0,06)	1,44 (±0,01)	47,61 (±0,11)	6,48 (±0,04)	5,63 (±0,04)	1,48 (±0,02)	0,00	36,18	18,87 (±0,09)	17,46

CONCLUSION

Elemental tests of spruce wood chips showed the positive impact of torrefaction on energy value increase and pellet production showed the positive impact on energy value density increasing the efficiency in handling and storing costs.

Barley, in comparison with spruce wood chip, has higher ash content and lower combustion heat and calorific value, but still may be used for energetic usage, if not used for other purposes (food, beer).

LITERATURE

Vnitrostátní plán České republiky v oblasti energetiky a klimatu, 2019. Available at: https://www.mpo.cz/cz/energetika/strategicke-a-koncepcni-dokumenty/verejna-konzultace-k-vnitrostatnimu-planu-ceske-republiky-v-oblasti-energetiky-a-klimatu--250509/

Commission Regulation (EU) 2015/1189 of 28 April 2015 implementing Directive 2009/125/EC of the European Parliament and of the Council with regard to ecodesign requirements for solid fuel boilers. Available at: https://op.europa.eu/en/publication-detail/-/publication/8809cda2-2f6e-11e5-9f85-01aa75ed71a1/language-en

GARCÍA, R., GIL, M.V., RUBIERA, F., PEVIDA, C. 2019. Pelletization of wood and alternative residual biomass blends for producing industrial quality pellets. Fuel 251, pp. 739-753.

MALAŤÁK, J., GENDEK, A., ANISZEWSKA, M., VELEBIL, J. 2020. Emissions from combustion of renewable solid biofuels from coniferous tree cones. Fuel 276,118001.

PIMCHUAI, A., DUTTA, A., BASU, P. 2010. Torrefaction of agriculture residue to enhance combustible properties. Energy and Fuels 24(9), pp. 4638-4645

RUDOLFSSON, M., STELTE, W., LESTANDER, T.A. 2015. Process optimization of combined biomass torrefaction and pelletization for fuel pellet production - A parametric study. Applied Energy 140, pp. 378-384

LYČKA, Z. 2011. Wooden pellet, cleared of myths. (Dřevní peleta, aneb, Peleta mýtů zbavená) Krnov: LING Vydavatelství, ISBN 9788090491403

Corresponding author:
Ing. Lukáš Jeníček, Department of mechanical engineering, Faculty of Engineering, Czech University of Life Sciences Prague, Kamýcká 129, Praha 6, Prague, 16521, Czech Republic, tel: +420724127798, email: jenicekl@tf.czu.cz

SMART FARMING APPLICATION: A LITERATURE REVIEW

Sri Murniani Angelina Letsoin[1,2], David Herak[1], RatnaChrismiari Purwestri[3,4]

[1]*Department of Mechanical Engineering, Faculty of Engineering, Czech University of Life Sciences Prague, Kamycka 129, 165 00 Praha-Suchdol, Czech Republic,letsoin@tf.czu.cz; herak@tf.czu.cz*
[2]*Faculty of Engineering, University of Musamus, Merauke Regency, Papua 99611, Indonesia*
[3]*Faculty of Forestry and Wood Sciences, Czech University of Life Sciences Prague, Kamycka 129, 16500 Praha-Suchdol, Czech Republic*
[4]*Institute of Nutritional Sciences, University of Hohenheim, Garbenstrasse 28, 70599 Stuttgart, Germany*

Since the agriculture sector nowadays is changing forward to become faster, reliable, remotely, and up to date information about productivity, pest detection, stock, or water controlling, then the farms should stand on the advancement of digital technology for instance autonomous and remotely recognition, advanced analytics, or smart devices. The presented work aims to review the currently smart farming application using literature study namely inOrdinatioindex.The literature review includes the scope of research that demonstrating on smart farming specifically in recognition study. As the result, in smart farming sector today supported by various embedded platform such as Internet of Things, as well as Unmanned Aerial System. These also involve various range of network protocol, for instance wired (Ethernet), middle range like wi-fi or wide range for example, LoRaWAN. Furthermore, smart farming application also relatable within different technology data processing, for instance, artificial intelligence, computer vision, machine learning, fuzzy, deep learning and also big data. Nevertheless further research and development is required to fulfil the smallholder needs as well the decision support for relevant parties.

Key words: remotely, smart detection, digital farming,inOrdinatio index

INTRODUCTION

Smart farming refers to the integrated use of Information and Communication Technologies supported by the latest technology in the agricultural sector. New technology involves the Internet of Things (IoT), cloud computing and applying robotics, various sensors, and the autonomous system, as well as Unmanned Aerial System, the artificial intelligence and deep learning model, are expected to robust this establishment into farming (Barreto et al. 2018, Darwin et al. 2021). This study aims to identify the smart farming application as well as to give the latest view about the smart agriculture research field using survey literature of the last 5 years.

MATERIAL AND METHODS

The Ordinatio ranking (Inordinatio index) was used to support the methodological literature review of the presented work. We have adopted the essential stage ofMethodiOrdinatio by calculating the InOrdinatio index, in choosing relevant articles according to the number of citations (CC), the length of publications in years (Py) as well as the impact factor of the journal (IF). Inordinatio calculation as follows: (de Carvalho et al. 2020.)

$$InOrdinatio = CC + \mathrm{IF} + (10 * \alpha) - (\alpha * \mathrm{Py}) \quad (1)$$

Here, the alpha constant refers to a weighting scheme chosen based on the researcher. In this paper,we combine the keywords usingBoolean search to achieve the research axes throughout the base engine, namely Web of Science Core Collection. Since our research line consists of agriculture and applied technology, thus, the keywords were smart farming application OR smart agriculture application, smart plant recognition, smart farming AND smart agriculture for recognition.Furthermore, the presented study examined the development of smart farming applications recently, particularly in recognition. In the next stage, the Zotero software was used to refine the journal, while Google Scholar was applied to support the verified stage. Additionally, Microsoft Excel software was usedas the auxiliary data storage of each publication, i.e., authors name, titles, journal name, publication year then also, the number of citations.

RESULTS

A total of 1172 articles in total were filtered by the search engine from the topic of interest. Throughout the examining phase, we identified the titles, abstracts and keywords relatable to the goal of this study, followed by an evaluation of InOrdinatio index, such as the number of citation,Impact Factor of the journal, and the length of publication in the last fiveyears, which resulted in 101 selected articles.Afterward, 45% of articles were discarded due to unrelated content to this study; while 41% were review articles, conference articles with un-traceable journals on the web of sciences core collection, and moreover, without impact factor (IF) information of the journal. The last phase evaluated 15 articles that can be accessed and selected as the papers under reviewed for the smart farming application study.

Table 1 Summary of smart farming application

Application	Embedded system	Network Protocols	Data Processing Technology	Challenges and Future Work	Authors
Soil management	Internet of Things, android based smartphone (LINE API), web application	Wireless Sensor Network (WSN)	Real data from IoT, data mining technique	Knowledge discovery Various control of spraying	Muangprathub ,etc. 2019
Machinery	Unmanned Aerial Vehicle (UAV), IoT, spraying robot	Ethernet, internet, OPC UA (Open platform Communications United Architecture), wifi	Watson Visual Recognition (WVR), PLC, cloud computing	Delay time	Salhaoui, M, etc., 2019 Sabanci,K.,etc . 2017
Pest, weed, disease recognition and classification	Resnet50 Architecture, Google Net, smart phone, IoT	Not identified, LoRaWAN	CNN, Recurrent Neural Network (RNN), deep learning	Integration of rich global and local visual interpretation, larger number and varietyof fruits and diseases, higher accuracy, Integration with big data	Pan, W., etc. .2019, Lee, S.H, etc. 2020 Kim,S,. 2018
Crop monitoring	Smartphone, RGB camera, OpenCV, IoT	LoRA 4G/5G	Machine vision, image processing technique, AI, data analytics	Lightening and distances, smallholder support, appropriate sensor with high accuracy	Laso Bayas, etc. 2020 Wang, etc. 2018 Koubaa, etc. 2020, Adhitya, etc., 2020
Crop harvesting	IoT, robotic arm, Raspberry PI, Keras	HTTP, Wireless network	AI, machine learning, NN	Various implementation	Khan, T., etc. 2020 Horng G, etc., 2020

CONCLUSION

Smart applications nowadays cover various themesnamely soil management, machinery, pest, weed or disease recognition, crop monitoring as well as crop harvesting. We reviewed also that smart farming applications supported by the different embedded platforms, for example, raspberry, UAV, Iot Cloud computing framework. And also various network protocols such as Ethernet (wired), Wifi (middle range), or LoRaWAN(Wide range).Further, the smart farming sector involves also data analytic as well as data processing technology likewise Artificial Intelligence, machine learning, deep learning, computer/machine vision, data mining, and big data approaches. However, some recommendations are required to be considered,about delay time due to the variety of platform environments and various implementation of smart farming.

This contribution has been prepared as a part of theon-going research in Smart Farming application in Papua of Indonesia.This study is supported by Internal Grant Agency (IGA) of the Faculty of Engineering, Czech University of Life Sciences Prague, with the grant number: 2021:31130/1312/3105.

LITERATURE

BARRETO, L.; AMARAL, A. SMART FARMING. 2018. Cyber Security Challenges. In Proceedings of the 2018 International Conference on Intelligent Systems (IS); IEEE: Funchal - Madeira, Portugal, September 2018; pp. 870–876.

DARWIN, B.; DHARMARAJ, P.; PRINCE, S.; POPESCU, D.E.; HEMANTH, D.J. 2021. Recognition of Bloom/Yield in Crop Images Using Deep Learning Models for Smart Agriculture: A Review. *Agronomy*, 11, 646, doi:10.3390/agronomy11040646.

de CARVALHO, G.D.G.; SOKULSKI, C.C.; da SILVA, W.V.; de CARVALHO, H.G.; de MOURA, R.V.; de FRANCISCO, A.C.; da VEIGA, C.P. 2020. Bibliometrics and Systematic Reviews: A Comparison between the Proknow-C and the Methodi Ordinatio. *Journal of Informetrics*, 14, 101043, doi:10.1016/j.joi.2020.101043.

Corresponding author:
Sri Murniani Angelina Letsoin, +420776569772, e-mail: letsoin@tf.czu.cz

OPTIMALIZATION OF COOLANT HEATER FOR RESEARCH OF CAR RADIATORS IN LABORATORY CONDITIONS

Marek Lipnický[1], Zuzana Brodnianská[1], Pavol Koleda[2]

[1]*Department of Environmental and Forestry Machinery, Faculty of Technology, Technical University in Zvolen, Studentska 26, 960 01, Zvolen, Slovak Republic, xlipnicky@tuzvo.sk, zuzana.brodnianska@tuzvo.sk*
[2]*Department of Manufacturing and Automation Technology, Faculty of Technology, Technical University in Zvolen, Studentska 26, 960 01, Zvolen, Slovak Republic, pavol.koleda@tuzvo.sk*

The paper presents a gradual design and optimization of a heating element for coolants in the experimental cooling circuit of a Skoda Fabia 1.4 MPI. The operating temperature of the coolant to be reached by the heater is 80 to 90 °C. The third variant of the manufactured heating element best suits the experimental conditions and its shape was designed with a circular cross-section ø 80 mm to achieve a cooling circuit volume specified by the manufacturer of 5.6 l.
Key words: engine cooling circuit, car radiator, heater, coolant, Skoda Fabia

INTRODUCTION

The experimental set up is intended for research of car radiators, their thermal parameters and used coolants in laboratory conditions. Since the engine model does not burn and thus does not generate any heat from the combustion chamber, the heat is generated by the heater. The size of the test circuit is an important factor for quality research (Singh *et al.* 2017). Electric heater with a power of 1500 W placed in the tank (volume 30 l) was used by the authors (Hussein *et al.* 2014) while the temperature was regulated in the range 60 – 80 °C. The authors (Peyghambarzadeh *et al.* 2013) heated coolant using two electric heaters (power 6000 W) to a temperature in the range of 50 – 80 °C. An 18 l tank was used in the experiment performed (Goudarzi & Jamali 2017). The tank contained 6 electric cells for heating the liquid to temperature of 80 °C. This paper is devoted to the development of the heating element to achieve a cooling circuit volume specified by the manufacturer of 5.6 l and real operating parameters of flow and heating time of coolants, and their smoother flow through the heating element.

MATERIAL AND METHODS

The laboratory engine cooling circuit is designed and constructed according to the real circuit in the car. The coolant temperature is measured by NTC thermistors located in the radiator inlet and outlet pipe, in the thermostat housing, and in the heating body. When the liquid heated by the coil flowed through it, thermal imaging images of the heater and its components were recorded by a Flir i7 thermal imaging camera. The design of the heater underwent gradual, based on test measurements, design changes and optimization (variants 1 to 3) to achieve real operating parameters of flow and heating time of coolants, and their smoother flow through the heater.

RESULTS

The Variant 1 of the heater consisted of an expansion tank for coolant from a Skoda Felicia vehicle with a heating coil of 500 W. A heating coil with three branches, but with a power of 1500 W, was used for Variant 2. Power supply and temperature regulation of the heating coil is solved by means of a triac regulator. The supporting element of the whole heating element assembly is an aluminum profile with dimensions of 80 × 80 × 300 mm. This profile also serves as a vessel into which a heating coil is inserted from the side through the plexiglass. The vent valve located in the upper part of the heating element serves for continuous venting of the entire small circuit. Air bubbles or excess coolant are returned to the expansion tank. In Variant 3, compared to Variant 2, the heating element is profiled steel with a thickness of 3 mm and the joints were not sealed with sealant, but with welds (Fig. 1a). The heating element forms one unit, which minimizes the possibility of coolant leakage even at high temperatures. Of the three branches of the heating coil, only 2 branches were connected, which provided us with sufficient power for our experiment (1000 W).

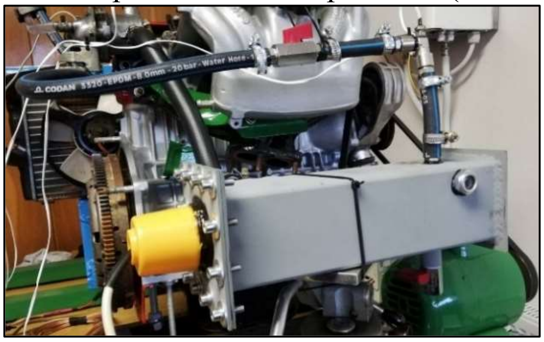

a)

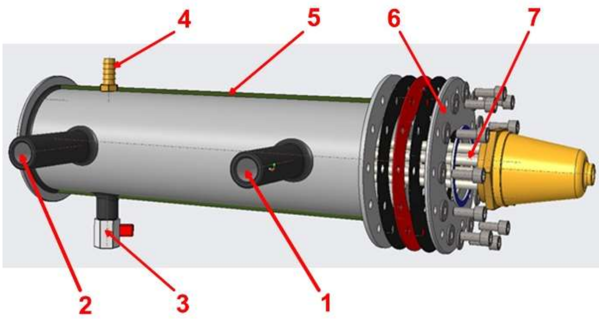

b)

Fig. 1 The heater element – Variant 3
a) connection to the experimental set up, b) optimized design
1 – coolant inlet, 2 – coolant outlet, 3 – drain ball valve, 4 – vent valve, 5 – mineral insulation, 6 – closing cover, 7 – heating spiral

CONCLUSION

The third variant of the heating element best suits the experimental conditions in the laboratory even under long-term loading (flow, temperature, pressure). However, when using a square cross-section of the heating element, the volume of the cooling circuit reaches approximately 6 l, therefore its shape has been adjusted to a circular cross-section of ø 80 mm to achieve a volume of cooling circuit specified by the manufacturer of 5.6 l (Fig. 1b).

Contribution has been prepared within the solving of scientific grant project VEGA 1/0086/18 " Research of temperature fields in the system of shaped heat exchange surfaces" and project IPA 2/2021 "Modification of cooling method of compact heat exchanger in engine cooling circuit car."

LITERATURE

GOUDARZI, K., JAMALI, H., Heat transfer enhancement of Al_2O_3-EG nanofluid a car radiator with wire coil inserts. In *Applied Thermal Engineering*, 2017, vol. 118, pages. 510-517, DOI: 10.1016/j.applthermaleng.2017.03.016.

HUSSEIN, A. M., BAKAR, R. A., KADIRGARGAMA, K., SHARMA, K. V., 2014. Heat transfer enhacement using nanofluids in an automotive cooling system. In *International Communications in Heat and Mass Transfer*, 2014, vol. 53, pp. 195-202. DOI: 10.1016/j.icheatmasstransfer.2014.01.003.

PEYGHAMBARZADEH, S. M., HASHEMABADI, S. H., NARAKI, M., VERMAHMOUDI, Y., 2013. Experimental study of overall heat transfer coefficient in the application of dilute nanofluids in the car radiator. In *Applied Thermal Engineering*, 2013, vol. 52, Issue 1, Pages 8-16, DOI: 10.1016/j.applthermaleng.2012.11.013.

SINGH, S., KUMAR, A., KHAN, F., 2017. Experimental study for heat transfer enhacement of car radiator using twisted inserts with coolants. In *International Journal of Interdisciplinary Research*, 2017, vol. 3, Issue 1, ISSN 2455-1600.

Corresponding author:
Ing. Marek Lipnický, tel.: +421455206 053, e-mail: xlipnicky@tuzvo.sk

THE USE OF DATA TRANSFER IN THE PREPARATION OF A TOTAL MIXED RATION IN A MIXER FEED WAGON

Gabriel Lüttmerding, Roman Gálik, Štefan Boďo

Department of Building Equipment and Technology Safety, Faculty of Engineering, Slovak University of Agriculture in Nitra, Tr. A. Hlinku 2, 949 76, Nitra, Slovakia, xluttmerding@uniag.sk

The total mixed ration represents an optimal composition of the very most needed raw materials in order to create the most optimal inputs the livestock needs, so farmer receives the highest possible quality outputs, such as high quality milk & meat, but most importantly the animal welfare must not be forgotten. Precision agriculture is seen as the future of agriculture and the data transfer is a crucial parameter for the digitalization in these days, or in the very near future. Dairy farming with the use of the data transfer between the feed mixer wagon and the farmer is the perfect combination to ease the work labour as well as to increase the level of the quality of work, and lastly but not least – the health of the livestock.

Key words: digitalization; precision agriculture; total mixed ration; dairy cattle; mixer feed wagon

INTRODUCTION

According to the well known literature, a total mixed ration (TMR) is a feeding system, used to provide consistent feed to animals and to stabilize rumen conditions as desired. Feeding activities have an important place in terms of animal health, performance, milk yield or meat production. The very each mouthful of the mixture consumed by an animal, must be homogenous and balanced, otherwide the animal can be negatively affected (Sova et al., 2014). These mixtures can be formulated for fresh cows, early lactation cows, mid-lactation as well as late-lactation, or close-up dry cows. The are many reasons to introduce different strategies for using TMR and there must be a decision of a farm manager, based on many aspects of the operations, research and personal preferences (Heinrichs & Kmicikewycz, 2016). The aim of this paper is to point out, how crucial the data transfer is for the farmer, to see the weight deviations of the set and the actual weight of the components, put into the TMRs. The data were obtained through a vertical mixer feed wagon and the results are put into the tables and graphs, which show how precise the loading of the components really is. In our work we established a hypothesis that the difference between the set and the actual loaded weight of the feed ration put into the mixer feed wagon, will not be greater than ± 5 %.

MATERIAL AND METHODS

Measurements for this article were made on a selected agricultural holding, using a Trioliet Solomix 2 1200 ZK (1 wheel axle) mixer feed wagon, shown on the Figure 1. The data of the selected feed rations were transfered from the mixer feed wagon to the usb stick. These data were exported into the PC and processed in the chosen software. We chose 3 groups of dairy cows with the highest milk yield. We could choose from many parametres, although we focused mainly on the set weight and the actual loaded weight. The weight differences were calculated from the chosen data. An acceptable permissible limit of ± 5 % was chosen by us. We chose data from the 10 days for the each group of cows. All the results were processed in tables and figures, which do show the difference between the set weight and the actual loaded weight of the feed ration components, exceeding the chosen maximal permissible limit.

Fig. 1 Trioliet Solomix 2 1200 ZK (1 wheel axle)

The chosen groups of animals were fed by the feed ration of the same structure, composed of four main components. The Table 1 shows the chosen components of the feed ration, and the numbers provided for the each component, which helped us to differ the data in our research.

Table 1 Charakteristics of components of selected groups of dairy cows

Number	Component
1	Core concentrate
2	Lantern haylage
3	Corn silage
4	Water

Analysis methods and evaluation of results

As we mentioned before, the set weight and the actual loaded weight of the feed ration were used. In order to find out the percentage deviations between the set and actual loaded weight in the group, we did use the following Equation 1:

$$w_d = \frac{w_{a_t} - w_{s_t}}{w_{a_t}} \,.\, 100 \qquad (1)$$

where w_d - weight difference [%],
w_{a_t} - total actual weight [kg],
w_{s_t} - total set weight [kg].

RESULTS

Group A

On the Figure 2 are shown the weight differences during the 10 days in the group A with an indication of the maximal and minimal permissible limit set by us.

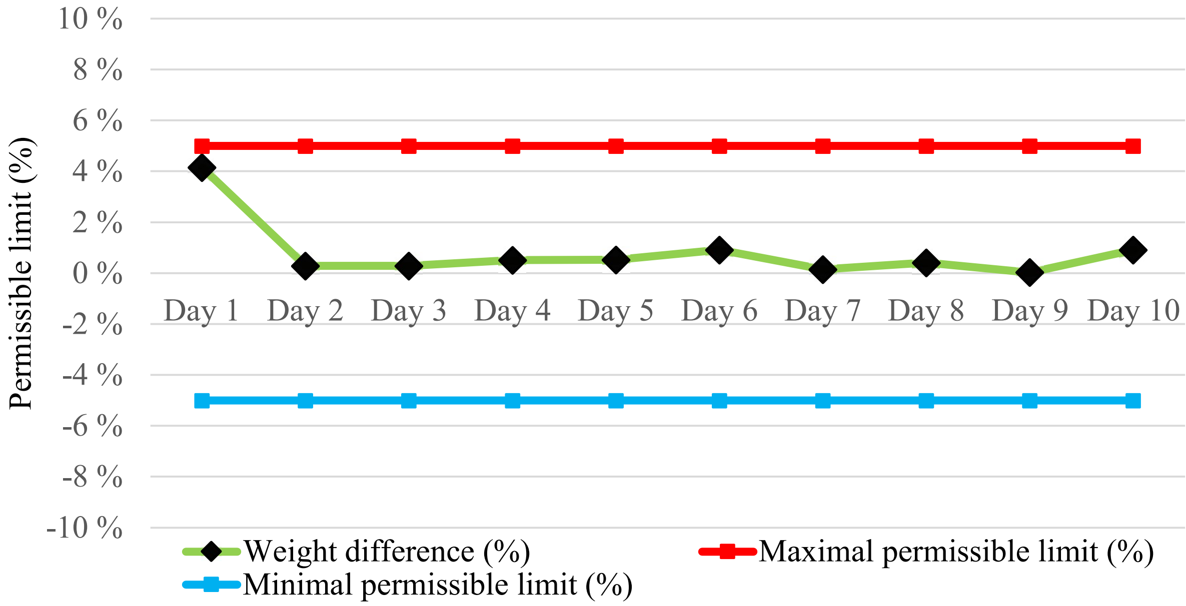

Fig. 2 Group A

Group B

On the Figure 3 are shown the weight differences during the 10 days in the group B with an indication of the maximal and minimal permissible limit set by us.

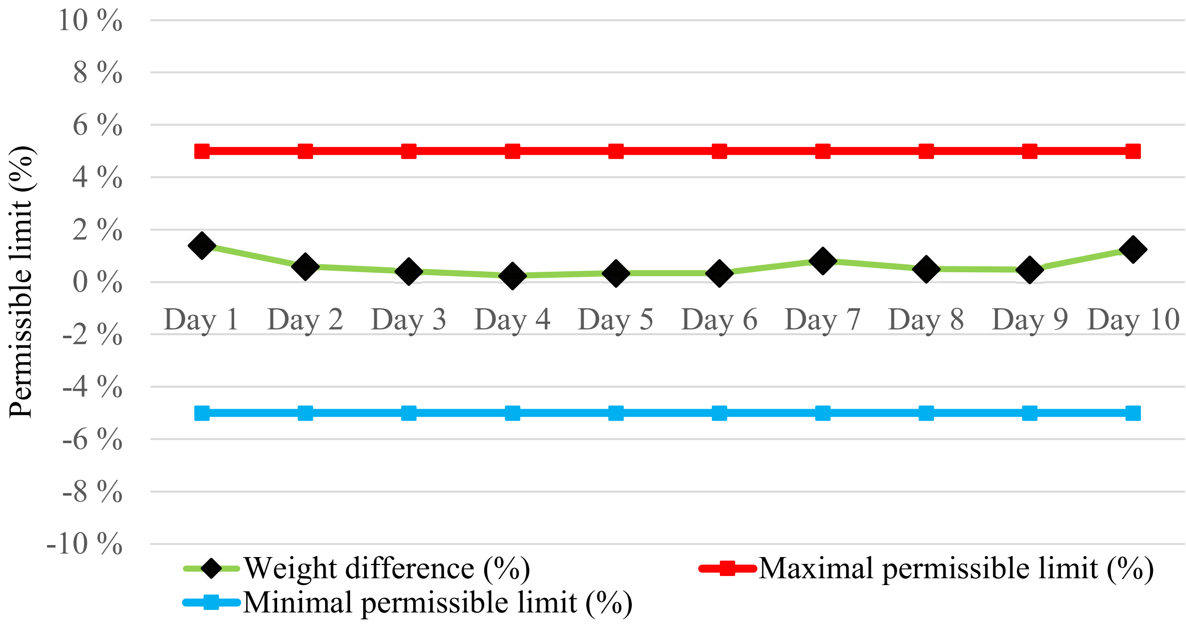

Fig. 3 Group B

Group C

On the Figure 4 are shown the weight differences during the 10 days in the group C with an indication of the maximal and minimal permissible limit set by us.

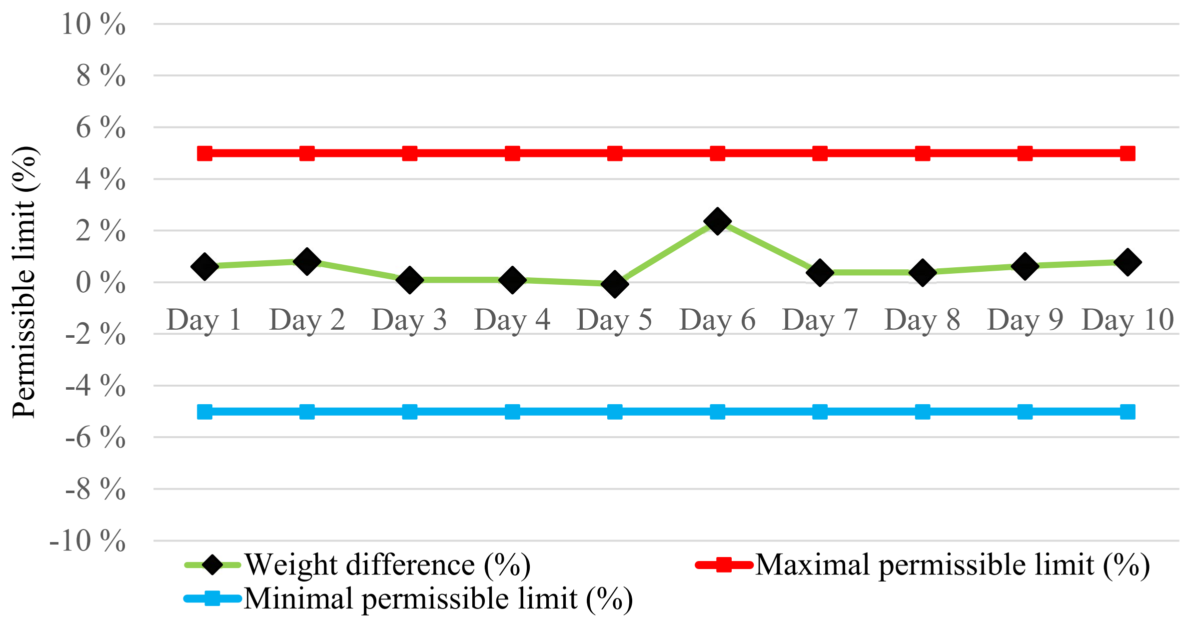

Fig. 4 Group C

CONCLUSION

We do can conclude the established hypothesis was confirmed. We did prove the weight differences of the feed ration did not exceed the set permissible limit ± 5 %. There is a lot of data, collected on a daily basis by the systems, programmed to help with the feed mixer wagon and it's accessories, for accurate loading and weighing of the feed ration components, thanks to constantly advancing technologies.

This publication was supported by the Operational Programme Integrated Infrastructure within the project: Sustainable smart farming systems taking into account the future challenges 313011W112, cofinanced by the European Regional Development Fund.

LITERATURE

HEINRICHES, J., KMICIKEWYCZ, A., 2016. Total Mixed Rations for Dairy Cows. [**online**]. Available at: <https://extension.psu.edu/total-mixed-rations-for-dairy-cows>.

SOLOMIX 2 - Mixer feeder wagons models 1000 - 3200. **[online].** Available at: <https://www.google.com/url?sa=t&rct=j&q=&esrc=s&source=web&cd=&cad=rja&uact=8&ved=2ahUKEwjAxJqlrd_wAhUBLewKHYm4DbIQFjADegQIBRAD&url=https%3A%2F%2Fwww.agriland.ee%2Fmedia%2Fcom_eshop%2Fattachments%2FTrioliet_Solomix2_EN_2017-2018-web.pdf&usg=AOvVaw3-4TGhh1iQ_Mh0Nfi_KoO5>.

SOVA et al., 2014. Accuracy and precision of total mixed rations fed on commercial dairy farms. *Journal of Dairy Science*. vol. 97, issue 1, pp. 562-571. ISSN 0022-0302. [**online**]. Available at: <https://www.sciencedirect.com/science/article/pii/S0022030213007492>.

Corresponding author:
Ing. Gabriel Lüttmerding, tel. +421 376 414 304, e-mail: xluttmerding@uniag.sk

INFLUENCE OF INDUCTANCE ON THE SHAPE OF OVERVOLTAGE CURRENT PULSE IN REAL CONDITIONS

Vladimír Madola, Dušan Marko, Vladimír Cviklovič, Ondrej Lukáč

Department of Electrical Engineering, Automation and Informatics, Faculty of Engineering, Slovak University of Agriculture in Nitra, Tr. Andreja Hlinku 2, 949 76, Nitra, Slovakia, xmadolav@uniag.sk

For economic reasons, we try to minimize the effects of atmospheric surges. When developing and testing surge protectors, it is necessary to expose them to energy effects that can be compared to real overvoltage. When simulating the effects of overvoltage, a capacitive generator is most often used to generate a current pulse. We created a simulation of a current pulse, the characteristics of which we obtained experimentally. When simulating the dynamic system, we aimed to identify the possible cause of model errors. We statistically proved a significant role of the variation of the self-inductance in the transition of shock pulses through the circuit. We performed all simulations in the Matlab & Simulink environment.

Key words: dynamic system, overvoltage, current pulse, simulation, measurement error

INTRODUCTION

The phenomenon of electrical overvoltage is the subject of intensive research. Technical experience knows the mathematical approximation of shapes surge pulses in current or voltage expressions at the time. In the technical conditions, generators are used to generate simulated overvoltage pulses, which are realized in the form of a capacitive battery with specific impedance (Wadhwa, 2007; Sheeba et al., 2012; Yebenbay et al., 2019).
The aim of the paper is to point out the influence of the inductance of the shaping impedance on the time parameters of the current pulse of the form 10/350 μs. The results will be obtained by simulating the calculated dynamic system and are compared with the experimental data measured on real device.

MATERIAL AND METHODS

We simulated the overvoltage current pulse according to the characteristics found on the selected device. We used a current pulse generator working on the capacitive principle. The function of the test pulse can be described analytically in general form (Eq. 1):

$$i(t) = \frac{I_m}{k} \cdot \left(e^{-\frac{t}{\tau_1}} - e^{-\frac{t}{\tau_2}}\right) \tag{1}$$

where i (t) – current function with time dependence [A],
k – wave shape factor [-],
t – time [s],
τ_1 – time constant of function fall [s],
τ_2 – time constant of function rise [s].

An analogy with the Rule 5τ can be used to derive time constants. We used dynamic system with electric capacity C ≈ 414 μF. The shape impedance was described by real part of impedance R = 1.10 Ω and self-inductance on idle state L = 3.00 μH calculated analytically. The dynamic system, which we used for experiment, was linear dynamic system 2nd order. It is possible describe by linear differential equation 2nd order with constant coefficients. Statistical investigation was performed by use Normal distribution with Student's critical quantiles and standard characteristics of variability.

RESULTS

After performing the measurements, we statistically evaluated the average front and tail time of the current function with a current pulse. Front time (time to reach first maximum from zero) was on average 65.00 μs (± 5.00 μs standard error of arithmetic mean). Tail time (time to reach one half from maximum value in negative derivative) was on average 350.00 μs (± 5.77 μs standard error of arithmetic mean). The current function with a complex variable was simulated in Matlab & Simulink. We prepare the function analytically using the Norton theorem on a complex RLC serial circuit. The current function equation before inductance correction (Eq. 2) showed a 76.67 % relative error at the front time compared to the experiment.

$$i(s) = \frac{1}{s} \cdot \frac{3.11 \cdot s}{1242 \cdot 10^{-12} \cdot s^2 + 455.4 \cdot 10^{-6} \cdot s + 1} \qquad (2)$$

The time constants of the experimental course were determined by the Euler method (τ_1 = 490.50 μs; τ_2 = 13.00 μs). By decomposition into partial fractions of equation (Eq. 2), we determined analytically the substitution inductance L = 15.40 μH. The simulation of the current function with the substitution inductance showed a relative error of 16.67 % determined on front time with comparison to experiment. Difference between idle self-induction and substitution inductance was 413.33 %.

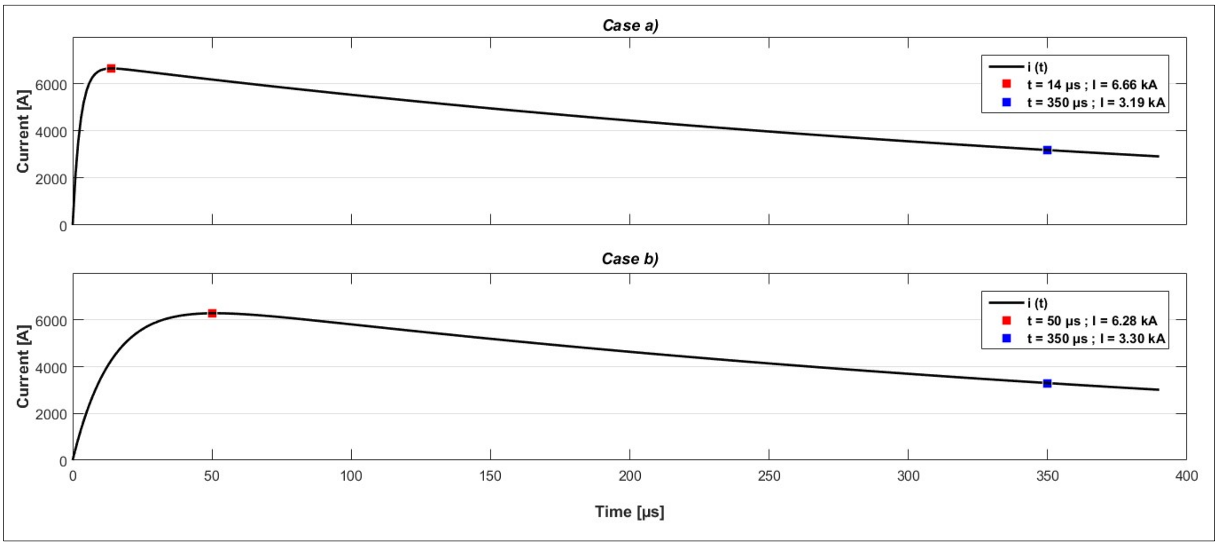

Fig. 1. Simulated complex functions of current pulses

At the significance level α = 0.05 we demonstrated an insignificant difference between the simulation and the experiment using substitution inductance. In Figure 1, Case a) showed the simulation of the current pulse without use the inductance correction (Eq. 2). Case b) is result from simulation with substitution inductance.

CONCLUSION

The paper aims to point out the issue of inductive phenomena in simulating overvoltage. The real effects of inductance were statistically determined at the level of significance (α = 0.05). The effect of the error by an unadjusted calculation results in a time deformation of the current course. The results can be interpreted to correct the ideal case in the mathematical simulation of overvoltage in time by substitution expression of complex impedance. From a physical point of view, a given dynamic system is described by a second-order transient phenomena.

The experimental measurements were created with cooperation with KIWA sk company during elaboration of thesis "Analysis of construct aspects of surge protective devices".

LITERATURE

GONOS, I. F., LEONTIDES, N., TOPALIS, F. V., STATHOPULOS, I. A. 2002. Analysis and design of an impulse current generator. *WSEAS Transactions on Circuits and Systems,* pp. 38 – 43. ISSN 1109-2734. [online] [cit. 2021-05-02]. Available in: <https://www.researchgate.net/publication/236855552>.

MADOLA, V. 2020. *Analysis of construct aspects of surge protective devices.* Diploma thesis. Nitra: SPU, 126 pp. (In Slovak: Analýza konštrukčných aspektov prepäťových ochrán).

SHEEBA, R., JAYARAJU, M., SHANAVAS, T. K. N. 2012. Simulation of Impulse Voltage Generator and Impulse Testing of Insulator using MATLAB Simulink. *World Journal of Modelling and Simulation,* vol. 8, no. 4, pp. 302 – 309. ISSN 1746-7233.

WADHWA, C. L., 2007. High voltage engineering. New Delhi: New Age International, 312 pp. ISBN 9788122423235.

YEBENBAY, Y., BAIGURMANOV, A., ALIMKHAN, A. 2019. Design and simulation of automatic surge generator. 6 pp. [online] [cit. 2021-05-01]. Available on: <https://www.researchgate.net/publication/332015358_Design_and_Simulation_of_Automatic_Surge_Generator>.

Corresponding author:
Ing. Vladimír Madola, tel. 037 / 641 47 23, e – mail: xmadolav@uniag.sk

COMPILATION METHODOLOGY OF EXPERIMENTAL MEASUREMENTS CHIPLESS CUTTING WOOD

Ján Melicherčík, Jozef Krilek, Ján Kováč, Tomáš Kuvik, Pavol Harvánek

Technical university in Zvolen, Faculty of technology, T.G. Masaryka 24, 960 01 Zvolen, xmelichercikj@is.tuzvo.sk

The paper focuses on the issue of primary wood processing in forestry. The solved problem is focused on the design of the methodology of experimental measurements of chipless wood cutting. The basic information in compiling the methodology was based on previous research and professional contributions, where the authors focused on the research of cutting tools – delimbing knife. The methodology is focused on laboratory measurements, which are performed on a special experimental device. The output parameters of the device correspond to the technical parameters of forest machines.

Key words: delimbing knife, harvester, cutting wood, harvester head

INTRODUCTION

Processing wood in forestry is greatly influenced by the development of machinery and equipment, the progress of which increases the efficiency of the process and reduces the economic costs of operation. Reducing the energy and material demands of wood processing, high reliability of machines and the incorporation of automation into this activity forces us to engage in research of the theoretical foundations of the use of forest technology in forestry (Dvořák et al. 2012). Automation and development of technology and technology is constantly developing a newer and more modern range of machines, while the processing time of wood is much faster and better. Productivity studies of mining equipment have been performed in many countries around the world, which have lasted for more than 25 years. These studies have shown that many factors affect the productivity of individual machines (Hiesl et.al., 2013).

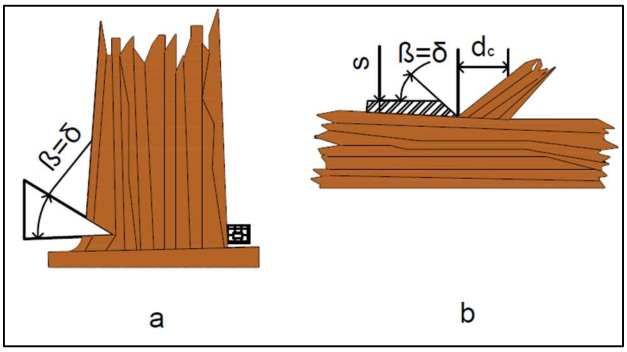

Fig. 2 a) cutting wood with a wedge knife, b) branching wood with a flat knife (Krilek et. al., 2018)

MATERIAL AND METHODS

The measurement will consist of a laboratory part, in which a jig will be used to attach a strain gauge force sensor to the experimental equipment and delimbing knives with different materials and different geometries.

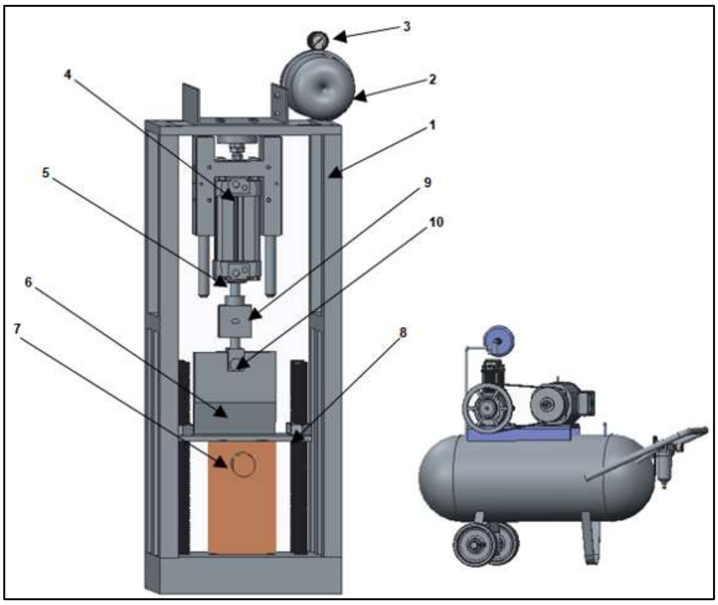

Fig. 2 Experimental equipment for chipless wood cutting

The experimental equipment is constructed of profiled steel and shaped elements by means of welded joints. The device has dimensions of 1404 x 500 mm, the branching knife is 400 mm away from the sample material. In the upper part of the stand there is an air tank, (2) which includes a barometer (3), on which I monitor the air pressure. A pneumatic double-acting cylinder (4) with parameters according to ISO 6431 is fastened by means of a screw connection. The strain gauge pressure and tension sensor HBM S9 (9) is placed on the piston rod (5) of the cylinder by means of the designed fastening jigs (10). The sensor is powered by connecting cables to the Quantum MX 840 measuring unit, which is an 8-channel measuring control panel. The advantage of the measuring unit is compatibility with HBM devices. The cutting device consists of a flat branching knife (6), which is located on the piston rod and is detected by a pin. After the piston rod is extended, the knife moves towards the wood sample (7), while there is a transverse division of the wood - delimbing. The course of measurements of the laboratory part will be realized on a flat delimbing knife, which is suitable for application to our experimental equipment. Its dimensions, shape and geometry are not real compared to the pruning knife of the harvester pruning head.

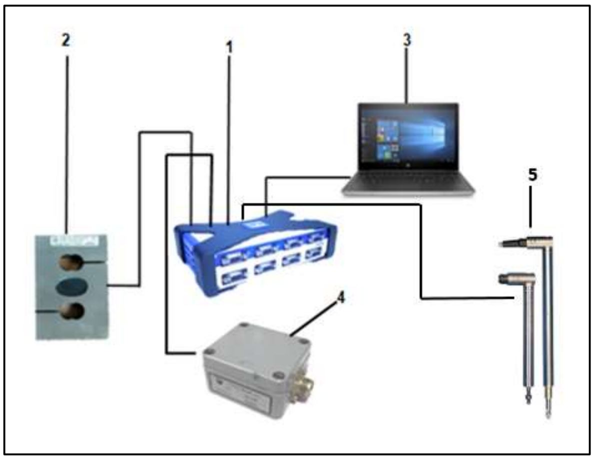

Fig. 3 Measuring chain diagram

1- Quantum MX 840 measuring control panel, 2 - strain gauge strain and pressure sensor HBM S9M 20kN, 3 - PC with evaluation software, 4-axis acceleration sensor SAI / L

Laboratory measurements will be performed according to the proposed measurement chain (Fig. 3). At the beginning of the experiment, the cutting speed during delimbing is determined using a uniaxial capacitive acceleration sensor. The cutting forces required for cutting wood will be measured using the HBM S9M sensor and recorded with the Quantum MX 840 measuring units. The delimbing knives with which the experiment will be carried out are made of the material STN 19 083, whose angular geometry is according to the parameters given in Table 1. On the delimbing knives, wear will be observed after delimbing of 100 pieces of sample material from selected wood diameters. During the measurements, 2 types of sample material of spruce and Scots pine will be changed. We will determine the moisture content of the wood by the gravimetric method. From the initial measurements, we determine the most suitable angular geometry of the knife and then 3 delimbing knives will be made of stainless steel.

Delimbing knife on experimental equipment

Its operating costs are much lower. From research at the department (Mikleš, M., 2009) and from foreign analyzes (Leonov, 1990, Voronicyn and Guglev, 1989), an analysis was developed in which the parameters for wood division - branching were determined. Based on these studies and analyzes of Krilek et al. (2018) at the department, it was found that the greatest influence on the cutting resistance when it penetrates into the wood has the thickness of the branching knife. Based on this, flat delimbing knives were made (Fig. 4). Parameters of the pruning knife are given in Table 1.

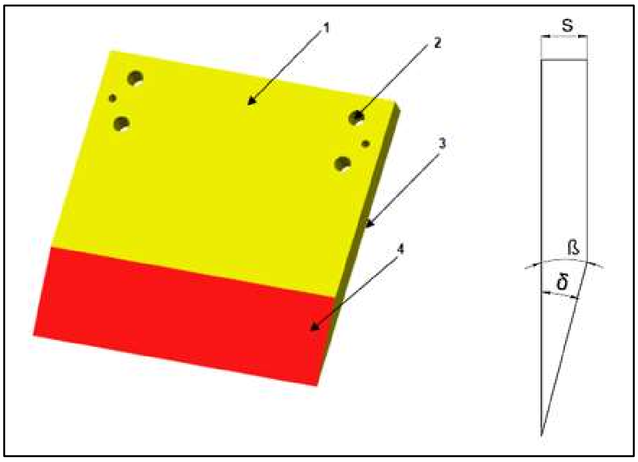

Fig. 3 Model and geometry of a branching knife on an experimental device

Table 3 Technical parameters of selected branching knives STN 19 083 (Krilek et.al., 2018)

Nr.	δ (°)	α (°)	s(mm)	ρ - cutting edge radius (mm)
1	20	7	15	0,012-0,025
2	15	4	15	0,012-0,025
3	20	4	15	0,012-0,025

RESULTS

The aim of the paper is to determine the influence of selected factors (cutting force, cutting speed, wear of pruning knives and their service life) in the process of chipless wood division - pruning on the basis of experimental measurements. Based on the processing and evaluation of the measured data, determine the weight of the influence of factors on the wear of the delimbing knife, with respect to the type of material and geometry according to which the knife will be manufactured and tested on experimental delimbing equipment.

CONCLUSION

The current situation in LH largely requires the use of multi-purpose forestry harvester machines in wood processing. Harvesters were used in countries with high wood production (Canada, Sweden, Finland), but over time they also reached Slovakia. In the end, this work determines the methodology of solving the dissertation with a description of laboratory measurements on experimental equipment. Based on research and theoretical knowledge, the cutting force and cutting speed will be evaluated in the branching process on the proposed experimental equipment. Delimbing knives of different geometries and different materials will be used in these measurements. In terms of cutting tool life t. j.

We will determine the wear of the pruning knife by the contact non-destructive method, in which the cutting edge and the radius of the cutting edge are observed.

The authors are grateful for the support of the Scientific Grant Agency of the Ministry of Education, Science, Research, and Sport of the Slovak Republic, project: VEGA 1/0609/20" Research of the cutting tools at the dendromass processing in agricultural and forestry production."

This publication is the result of the project implementation:Progressive Research into Utility Properties of Materials and Products Based on Wood (LignoPro), ITMS 313011T720 supported by the Operational Programme Integrated Infrastructure (OPII) funded by the ERDF."

LITERATURE

DVOŘÁK, J., NATOV, P., HRÍB, M., NATOVÁ, L., HOŠKOVÁ, P., BYSTRICKÝ, R., KOVÁČ, J., KRILEK, J.,LIESKOVSKÝ, M. 2012. Využití harvestorových technológií v hospodářských lesích. Kostelec nad Černými lesy,2012. ISBN 978-80-7548-028-4

HATTON, B.; POT, G.; BOUZGARROU, B. CH.; GAGNOL, V.; GOGU, G. 2015. Experimental determination of delimbing forces and deformations in hardwood harvesting, Croatian journal of forest engineering. ISSN 1845-5719, 2015, vol. 36, no. 1, pp. 43-53.

HIESL, P.,WARING, TM., BENJAMIN, JG. 2015. The effect of hardwood component on grapple skidder and stroke delimber idle time and productivity – An agent based model, Kidlington, Oxford ox5 1gb, oxon, England, Computers and Electronics in Agriculture 118 (2015) s. 270–280

KRILEK, J., KOVÁČ. J., DVOŘÁK, J., MIKLEŠ, J. 2018. Výskum rezných mechanizmov v lesníctve. Zvolen : Vedecká monografia. Technická univerzita vo Zvolene.ISBN 978-80-228-3056-0

LEONOV, A., L. 1990. Matematičeskaja model optimalizácii parametrov mechanizma prižima sučkoreznogo noža. IVUZ Lesnoj žurnal, č. 2, Archangelsk, 1990, s. 52 – 56.

MIKLEŠ, M. 2009. Štúdium geometrie nožov odvetvovacej hlavice. Acta Facultatis Technicae, XIV , 2009 (2) : p. 121 – 129, ISSN 1136 – 4472

MIKLEŠ, J., MIKLEŠ, M. 2015. Určenie technických parametrov odvetvovacej hlavice z hľadiska tvaru a počtu nožov : Determination of the technical parameters of delimbing head the viewpoint of their number and their shape. *Acta facultatis technicae*: vedecký časopis Fakulty enviormentálnej a výrobnej techniky. Zvolen:Technická univerzita vo Zvolene,2015,20(2),97-108. ISSN 1336-4472

PATHAK, A.D., WARHANE, R.S.,DEOKAR, S.U. 2017. Optimization of cutting parameters in Dry Turning of AISI A2 Tool Steel using Carbide Tool by Taguchi Based Fuzzy Logics. ScienceDirect- Material Today: Proceedings 5 (2018) ISSN 5082- 5090

SUCHÁNEK, J., 2009. Abrazivní opotřebení kovových materiálů. 2009. [online], [cit. 05. 12. 2017]. Dostupné na internete: <http://www.tribotechnika.sk/>

VORONICYN, K. I., GUGELEV, S. M. 1989 Mašinnaja obrezka sučjev na lesoseke. Lesnaja promyšlennosť, 1989, 272 s.

WATSON W.F., TWADDLE AA., HUDSCON JB., 2013 Review of Chain Flail Delimbing-Debarking, Forest Research Institute Rotorua, New Zealand, J. B. Hudson University of Aberdeen Aberdeen, Scotland, Journal of Forest Engineerin,2013

Corresponding author:
Ing. Ján Melicherčík, PhD, Fakulta techniky, Katedra environmentálnej a lesníckej techniky, Študentská 26, Zvolen 960 01, janmelichercik88@gmail.com

ANALYSIS OF HYDROGENATED VEGETABLE OIL INJECTION USING A HIGH-SPEED CAMERA

Jaroslav Mrázek, Jakub Čedík, Martin Pexa, Michal Holubek

Department for Quality and Dependability of Machines Czech University of Life Sciences Prague, Faculty of Engineering, Kamýcká 129, 165 21, Prague 6, Czech Republic, mrazekjaroslav@tf.czu.cz

One of the biofuels that have the potential to replace fossil fuels as internal combustion engine propulsion is hydrogenated oil (HVO). Hydrogenated oil has parameters that are close to diesel, yet they are not the same. Different parameters include, for example, the viscosity and density of the fuel, which will affect the way the fuel is sprayed in the combustion chamber and thus also the operating parameters of the engine. The paper focuses on the analysis of HVO spraying at different levels of concentration (HVO_5, HVO_10 and HVO_100). For comparison, a spray of standard diesel (D100) was used as a standard. A high-speed camera was used to obtain data, and the subsequent analysis dealt with the maximum width of the sprayed cone, the spray angle, the aerosol propagation rate and its acceleration.

Key words: Biofuel, HVO (hydrogenated vegetable oil), Injection, High-speed camera

INTRODUCTION

Vegetable oils are a raw material for the production of biofuels used as alternative fuels (Čedík et al. 2018, Elango and Senthilkumar 2011, Esteban et al. 2012). In the form of biodiesel, they are the dominant biofuel used to power diesel engines (Pechout et al. 2019, Sondors et al. 2019). Much better quality diesel fuel than conventional biodiesel can be produced from vegetable oils by their hydrogenation.

HVO as a possible alternative fuel for engines has shown excellent combustion and emission characteristics in many studies (Birzietis et al. 2017, Bohl et al. 2018, Bortel et al. 2019, Heikkilä et al. 2012, Omari et al. 2017). It can be produced from various sources - such as waste oil, rapeseed oil or palm oil and animal fat (Soam and Hillman 2019, Zeman et al. 2019). A study (Vojtíšek-Lom 2018) reported that cold starts led to an increase in the concentration of particulates and bound organic compounds in emissions of approximately 15% compared to warm starts.

More than 60% of the raw material of waste character = 2nd generation biofuels are used for the production of HVO. Compared to biodiesel, HVO has the advantage as a fuel of its hydrocarbon nature. HVO is materially compatible with the fuel system and is characterized by good oxidative stability (Krivopolianskij et al. 2019, Pexa et al. 2014, Rodríguez-Fernández and Sánchez-Valdepeñas 2017, Sunde et al. 2011). HVO has some better properties than diesel (sulfur content, cetane number, low aromatic hydrocarbons). HVO can be added to diesel in any amount. The relatively low HVO density reduces the density of the blended fuel (at 30% by volume of HVO in diesel, the density approaches the lower limit (EN-590)). At the same time, at 30% of the HVO content in the fuel, an increase in the cetane number of up to 10 units can be expected (Gailis et al. 2017, Pechout and Macoun 2019, Sondors et al. 2019, Suarez-Bertoa et al. 2019).

The aim of this research was to obtain data on the spraying of HVO at different levels of concentration (HVO_5, HVO_10 and HVO_100) and then compare it with the spraying of standard diesel (D100).

MATERIAL AND METHODS

The evaluation of the spray was performed on the basis of the recording from the speed camera. Shooting was carried out with a high-speed camera Photron Fasctam NOVA S9. The frame rate was selected at 15,000 frames per second. In addition to the mentioned fuel mixtures HVO_5 and HVO_10 and reference fuel D100, pure HVO (HVO_100) was also used to evaluate the influence of fuel on its spray.

Regarding the spray itself, 4 criteria were evaluated for each fuel - the maximum width of the sprayed cone, the spray angle, aerosol spread rate and acceleration. To measure the width and angle of the spray, 10 measuring points were determined from the beginning of the injection to the end. The speed of the fuel sprayed was measured from the start of the spray to the edge of the camera so that 10 measuring points were determined again and the distance by which the aerosol changed its position for a given number of images was measured using the distance measurement function in the program.

RESULTS

The HVO_5 and HVO_10 fuel blends have shown very similar widths for most of the time. HVO_100 fuel, on the other hand, showed a significantly lower width, which may be associated with higher viscosity and poorer evaporation capacity of HVO. In terms of the maximum achieved width values, a decrease of 18.4% was recorded for HVO_5, 4.1% for HVO_10 and 21.2% for HVO_100.

Achieved spray angle for all tested fuels shows, that both mixed fuels and HVO fuel showed a significantly smaller spray angle than the reference fuel D100. This may again be due to the higher viscosity of blended fuels compared to D100. Compared to D100 fuel, the HVO_5 fuel mixture showed a decrease in the spray angle by 23.8%, HVO_10 by 19.6% and HVO_100 fuel by 28%.

The spray rate of the aerosol for all fuels is shows that the velocity over time is very similar for all fuels, especially for fuels containing HVO (HVO_5, HVO_10 and HVO_100). For the D100 fuel, a lower increase in speed is seen in the second phase, following the initial opening of the nozzle. The maximum achieved aerosol spread rate was thus higher for HVO_5 fuel by 10.6%, for HVO_10 fuel by 5.1% and HVO_100 by 18%.

Aerosol itself can be only slow down after leaving the nozzle due to the resistance of the environment. The maximum acceleration achieved was 12.4% higher for HVO_5 fuel, 4.9% higher for HVO_10 fuel and 3.3% higher for HVO_100 compared to D100. In contrast, in terms of maximum deceleration, fuels showed significantly higher differences, for HVO_5 fuel it was higher by 51.4%, for HVO_10 fuel by 22.9% and HVO_100 by 77.1%. For each fuel, 6 images were selected to capture the course of the injection and one image as the initial one before the start of the injection. The time interval between the displayed images is approximately 0.0004 s. The images show the gradual propagation of the sprayed fuel away from the nozzle and the last 2-3 images already show the entire fuel spray cone. These images were also used to evaluate the spray angle and the maximum width of the fuel spray cone, to evaluate the speed and acceleration it was necessary to use images with a shorter time interval (approximately half), this section always captures the first 4-5 images.

CONCLUSION

The paper evaluated the spraying of hydrogenated oil in various concentrations with diesel fuel (5, 10 and 100%). Pure diesel was used as a benchmark.

- The HVO_5 and HVO_10 fuel blends showed a very similar width most of the time. HVO_100 fuel, on the other hand, showed a significantly lower width, which may be associated with higher viscosity and poorer evaporation capacity of HVO (HVO_5 by 18.4%, HVO_10 by 4.1% and HVO_100 by 21.2%).

- Both mixed fuels and HVO fuel showed a significantly smaller spray angle than the reference fuel D100 (HVO_5 by 23.8%, HVO_10 by 19.6% and HVO_100 by 28%).

- The course of the spray cone propagation rate is very similar for all fuels, especially for fuels containing HVO (HVO_5, HVO_10 and HVO_100). For fuel D100, a lower increase in speed is seen in the second phase, following the initial opening of the nozzle (HVO_5 by 10.6%, HVO_10 5.1% and HVO_100 by 18%).

The analysis of fuel spraying showed mainly the effect of higher viscosity of blended fuels and pure HVO, which is evidenced mainly by the lower measured width of the sprayed aerosol cone and the smaller spray angle compared to D100 fuel.

This research was funded by Internal Grant Agency of Czech University of Life Sciences Prague, Faculty of Engineering - IGA CULS - 2020: 31190/1312/3111.

LITERATURE

BIRZIETIS, G., PIRS, V., DUKULIS, I., GAILIS, M. 2017. Effect of commercial diesel fuel and hydrotreated vegetable oil blend on automobile performance. Agronomy Research, 15(S1), 964–970.

BOHL, T., SMALLBONE, A., TIAN, G., ROSKILLY, A. P. 2018. Particulate number and NOx trade-off comparisons between HVO and mineral diesel in HD applications. Fuel 215, 90-101.

BORTEL, I., VÁVRA, J., TAKÁTS, M. 2019. Effect of HVO fuel mixtures on emissions and performance of a passenger car size diesel engine. Renewable Energy 140(September), 680-691.

ČEDÍK, J., PEXA, M., PETERKA, B., HOLŮBEK, M., MADER, D. AND PRAŽAN, R. 2018. Effect of biobutanol-sunflower oil-diesel fuel blends on combustion characteristics of compression ignition engine. Acta Technologica Agriculturae, 4, 133–138.

ELANGO, T., SENTHILKUMAR, T. 2011. Performance and emission characteristics of CI engine fuelled with non edible vegetable oil and diesel blends. Journal of Engineering Science and Technology 6(2), 252–262.

ESTEBAN, B., RIBA, J.-R., BAQUERO, G., RIUS, A., PUIG, R. 2012. Temperature dependence of density and viscosity of vegetable oils. Biomass and Bioenergy 42, 164–171.

GAILIS, M., RUDZITIS, J., KREICBERGS, J., ZALCMANIS, G. 2017. Experimental analysis of hydrotreated vegetable oil (HVO) and commercial diesel fuel blend characteristics using modified CFR engine. Agronomy Research 15(4), 1582–1601.

HEIKKILÄ, J., HAPPONEN, M., MURTONEN, T., LEHTO, K., SARJOVAARA, T., LARMI, M., KESKINEN, J., VIRTANEN, A. 2012. Study of miller timing on exhaust emissions of a hydrotreated vegetable oil (HVO)-fueled diesel engine. Journal of the Air and Waste Management Association 62(11), 1305-1312.

KRIVOPOLIANSKII, V., BJØRGEN, K. O. P., EMBERSON, D., USHAKOV, S., ÆSØY, V., LØVÅS, T. 2019. Experimental study of ignition delay, combustion, and NO emission characteristics of hydrogenated vegetable oil. SAE International Journal of Fuels and Lubricants 12(1).

OMARI, A., PISCHINGER, S., BHARDWAJ, O. P., HOLDERBAUM, B., NUOTTIMÄKI, J., HONKANEN, M. 2017. Improving engine efficiency and emission reduction potential of HVO by fuel-specific engine calibration in modern passenger car diesel applications. SAE International Journal of Fuels and Lubricants 10(3).

PECHOUT, M., MACOUN, D. 2019. Experimental investigation of combustion timing of HVO, RME and diesel fuel in a Euro6 car engine during transient driving cycles. SAE Technical Papers 2019(September).

PECHOUT, M., KOTEK, M., JINDRA, P., MACOUN, D., HART, J., VOJTISEK-LOM, M. 2019. Comparison of hydrogenated vegetable oil and biodiesel effects on combustion, unregulated and regulated gaseous pollutants and DPF regeneration procedure in a Euro6 car. Science of the Total Environment 696, article no. 133748.

PEXA, M., MAŘÍK, J., ČEDÍK, J., ALEŠ, Z., VALÁŠEK, P. 2014. Mixture of oil and diesel as fuel for internal combustion engine. In: 2nd International Conference on Materials, Transportation and Environmental Engineering. CMTEE, Kunming, 1197–1200

RODRÍGUEZ-FERNÁNDEZ, J., LAPUERTA, M., SÁNCHEZ-VALDEPEÑAS, J. 2017. Regeneration of diesel particulate filters: Effect of renewable fuels. Renewable Energy 104(April), 30-39.

SOAM, S., HILLMAN, K. 2019. Factors influencing the environmental sustainability and growth of hydrotreated vegetable oil (HVO) in sweden. Bioresource Technology Reports 7(September).

SONDORS, K., BIRKAVS, A., PIRS, V., BIRZIETIS, G., DUKULIS, I. 2019. Comparison of vehicle performance using fossil diesel fuel blends with biodiesel and HVO fuel. Paper presented at the Engineering for Rural Development 18, 964-970.

SUAREZ-BERTOA, R., KOUSOULIDOU, M., CLAIROTTE, M., GIECHASKIEL, B., NUOTTIMÄKI, J., SARJOVAARA, T., LONZA, L. 2019. Impact of HVO blends on modern diesel passenger cars emissions during real world operation. Fuel 235(January), 1427-1435.

SUNDE, K., BREKKE, A., SOLBERG, B. 2011. Environmental impacts and costs of hydrotreated vegetable oils, transesterified lipids andwoody BTL-A review. Energies, 4(6), 845-877.

VOJTÍŠEK-LOM, M., BERÁNEK, V., MIKUŠKA, P., KŘŮMAL, K., COUFALÍK, P., SIKOROVÁ, J., TOPINKA, J. 2017. Blends of butanol and hydrotreated vegetable oils as drop-in replacement for diesel engines: Effects on combustion and emissions. Fuel 197, 407-421.

ZEMAN, P., HÖNIG, V., KOTEK, M., TÁBORSKÝ, J., OBERGRUBER, M., MAŘÍK, J., HARTOVÁ, V. PECHOUT, M. 2019. Hydrotreated vegetable oil as a fuel from waste materials. Catalysts 9(4), article no. 337.

Corresponding author:
Jaroslav Mrázek, phone +420 605 025 914, e-mail: mrazekjaroslav@tf.czu.cz

PRETREATMENT OF THE STEEL SURFACE FOR POWDER COATING

Michal Neškudla

Department of Technological Equipment of Buildings, Czech University of Life Sciences Prague, Prague, Czech Republic, neskudla@tf.czu.cz

This article is about pretreatment of the steel surface for a better adhesion of powder coating. Different level of pretreatment were used and the score of final painted parts were compared each other. The grid method showed that the final outcome is strongly affected by the diverse types of pretreatment methods.

Key words: powder coating, pretreatment, surface, blasting, degreasing, grid method

INTRODUCTION

Electrostatic application of plastics is a widely used surface treatment of parts made of various materials worldwide. Powder coating is mainly used for steel components that are exposed to corrosive or otherwise degrading environments (Frey and Hamid 2015). Powder coatings are valued not only for their final aesthetic appearance, but also for their protective properties, which increase the life of products, affect their functionality.

MATERIAL AND METHODS

In this experiment a steel sheets of 50cm x 50cm were used to find out the affection of different pretreatment methods for the adhesion of painted on the final product. There were 4 different level of pretreatment – without any, mechanical, chemical and mechanical plus chemical.

RESULTS

Forty different measurements were carried out to find out the significancy of pretreament to the quality of final product. 10 measurements were carried out without any pretreatment, 10 with blasting only, 10 with degreasing only and 10 with blasting and degreasing subsequently.

Sand blasting

It is visible that blasting time affects some of evaluation test but not necessary all of them. Grid method reports very bad figures 5 without any blasting, much better of 1 with two or fifteen minutes and the best of 0 with five minutes. Powder with is absolutely independent from blasting time at all. Aesthetical test showed bad figures of around 3,5 in zero and fifteen blasting time together with an excellent 0 in two and five minutes. The measured figures are in accordance with an assumption.

CONCLUSION

There is a strong connectivity between the pretreatment and the quality of the final painted product. Mechanical pretreatment only is far better that nothing and slightly worse than the chemical one. Combination of mechanical and chemical pretreatment showed the best option and secured almost flawless results.

Powder width is not affected by time blasting whilst optimal time blasting of 5 minutes secures the best outcome as of grid method and aesthetical test. The longer time blasting the better outcome does not apply.

LITERATURE

FREY, H. and HAMID, R. K. 2015. Handbook of thin-film technology. Berlin:Springer, 2015, xiiii, 379 stran: ilustrace. ISBN 978-3-642-05429-7

Corresponding author:

Ing. Michal Neškudla, Department of Technological Equimpent of Buildings, Faculty of Engineering, Czech University of Life Sciences Prague, Kamýcká 129, Praha 6, Prague, 16521, Czech Republic, email: neskudla@tf.czu.cz

VERIFICATION OF DECLARED DRIVING CHARACTERISTICS OF ELECTRIC VEHICLES IN REAL OPERATION

Štěpán Pícha, Veronika Štekerová, Martin Kotek, Veronika Hartová

Department of Vehicles and Ground Transport, Faculty of Engineering, Czech University of Life Sciences Prague, Kamýcká 129, Praha 6, Prague 16521, Prague, Czech Republic, pichas@tf.czu.cz

This paper is focused on the selected electric vehicles and their driving parameters. Each vehicle has the driving characteristics declared by the manufacturer. This paper tries to verify these declared driving parameters and draw conclusions from them. The selected vehicles drove the same predetermined route, which was 56,1 km long. The aim of this paper is to verify the operating parameters and driving characteristics of electric vehicles in real operation. The obtained data are used not only to verify the declared parameters of the manufacturer, but also to study factors that fundamentally affect these operating parameters.

Key words: electric vehicles, operating parameters, real range, recuperation

INTRODUCTION

The constantly increasing number of vehicles is causing problems all around the world, whether it is traffic congestion, parking or, last but not least, air pollution. The vast majority of today's car uses an internal combustion engine, either gasoline or diesel. It is these engines that cause air pollution and make human lives uncomfortable in large urban agglomerations, where tens of thousands of these engines can run at once. Furthermore, the impending shortage of fossil fuels, along with the increasing environmental pollution in recent years have led to fundamental changes in the development of the automotive industry. In everyday life, these changes can be felt mainly in the area of emission limits and the tightening of emission regulations for the entry of vehicles into selected cities. Exhaust emissions scandals have also played a role in short-term history, bringing with them, among other things, growing skepticism about internal combustion engines. Electromobility is currently considered to be an effective way to reduce the production of these harmful emissions from transport and thus prevent further environmental pollution and associated global warming (May 2017).

MATERIAL AND METHODS

The measurement of operating parameters of selected electric vehicles took place on a pre-selected route, which was completed by all vehicles. The measurement was performed using TEXA, Bosch or VAG-COM diagnostic devices, which communicated with the electric drive control unit during the measurement, from which instantaneous values of operating parameters were obtained (especially battery voltage and current, state of charge, electric motor speed, vehicle speed).

These values were continuously recorded and stored by the system. In addition, the vehicles were equipped with a device for tracking the current position using the Garmin GPS 18x USB navigation unit.

Electic vehicles

For the purpose of analyzing the operating parameters of electric vehicles, several electric vehicles were rented:

- BMW i3s
- Škoda CITIGOe iV
- Fiat 500e
- Volkswagen ID.3

Test route

The test route was based on the WLTP (World Harmonized Light-duty Procedure) vehicle type-approval regulation, in particular the RDE (Real Driving Emissions) part. The test route must include urban, extra-urban and motorway traffic according to precise specifications, which further define the achieved average speed, route elevation, route timing, climatic conditions and more. The total length of the route was 56.1 km. The proposed test route was always driven in both directions. The starting point for the start of the ride was the CULS TF workshops.

RESULTS

Table 2. summarizes the basic results of the performed experiments. The aim of the measurement was to verify the declared range of selected electric vehicles in real operation. During the measurement, it was not possible to establish communication between the vehicle control unit and the diagnostic device in some vehicles. Alternatively, the connection was not reliable and data was lost.

The average speed of vehicles was affected only by the immediate traffic situation, as the defensive driving style and compliance with traffic regulations. The achieved average speed of the tested vehicles ranges from 40 to 47 km/h and did not show significant fluctuations. In the case of the BMW i3s, the measured consumption value was by 0.8 kWh/100 km higher than declared. On the other hand, the Škoda CITIGOe iV and Fiat 500e showed lower electricity consumption. Analogic values were, in the case of the Škoda CITIGOe iV 2.2 kW/100 km and in the case of the Fiat 500e by up to 5.7 kWh/100 km. The highest electricity consumption was achieved by the VW ID3 vehicle, namely 22.4 kWh/100 km, ie 6.3 kWh/100 km - higher than the declared value.

Table 2 Basic summary results

	Declared energy consumption	**Average consumption during the test**	**The difference between declared consumption and measured consumption**	**Average speed**	**Date**	**Outside temperature**
Vehicle	kWh/100 km	kWh/100 km	kWh/100 km	km/h	-	°C
BMW i3s	13,1	13.9	0.8	46	13.01.2021	1
CITIGOe iV	14,8	12.6	2.2	42	14.10.2020	6.5
Fiat 500e	18	12.3	5.7	40	21.10.2020	12
VW ID3	16,1	22.4	6.3	47	11.02.2021	-10

CONCLUSION

As part of the verification of the declared parameters by the manufacturer, a total of 4 electric vehicles were tested, some even repeatedly (according to the immediate situation and availability of cars). For the time being, there is still the problem of complex sensing of the instantaneous operating parameters of the electric drive, or the electric vehicle as a whole.

Despite these difficulties, during the measurement it was confirmed that the data of the operating parameters of the vehicles, which are verified during the homologation procedure (according to the new WLTP methodology), correspond to real traffic. The general traffic that had led to lower average speed had reasonable effect on reduction of energy consumption how it can be seen on example of Fiat 500e. The instantaneous climatic conditions could be the explanation of higher energy consumption in the case of the VW ID3 and contemporary it was the biggest and the heaviest from tested vehicles.

Experiments have shown that the declared range of vehicles was in general verified in real traffic. Although, the real climatic conditions, traffic situation or driving style of the driver had additional significant effect.

The work was supported by the internal research project of Czech University of Life Sciences Prague of Faculty of Engineering IGA 2020:31150/1312/3102.

LITERATURE

[1] MAY, Nadine. Local environmental impact assessment as decision support for the introduction of electromobility in urban public transport systems. *Transportation Research Part D: Transport and Environment* [online]. 2017, **64**(July 2017), 192–203. ISSN 13619209. Dostupné z: doi:10.1016/j.trd.2017.07.010

MAY, N. 2017. Local environmental impact assessment as decision support for the introduction of electromobility in urban public transport systems. Transportation Research Part D: Transport and Environment [online]. 2017, 64(July 2017), 192–203. ISSN 13619209. Dostupné z: doi:10.1016/j.trd.2017.07.010

Corresponding author:
Ing. Štěpán Pícha, e-mail: pichas@tf.czu.cz

INFLUENCE OF DEFORMATION RATE ON THE STRENGTH OF POLYMER COMPOSITE MATERIAL WITH FILLER BASED ON WOOD POWDER INTENDED FOR ADDITIVE TECHNOLOGIES

Dominik Piš; Hana Pouzarová

[1]*Department of Material Science and Manufacturing Technology, Faculty of Engineering, Czech University of Life Sciences Prague, Kamycka 129, Prague 6 - Suchdol, 165 00 Prague, Czech Republic; pisd@tf.czu.cz, pouzarova@tf.czu.cz*

The article deals with the influence of the strain rate on the strength of a polymer composite material with a filler based on wood powder intended for additive technologies. The aim of the article is to compare the influence of the strain rate on the maximum stress and elongation of the composite material. The tensile test was performed on the universal testing machine LabTest 5.50ST type (LaborTech, Opava, Czech Republic) was performed for 6 different deformation speeds (1 mm / min, 2.5 mm / min, 5 mm / min, 10 mm / min, 15 mm / min and 20 mm / min). The maximum strength limit reached was 34.19 MPa at a strain rate of 20 mm / min and the minimum strength limit was 27.37 MPa at a strain rate of 1 mm / min. The maximum elongation was 4.35 mm at 1 mm / min and the minimum elongation was 2.55 mm at 20 mm / min. Significant porosity of the material was found by microscopic analysis of the ruptured material.

Keywords: 3D printing, strain rate, bio-composite, PLA, mechanical properties, tensile strength

INTRODUCTION

The market for polymer composites with wood-based fillers is growing, especially in the automotive and construction industries (Jeske et al. 2012). Wood particles for polymer composite are used mainly due to their low density, mechanical properties, ecological nature and low cost (Farsi 2010). Majority wood-based polymer composites are made from oil-based polymers, which include polyethylene, polyvinyl chloride, polypropylene and etc. (Friedrich 2018, Espert et al. 2004). Oil-based polymers are only partially biodegradable and difficult to recycle. With regard to the environment, efforts are being made to replace them with biopolymers (Spear et al. 2015, Robledo-Ortíz et al. 2021).

A very perspective biopolymer is polylactic acid (PLA) and polyhydroxybutyrate (PHB); both of these polymers are biodegradable (on an industrial scale) and used extensively in industry (Gue et al. 2018, Torres-Tello 2017). PLA is made from lactic acid monomer, which is obtained by fermentation of corn, potatoes or sugar beet. These are majority often the synthesis and polymerization of lactides (Briassoulis 2006, Zhang et al. 2017).

These biopolymers have some significant disadvantages, such as low resistance to higher temperatures and brittleness; the properties of these polymers can be modified by mixing them or by using different fillers

The growing market for biopolymers has made these polymers more availability, but they still have higher production costs than conventional polymers. Achieving lower end costs can be achieved by combining biopolymers with low-cost materials; such material may be wood particles (Petinakis et al. 2009).

The aim of the experiment was to compare the effect of material deformation rate on material strength and specific elongation in test specimens made of PLA with wood powder printed using FDM 3D printing technology.

MATERIAL AND METHODS

The test specimens are made of a filament of PLA polymer with 20% by weight of wood powder filler. The used filament was made by SUNLU INDUSTRIAL CO., LTD. The manufacturer does not state the origin, size of the wood filler, or whether the filler has been modified.

RESULT AND DISCUSSION

Figure 1 shows that the tensile strength has an increasing tendency with increasing strain rate of the tensile test. The maximum average stress achieved during the experiment was reached at a strain rate of 20 mm/min.

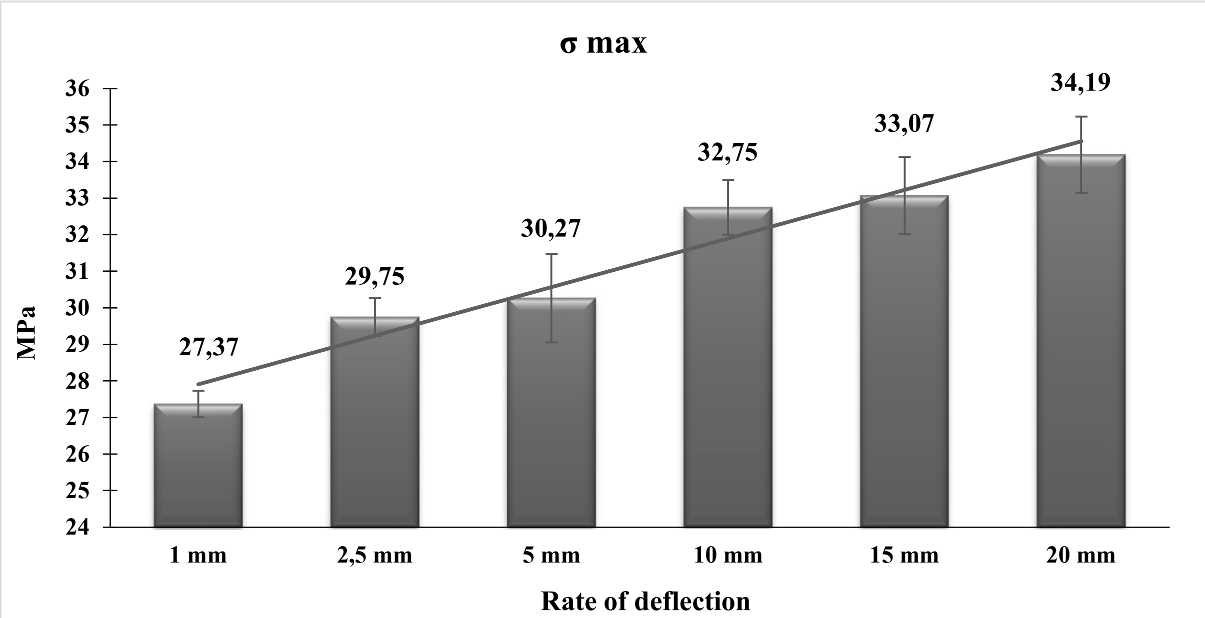

Fig. 1 Tensile strength

Figure 2 shows that the maximum elongation has a decreasing tendency with increasing strain rate of the tensile test. The maximum average elongation achieved during the experiment was reached at a strain rate of 1 mm/min.

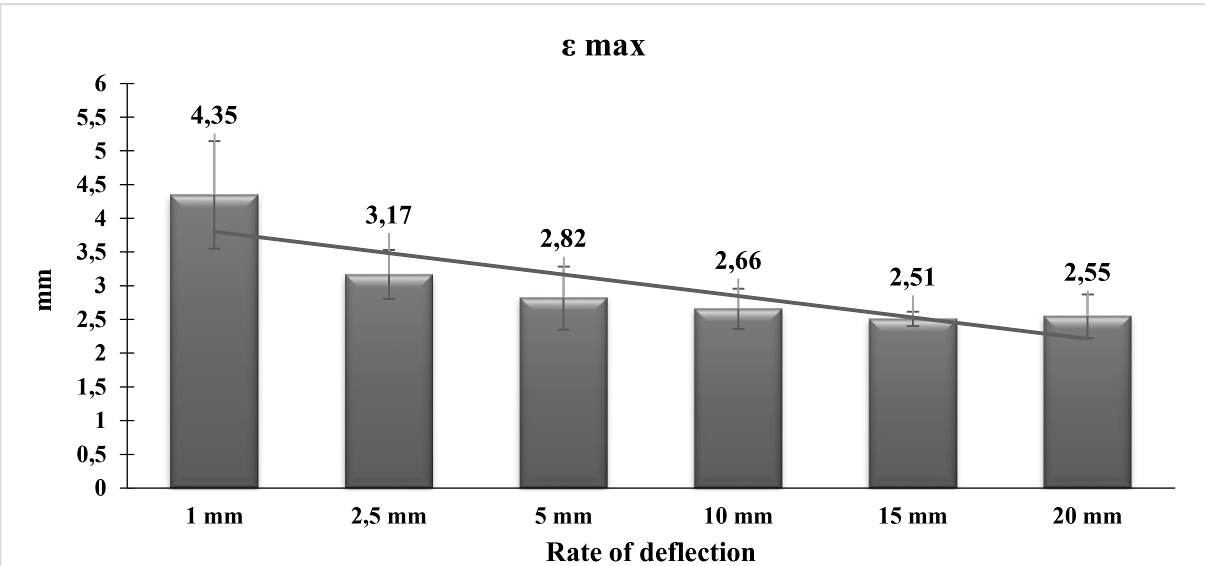

Fig. 2 Elongation

CONCLUSION

The aim of the article was to compare different strain rates for PLA test specimens with wood powder made by additive 3D printing technology. The results of the article show that the maximum stress of 34.19 MPa was reached at a speed of 20 mm/min. The maximum elongation of 4.35 mm was reached at a speed of 1 mm/min. The rate of deformation affects the maximum strength of the material and the elongation. The reduced strength of the material in 3D printing could be caused by air pores inside the material. These pores could have formed for various reasons.

ACKNOWLEDGMENT

Contribution has been prepared within the solving of scientific grant project IGA 2021:31140/1312/3115 "Degradation of polymer composite materials printed by 3D printing with cellulose-based fille

REFERENCES

JESKE, H., SHIRP, A. CORNELIUS, F. 2012 Development of a thermogravimetric analysis (tga) method for quantitative analysis of wood flour and polypropylene in wood plastic composites (wpc). *Thermochimica acta* 543, 165–171.

FARSI, M. 2010. Wood-plastic composites: influence of wood flour chemical modification on the mechanical performance. *Journal of reinforced plastics and composites*, 29(24), 3587–3592.

FRIEDRICH, D. 2018. Comparative study on artificial and natural weathering of wood-polymer compounds: a comprehensive literature review. *Case studies in construction materials*, 9, e00196.

ESPERT, A., VILAPLANA, F., KARLSSON, S. 2004. Comparison of water absorption in natural cellulosic fibres from wood and one-year crops in polypropylene composites and its influence on their mechanical properties. *Composites part a: applied science and manufacturing*, 35(11), 1267–1276.

SPEAR, M. J., EDER, A., CARUS, M. 2015. Wood polymer composites. In: *wood composites*. B.m.: Elsevier inc., 2015, s. 195–249. Isbn 9781782424772.

ROBLEDO-ORTÍZ, J. R., GONZÁLEZ-LÓPEZ, M. E., MARTÍN DEL CAMPO, A. S., PÉREZ-FONSECA A. A. 2021. Lignocellulosic materials as reinforcement of polyhydroxybutyrate and its copolymer with hydroxyvalerate: a review. B.m.: Springer.

GUO, R., REN, Z., BI, H., SONG, Y., XU, M. 2018. Effect of toughening agents on the properties of poplar wood flour/poly (lactic acid) composites fabricated with fused deposition modeling. *European polymer journal*, 107, 34–45.

TORRES-TELLO, E. V., ROBLEDO-ORTÍZ, R. R., GONZÁLEZ-GARCÍA, Y., PÉREZ-FONSECA, A. A., JASSO-GASTINEL, C. F., MENDIZÁBAL, E. 2017. Effect of agave fiber content in the thermal and mechanical properties of green composites based on polyhydroxybutyrate or poly(hydroxybutyrate-co-hydroxyvalerate). *Industrial crops and products*, 99, 117–125.

BRIASSOULIS, D. 2006. Mechanical behaviour of biodegradable agricultural films under real field conditions. *Polymer degradation and stability*, 91(6), 1256–1272.

ZHANG, L., LV, S., SUN, C., WAN, L., TAN, H., ZHANG, Y., 2017. Effect of mah-g-pla on the properties of wood fiber/polylactic acid composites. *Polymers*, 9(11), 591.

PETINAKIS, E., YU, L., EDWARD, G., DEAN, K., LIU, H., SCULLY, A. D. 2009. Effect of matrix-particle interfacial adhesion on the mechanical properties of poly(lactic acid)/wood-flour micro-composites. *Journal of polymers and the environment*, 17(2), 83–94.

Corresponding author:

Dominik Piš, pisd@tf.czu.cz

TECHNICAL SOLUTION OF FIRE-FIGHTING ADAPTER FOR FOREST FIRE PREVENTION

Matej Priatka[1], Michaela Hnilicová[2], Ivan Chromek[3], Richard Hnilica[4]

[1] Department of Forest Harvesting, Logistics and Ameliorations; Faculty of Forestry; Technical University in Zvolen; T.G. Masaryka 24, 960 01 Zvolen, Slovak Republic
[2] Department of Mechanics, Mechanical Engineering and Design; Faculty of Technology; Technical University in Zvolen; T.G. Masaryka 24, 960 01 Zvolen, Slovak Republic
[3] Department of Fire Protection; Faculty of Wood Sciences and Technology; Technical University in Zvolen; T. G. Masaryka 24, 960 53 Zvolen, Slovak Republic
[4] Department of Manufacturing Technology and Quality Management; Faculty of Technology; Technical University in Zvolen; T.G. Masaryka 24, 960 01 Zvolen, Slovak Republic

The forest wheeled skidder has been developed from its beginnings as a single-purpose machine for the needs of skidding in the forest. The paper deals with the analysis of input factors that predispose this type of construction to ensure the transport of water supply in case of fire brigades in forest fires. The input factors for the use of LKT mainly include analysis of the terrain, which is capable of this type of equipment to move, analyze the appropriateness of placing the adapter for the transport of water, the selection of appropriate materials, design and construction solutions. The aim of these analytical procedures is to conservation the original features and to extend the target use of special machines.

Key words: fire, forest wheeled skidder, adapter, slope gradient, forest

INTRODUCTION

Ongoing climate change and its consequences are often discussed in professional circles as the main cause of future increased frequency of natural disasters, including fires in the natural environment. Climate change affects forest fires directly through weather conditions, which influence the onset and spreading of fire, and indirectly through its impact on vegetation and combustible material. It is assumed that the risk of fire occurrence in Europe will increase with the most extreme fires occurring more frequently, which destroy vast areas and have long-term consequences. Results of studies on fires, which occurred in the European continent in the last 30 years, show an increase in the duration of a fire season and it is assumed that a fire regime will change almost everywhere across Europe. While the total area in the South European countries destroyed by fire is increasing each and every year, northern areas like Scandinavia are afflicted by unprecedented forest fires. Due to global warming and increasing aridity, the risk of increased frequency and extent of wildfires is very high. Many regions of the world have experienced an increasing trend of excessive wildfires and an increasing occurrence of extremely severe fires (FAO Fire management 2006). The total area of forest fires in the EU over the last 20 years has been around 8.7 million hectares, with an annual average of around 415,000 hectares. The most extensive fires were recorded in 2000, 2003, 2005, 2007, 2012 and 2017. The fires in these years were above the annual average. (San-Miguel-Ayanz et al. 2020) In 2017, wildfires burnt be around 1 million hectares of natural lands in the EU. The European Forest Fire Information System estimated the amount of fire-related losses to be around 10 billion Euros (San-Miguel-Ayanz et al. 2018).

Forest fires in Slovakia often occur in the areas inaccessible to fire-fighting machinery with insufficient or rather inadequate water supply for fire-fighting purposes. The facts provided above are based on statistically processed data on fire in state forests of the Slovak Republic in the last ten years. The results are presented in the Figures 1.

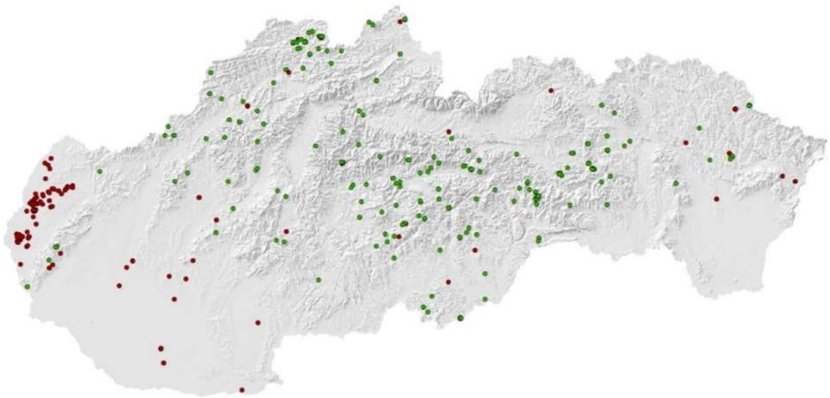

Fig. 1 Map of fires in forests of the Slovak Republic in 2010 – 2020, red marks - fires in the terrain with a slope until 16 %, green marks - fires in the terrain with a slope over 16 %

According to these results, there can be concluded that the greatest damage is caused by fires in the forests of the Slovak Republic at a slope gradient of 16 %. As a result, our research was aimed in this direction.

MATERIAL AND METHODS

The main task of LKT is to move wood from the forest to the place of further manipulation. In the case of a transport of an extinguishing agent, it is a change of the basic working algorithm. The space remains, the direction of movement changes only. For this reason, when considering how to use existing LKT for these purposes, the design of the fire-fighting adapter will be based on the following basic concepts of its use:

- the use of base machine (LKT) in the form of a pulling device to increase the CAS's accessibility – concept I,
- the use of base machine (LKT) as a pulling device for pulling a one-axle or two-axle trailer – concept II,
- the use of base machine (LKT) as a carrier for the transport of water (a special purpose machine) – concept III,
- the use of base machine (LKT) as a carrier for a removable water transport body – concept IV.

When designing an alternative location adapter (body) was based on two options. Design of a special platform for the rear axle LKT, or an adapter for the rear LKT shield. After considering all the pros and cons, the adapter was developed, using the rear LKT shield.

RESULTS AND DISCUSSION

The basic essence of the technical solution of the fire-fighting adapter is to ensure sufficient water transport with the necessary firefighting equipment for firefighting purposes in conditions of mountain forests. The resulting technical solution of the fire-fighting adapter (Fig. 2) is adapted to the parameters of the base machine LKT, on which the adapter is supported, resp. semi-mounted (floating position) on the rear LKT shield. The adapter can be removed and transported by other means of transport to the place of intervention.

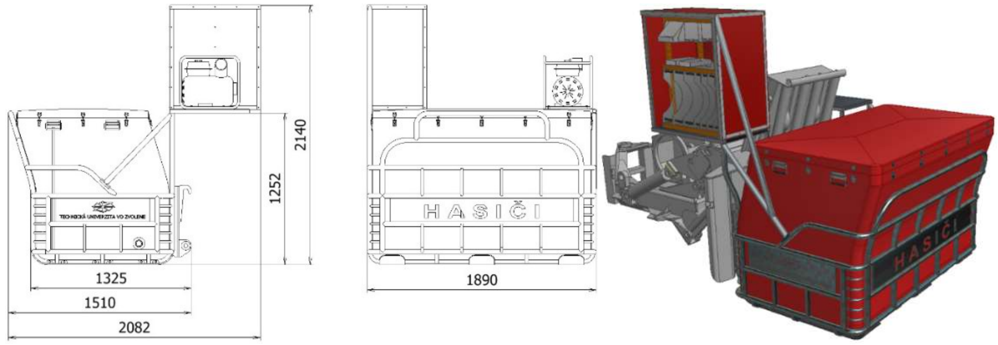

Fig. 2 The design of the fire-fighting adapter

Additional equipment of the fire-fighting adapter to the demands of accepted practice:

- water pump,
- 2" suction hose (length 125 *cm*),
- 2" suction hose with strainer (length 250 *cm*),
- hose "C" (fire hose with connector) 3x20 *m*,
- hose "D" (fire hose with connector) 4x20 *m*,
- dividing breeching C - DCD,
- hand branchpipe ("C" Profi, "D" Profi),
- ball valve "C" with connectors,
- the ax-hoe, the spade and the shovel.

This equipment is intended to ensure an autonomous capacity to refill the tank of fire-fighting adapter from the nearest natural water source, as well as to manage the intervention itself in a complicated terrain.

Fire adapter (Fig. 3) its technical design allows transport of water into the area of fire and firefighting forest fires in connected to the base machine LKT. It has an autonomous drive (own motor pump) for filling from a water source and to supply a hose, offensive line. This ensures its full functionality even after disconnecting the base machine LKT.

Fig. 3 Fire-fighting adapter

Besides being used for fighting forest fires, the fire-fighting adapter can also be used for transport of water to forest nurseries (irrigation), freshly planted areas in the event of prolonged drought, filling of watering-places for forest animals and filling puddles in the dry season and cleaning of culverts.

In conclusion, the statistically processed results of operating tests show that the deployment speed of the fire-fighting adapter from its import to intervention is relatively short. Time depends to a large extent on the volume of loaded extinguishing agent. Of course, the delay increases with a full tank. LKT travels 100 *m* distance with a full tank (2,000 *L*) in 3 *mins* 37 *secs*, while LKT loaded with 1,000 *L* of extinguishing agent travels the same distance in 2 *mins* and 16 *secs*.

Results of slope gradient have shown a difference in the transport of the fire-fighting adapter with a full and half-full tank. It can be said that the time of the adapter deployment increases with a volume of extinguishing agent in a tank and depends on a gradient and distance. Slope gradient limits of the adapter for the purpose of our measurements can be deduced from operating measurements. The adapter attached to LKT riding with a full tank has had a slope gradient limit of 30 *%*. In the case of a half-loaded tank, it can be said that LKT has a slope gradient limit of 40 *%*. Operating tests, observations, and consultations with LKT operators have been a prerequisite for improving these parameters. This follows from the technical and performance specifications of base machine LKT. Counterweight installed on the front blade for example in the form of a 500 *L* tank could improve the stability of a base machine when riding up the slope. It was assumed that the front axle had been lifted at limited gradients and therefore its centre of gravity was displaced. This issue is currently being worked on together with subsequent tests right under operating conditions.

CONCLUSION

At present, the representation of base machines of the LKT type predominates in the forests of the Slovak Republic, but do not have a similar extension, introduced in the present article. Based on the above analysis, it would be appropriate to prepare a proposal on the basis of which a fire-fighting adapter of the said construction would be incorporated into the vehicle fleet. The adapter can be quickly mounted on a LKT base machine, which creates an effective tool in extinguishing fires, especially in inaccessible terrain

ACKNOWLEDGMENT

This work was supported by "Agentúra na podporu výskumu a vývoja MŠVVaŠ SR" under the grant number APVV-14-0468

LITERATURE

FAO *Fire management: Review of international cooperation. Fire Management Working Paper FM18E*. 2006. [online] [cit. 2021-04-14] https://www.fao.org/3/j9406e/j9406e00

SAN-MIGUEL-AYANZ, J.; DURRANT, T.; BOCA, R.; MAIANTI, P.; LIBERTÀ, G.; ARTES-VIVANCOS, T.; OOM, D.; BRANCO, A.; DE RIGO, D.; FERRARI, D.; PFEIFFER, H.; GRECCHI, R.; NUIJTEN, D.; LERAY, T. 2020. *Forest Fires in Europe, Middle East and North Africa 2019*. Publications Office of the European Union 2020; pp. 164. doi:10.2760/468688

SAN-MIGUEL-AYANZ, J.; DURRANT, T.; BOCA, R.; LIBERTÀ, G.; BRANCO, A.; DE RIGO, D.; FERRARI, D.; MAIANTI, P.; ARTES-VIVANCOS, T.; COSTA, H.; LANA, F.; LÖFFLER, P.; NUIJTEN, D.; AHLGREN, A.CH.; LERAY, T. 20218. *Forest Fires in Europe, Middle East and North Africa 2017*. Publications Office of the European Union

Corresponding author:
Michaela Hnilicová, +421-45-52066876, michaela.hnilicova@gmail.com

ENERGETIC EFFICIENCY OF MERANTI WOOD MILLING

Ľubomír Rajko, Peter Koleda, Štefan Barcík

Department of Machinery Control and Automation, Faculty of Technology, Technical University in Zvolen, 26 Študentská street, Zvolen, 960 01, Slovakia

Experimental measurement of energy efficiency of meranti wood milling was performed on samples that were thermally modified by four treatments (T = 160, 180, 200 and 220 °C) while one sample was in the native state. The technological parameters of milling were: feed speeds (6, 10, 15 m.min^{-1}), cutting speeds (20, 40, 60 m.s^{-1}), tool rake angles (20, 25, 30°). Experimental measurement of cutting power was performed using a frequency converter. The experiments obtained the effects of individual parameters in the following order: cutting speed, feed speed, angular geometry, and heat treatment of the material.

Keywords: cutting power, cutting speed, thermo modification of wood, feed rate

INTRODUCTION

The energy intensity of the manufacturing process in practice requires high demands on the wood cutting process (Siklienka and Kminiak 2013). During milling, the energy intensity is influenced by various factors, such as the material of the cutting tool, the geometry of the tool, or the cutting conditions (Prokeš 1982, Lisičan 1996, Coelho *et al*. 2007, Kubš *et al*. 2016, Pervaiz *et al*. 2019). When machining a material, the energy intensity is most often observed through the cutting power (Nasir *et al*. 2020 Koleda *et al*. 2021).

EXPERIMENTAL

Surface induction hardened knives with dimensions of 45 x 35 x 6 mm (h × w × d) made from tool steel 19 573 (STN 41 9573) were used for experimental measurements. Chemical composition of knives is in the Tab. 1.

Table 1 Chemical composition of used knives

Tool steel 19 573							
Co	**Mn**	**Si**	**P**	**S**	**Cr**	**Mo**	**V**
1,4 ÷ 1,65	0,2 ÷ 0,45	0,2 ÷ 0,45	0,03	0,035	11 ÷ 12,5	0,6 ÷ 0,95	0,8 ÷ 1,20

Exotic wood Meranti (Shorea) from Malaysia was used as material for the samples. Boards made of radial central lumber with a thickness of 25 mm were handled from the log on a log band saw (MEBOR MTZ 1000) at workshop of Technical university in Zvolen. The boards were dried to humidity of 10 % in a lumber kiln. Subsequent processing of the boards, samples were obtained using a DMMA 35 circular saw (Rema s.a., Reszel, Poland) and a F2T80 thicknesser (TOS Svitavy, Czech Republic). The final dimensions of the samples were 700 mm in length, 100 mm in width and 25 mm in thickness. One set of samples was not heat treated and was examined as a natural material. The remaining samples were heat treated. Thermal modification of the other samples was performed using ThermoWood technology with the method described by Hrčková *et al*. (2018).

The milling of the samples was carried out on an experimental device, which was the lower spindle milling machine ZDS-2 (360/220 V, 4 kW) (Liptovské strojárne, Slovakia).

Feeding was ensured using a Frommia ZMD 252/137 (380 V, 2800 m.min^{-1}) feeding device (Maschinenfabrik Ferdinand Fromm, Fellbach, Germany).

The UNIFREM 400 007M frequency converter (5.5 kW for constant load) (Vonsch, Slovakia) was used to measure power consumption during milling,. From the current, voltage, and power factor of the motor, the power and power input of the motor were determined without loss and recorded *via* Vonsch Drive Studio 2.2 (VONSCH S. R. O., Brezno, Slovakia). The output voltage of the converter was smoothed by a SKY3FSM25 sine filter (VONSCH S. R. O., Brezno, Slovakia).

RESULTS AND CONCLUSION

Consumption of cutting power depends on the monitored factors, which were in the following order: 1) cutting speed; 2) feed speed; 3) angular geometry; 4) heat treatment.

Based on the obtained results, it is recommended to use a cutting speed of 20 m.s^{-1} at which the lowest value of cutting power was reached (approx. 28.7 W), in almost all examined samples. A slight deviation of the cutting power was shown for natural wood, where the value of the cutting power was higher (approx. 48 W). On the contrary, the highest value of cutting power was shown at a cutting speed of 60 m.s^{-1} in all examined samples (90 – 110 W).

In terms of feed rate, the lowest cutting power for thermally treated wood was 160 °C using a feed rate of 10 m.min^{-1} (approx. 48 W). On the contrary, the highest value of cutting power was measured at milling native sample of wood material at feed speed of 15 m.min^{-1} (approx. 98 W).

The lowest value of the cutting power was achieved with a rake angle of 20° at a temperature of 160 °C, whereas the highest value of the cutting power was at a rake angle of 25° with the untreated sample.

Thermal modification of wood was one of the least significant factors that affected the cutting power. The lowest value of cutting power was achieved with a thermally treated sample at 180 °C (approx. 57.6 W), on the contrary, the highest value of cutting power was with a natural sample of wood material (approx. 77 W).

ACKNOWLEDGMENTS

The paper was written within the project: VEGA 1/0315/17, "Research of relevant properties of thermally modified wood at contact effects in the machining process with the prediction of obtaining an optimal surface" the project of Internal Project Agency No. 2/2019 an the "Impact of selected technological, tool and material factors on the surface finish quality and energetic intensity at plane milling of thermally modified spruce wood" and with the support of project APVV 17/0456 "Thermal modification of wood with water vapor for purposeful and stable change of wood color".

LITERATURE

COELHO, L.C., CARVALHO, L.M.H., MARTINS, J.M., COSTA, C.A.V., MASSON, D., MÉAUSOONE, P. 2007. Method for evaluating the influence of wood machiningconditions on the objective characterization andsubjective perception of a finished surface. *Wood Sci. Technol*. 42, pp. 181-195

HRČKOVÁ, M., KOLEDA, P., KOLEDA, P., BARCÍK, Š., ŠTEFKOVÁ, J. 2018. Color change of selected wood species affected by thermal treatment and sanding. *BioResources* 13(4), pp. 8956-8975. DOI: 10.15376/biores.13.4.8956-8975

KOLEDA, P., BARCÍK, Š., KORČOK, M., JAMBEROVÁ, Z., CHAYEUSKI, V. (2021). "Effect of technological parameters on energetic efficiency when planar milling heat-treated oak wood," *BioResources* 16(1), 515-528. DOI: 10.15376/biores.16.1.515-528

KUBŠ, J., GAFF, M., BARCÍK, Š. 2016. Factors affecting the consumption of energy during the milling of thermally modified and unmodified beech wood. *BioResources* 11(1), pp. 736-747.

LISIČAN, J. (1996). *Teória a Technika spracovania dreva* [*Theory and technique of wood processing*], Matcentrum, Zvolen (in Slovak).

PERVAIZ, S., KANNAN, S., DEIAB, I., KISHAWY, H. 2019. Role of energy consumption, cutting tool and workpiece materials towards environmentally conscious machining: A comprehensive review. *Proceedings of the Institution of Mechanical Engineers, Part B: Journal of Engineering Manufacture*, 234 (3), pp. 335-354. DOI: 10.1177/0954405419875344

PROKEŠ, S. 1982. *Obrábění dřeva a nových hmot ze dřeva* [*Machining of wood and new wood materials*], SNZI, Prag, Czech Republic

SIKLIENKA, M., KMINIAK, R. 2013. *Delenie a obrábanie dreva. 1. vyd.* [Cutting and machining of wood. 1st edition] Zvolen, Technical University in Zvolen, 207 s. ISBN 978-80-228-2618- 1

NASIR, V., MOHAMMADPANAH, A., COOL, J. 2020. The effect of rotation speed on the power consumption and cutting accuracy of guided circular saw: Experimental measurement and analysis of saw critical and flutter speeds, *Wood Material Science & Engineering*, 15(3), pp. 140-146, DOI: 10.1080/17480272.2018.1508167

Corresponding author
Peter Koleda, Department of Machinery Control and Automation, Faculty of Technology, Technical University in Zvolen, peter.koleda@tuzvo.sk

COMPARISON AND STATISTICAL EVALUATION OF THERMAL FEATURES OF VEHICLE CATEGORIES

David Švorc, Miroslav Růžička

Department of Vehicles and Ground Transport, Faculty of Engineering, Czech University of Life Sciences Prague, Kamýcká 129, 165 00 Czech Republic, ruzicka@tf.czu.cz, svorcd@tf.czu.cz

The main aim of this paper is to show a new possibility for detection and recognition of different categories of electric and conventional (equipped with combustion engines) vehicles with help of a thermal video camera. We proposed a draft of possible detection and classification system combines thermal analyses and methods of machine learning. The differences in thermal features of different vehicle categories were found out and statistically proved. The thermal images, obtained through an infrared thermography camera, were used to create an image database. The results confirmed the hypothesis that it is possible to use infrared thermography for the vehicle drive type categorization according to the thermal features of vehicle exteriors together with using methods of machine learning for vehicle type recognition.

Key words: Thermal analysis, Vehicle classification, Electric vehicles, Thermal detection, Detection and classification system

INTRODUCTION

In the last decades automobile in urban areas have been increasing all over the world bringing serious problems such as a congestion, traffic accident, air pollution to large cities, affecting them at both social, economic and environmental levels (Vilarinho, Tavares, & Rossetti, 2017). Electromobility presents a significant way toward to reduction of carbon gas emissions and dependence of gasoline or diesel fuel and is gaining popularity in the present society due to reason of reduction energy consumption (Li, Guo, Wang, & Jiang, 2019). In traffic planning, management and transport, safety is for all types of transportation data collection necessity (Robert, 2009). Traffic data acquisition in last decades has been limited to manual methods or induction loop collection in stationary positions (Bahler, Kranig, & Minge, 1998). Traffic control need to be adapted in real time, hence is necessary to monitor traffic flow in such a way (Ni, 2007).

Actual ITS applications to be competitive, need to establish categorization of vehicle type according their emissions standards or type of engine unit for tool way, emissions zone, emergency systems, safety, and so on.

Nowadays traffic control systems mainly use conventional methods using visual cameras but it is necessary to replace or complement due to low accuracy in bad weather, such as fog, snow, heavy rain with infrared cameras (Fu, Stipancic, Zangenehpour, Miranda-Moreno, & Saunier, 2017). Thermal images of vehicles are promised to provide continuous and reliable detection of vehicles on the conditions in their surroundings (Fu et al., 2017).

In recent years, several approaches to automatic vehicle detection and classification are made. The author (Avery, Wang, & Rutherford, 2004) proposed a classification solution based on information about the length of the vehicle. A similar approach is also chosen by another author (Zhang, Avery, & Wang, 2007). Image-based methods were developed to speed up the video detection processing time. Systems for image classification based on artificial intelligence were adopted (Goyal & Verma, 2007; Iwasaki, Kawata, & Nakamiya, 2011; Thi, Robert, Lu, & Zhang, 2008).

MATERIAL AND METHODS

Distinction of vehicles into electric vehicles (EV's) or internal combustion engine vehicle (ICEV) is achieved using set parameters region of interest (ROI) of the vehicle mask. This area is differentiation from others parts of the vehicle mask by that thermal energy generated by an engine and other operating parts is emitted in this area. Thanks to a knowledge of the temperatures present by of value of each pixel in the image is possible to set the boundary value and accordingly determine the type of engine units.

Each detects vehicle is processes by manual analysis. It consists the selection of the ROI of the vehicle mask, extraction of the pixels values of this ROI by the thermal analysis program. It follows the calculations of the average temperatures from extracted values of pixels and calculations of the standard deviations for each detected vehicle according to theirs categories. Automatic evaluation of belonging individual vehicles to each category is based on this information. The algorithm will proceed according to the formula below (1) to decide whether average temperatures (extracted and calculated the value of pixels) of ICEV or EV's are inside of the boundaries of intervals for these categories.

$$T=\begin{bmatrix} t_{11} & t_{12} & \cdots & t_{1c} \\ t_{21} & t_{22} & \dots & t_{2c} \\ \vdots & \vdots & \ddots & \vdots \\ t_{r1} & t_{r2} & \cdots & t_{rc} \end{bmatrix}=\mu_{(t_{11},\ t_{12},\dots t_{rc})} \quad (1)$$

According to the calculated mean of temperatures by this formula is accordingly calculated standard deviation and decision process is set as follow:

1. calculation of σ"... if standard deviation < then threshold -"σ", vehicle is supposed to be electric car
2. calculation of σ"... if standard deviation is between thresholds -" σ",+" σ" vehicle is supposed to be conventional car"

If the calculated average ROI temperature, or its standard deviation, is in the temperature range of the combustion vehicle and outside the range of the electric vehicle category, the algorithm enters logic "1" in the register, which indicates the vehicle with the internal combustion engine. If the temperature is within the range of the electric vehicle category, the temperature detector writes a logic "0" which indicates the electric vehicle.

METHODOLOGY OF MEASUREMENT

Image data was captured in August to verify the functionality of the engine thermal signature recognition. The smallest difference between the atmospheric temperature and the temperature of the mask of the vehicle heated by the engine occurs in the summer months and is therefore suitable for evaluation. Measurements made in previous measurements in the winter have shown us that this system will have difficulties, especially at higher outdoor temperatures from May to September in Central Europe.

Measurement continues the results of previous laboratory measurement, where the hypothesis of detection of electric vehicles based on thermal signature was confirmed (Svorc, Tichy, & Ruzicka, 2020). Hence, this hypothesis was necessary to confirm or decline even in conditions of real traffic and weather. Three cameras were used for measurement; two visual cameras, first for collection of registration plates of vehicles, the second one for continuous recording of traffic, and the third one was the thermal camera. The reason for the usage of a visual camera with the continual video stream is mainly due to the manual control of classified vehicles from the thermal video stream. The infrared thermal camera has small resolution and therefore we used the visual camera with the option of collection registration plates start with letters "EL" for classification of electric vehicles from the thermal stream.

The location for measurement was selected near to exit from an intersection on the road with three lines with huge density traffic. Cameras were placed under the bridge in Argentinska street in Prague (https://mapy.cz/s/penurehace). The position of the thermal camera was selected based on two reasons. First one was the suitable position of a recording towards approaching vehicles thus recording height and angle of recording towards approaching vehicles. The second one was the possibility of video record, which was less affected by weather conditions because cameras were placed under the bridge thus record cameras would not be damaged occurring bad raining weather. The record was made in these particular positions so the cameras captured in one moment the mask and the side of the vehicles.

Thorough setup of measure parameters went before measurement. In case of the thermal camera, it was settings of lengths measurement points, emissivity and reflected temperature. For visual cameras were important precise lens focusing as well as defining areas (lanes) for vehicle license plate detection and registration. Record of the video stream was send in case of a thermal camera to the prepared notebook or saved as a video stream to internal camera memory in case of visual cameras.

Due to the small number of electric vehicles moving in the traffic flow, a Tesla car was lent to provide pictures of the electric vehicle in real operating conditions. The vehicle was preheated to operating temperature, thanks to a half-hour drive in city traffic. Subsequently, the vehicle was driven several times under the prepared cameras to achieve the necessary images.

RESULTS

Normality validation of the data of average temperature as a condition for statistical evaluation was first to proceed. Figure 3 below shows that data recorded from the thermal camera and proceed by thermal analysis program comes from the normal distribution and thus is possible to create a statistical test ANOVA (Analysis of variance). ANOVA test compares the means of four categories of vehicle, specifically personal car with a combustion engine, electric personal car, van with combustion engine and bus with the combustion engine.

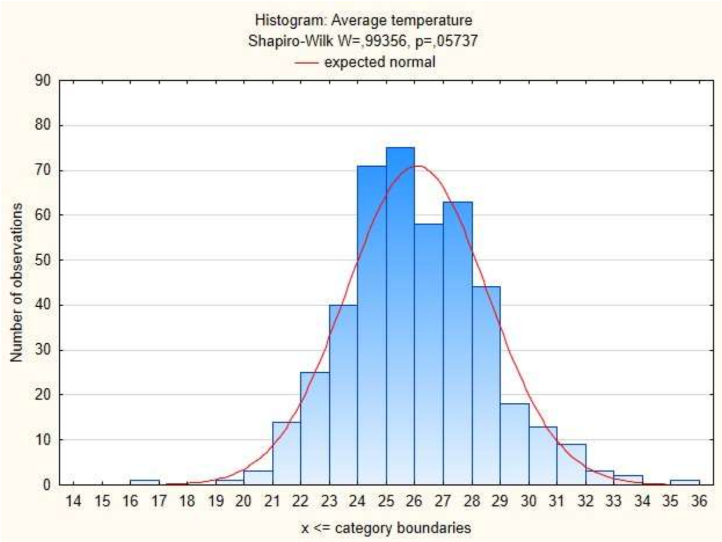

Fig.3 Histogram of normality validation

The test was based on the confirmation of the alternative hypothesis so that among average temperatures of ROI mask of the vehicle of each category exists a significant difference. Result shows that probability "p" is less than a pre-specified threshold (0,5), hence is possible to claim the mentioned hypothesis. There was a statistically significant difference between groups as determined by one-way ANOVA ($F(3,437) = 10,781$, $p = 0,000001$).

There is still gap to observe among the groups. We found out due to statistic post-hoc Sheffe test, that significant difference is just between the groups of personal vehicles (PV) and VAN's see table 1 below.

Tab. 1 Sheffe test result

Category of vehicles	Scheffe test;level of significant p < ,05000 {1}	{2}	{3}	{4}
PV average temperature {1}		0,000001	0,900207	0,129651
VAN average temperature {2}	0,000001		0,854726	0,957246
El. PV average temperature {3}	0,900207	0,854726		0,966665
BUS average temperature {4}	0,129651	0,957246	0,966665	

The results of Sheffe test show that there is no statistically significant difference between two rest categories ie electric PV and BUS but statistically significant difference did not occur even toward other categories. The problem is, that we captured not enough images of electric PV's and buses (9 PV, 32 BUS), so the data are unclear for the comparison in this time.

Hence is essential to capture more of the images data of the buses and the electric PV's to specify the results. Due to this lack of data the conclusion of possible detection based on thermal analysis are not complete and thus is not possible to mention partial results.

CONCLUSION

The results partially confirm the hypothesis from the previous laboratory measurement (Svorc et al., 2020), ie that it is possible to build a detection and categorization system of vehicles in the traffic flow based on thermal analysis and correct targeting of the thermal camera. This can be achieved even in the summer, when the ambient air temperature approaches the temperature of the car's heated mask. The results give hope that if a difference in the categories of internal combustion cars and VANs was found due to the measured date, this difference will also be found with a larger amount of data between the other categories. The measurement shows the pitfalls associated with the lack of electric vehicles in the traffic flow. It mainly raises the problem of lack of data for verifying pixel values (temperatures) and determining the limits of the temperature interval for reliable detection of this category. The sufficient resolution of the thermal images is also necessary to obtain in further research. The proposed method of calculating thermal data is a promising start for the development of an automatic system for detecting vehicles in a traffic flow, for example when connected to a vehicle recognition system using neural networks. This system should have an advantage over other detection systems, especially in the independence of detection on ambient conditions and in the categorization of passing vehicles according to the engine unit of the vehicles. In the future, it is necessary to record other parts of vehicles, especially the stern, where the assumption of advantageous detection based on the absence of exhaust system of electric vehicles, which represents the temperature difference compared to a combustion vehicle with this exhaust system.

LITERATURE

Avery, R. P., Wang, Y., & Rutherford, G. S. (2004). Length-based vehicle classification using images from uncalibrated video cameras. *IEEE Conference on Intelligent Transportation Systems, Proceedings, ITSC*, 737–742. https://doi.org/10.1109/itsc.2004.1398994

Bahler, S. J., Kranig, J. M., & Minge, E. D. (1998). Field Test of Nonintrusive Traffic Detection Technologies. *Transportation Research Record: Journal of the Transportation Research Board*, *1643*(1), 161–170. https://doi.org/10.3141/1643-20

Fu, T., Stipancic, J., Zangenehpour, S., Miranda-Moreno, L., & Saunier, N. (2017). Automatic Traffic Data Collection under Varying Lighting and Temperature Conditions in Multimodal Environments: Thermal versus Visible Spectrum Video-Based Systems. *Journal of Advanced Transportation*, *2017*(May), 1–15. https://doi.org/10.1155/2017/5142732

Goyal, A., & Verma, B. (2007). A neural network based approach for the vehicle classification. *Proceedings of the 2007 IEEE Symposium on Computational Intelligence in Image and Signal Processing, CIISP 2007*, (Ciisp), 226–231. https://doi.org/10.1109/CIISP.2007.369173

Iwasaki, Y., Kawata, S., & Nakamiya, T. (2011). Vehicle detection even in poor visibility conditions using infrared thermal images and its application to road traffic flow monitoring. *Lecture Notes in Electrical Engineering*, *151*, 997–1009. https://doi.org/10.1007/978-1-4614-3558-7_85

Li, C., Guo, H., Wang, W., & Jiang, X. (2019). Stabilization Analysis of Mixed Traffic Flow with Electric Vehicles Based on the Modified Multiple Velocity Difference Model. *Lecture Notes in Electrical Engineering*, 251–261. https://doi.org/10.1007/978-981-13-0302-9_25

Ni, D. (2007). Determining Traffic-Flow Characteristics by Definition for Application in ITS. *IEEE Transactions on Intelligent Transportation Systems*, *8*(2), 181–187. https://doi.org/10.1109/TITS.2006.888621

Robert, K. (2009). Night-Time Traffic Surveillance: A Robust Framework for Multi-vehicle Detection, Classification and Tracking. *2009 Sixth IEEE International Conference on Advanced Video and Signal Based Surveillance*, 1–6. https://doi.org/10.1109/AVSS.2009.98

Svorc, D., Tichy, T., & Ruzicka, M. (2020). Detection of the electric vehicle using thermal characteristics. *2020 Smart City Symposium Prague (SCSP)*, 1–5. https://doi.org/10.1109/SCSP49987.2020.9133981

Thi, T. H., Robert, K., Lu, S., & Zhang, J. (2008). Vehicle Classification at Nighttime Using Eigenspaces and Support Vector Machine. *2008 Congress on Image and Signal Processing*, *2*(June 2008), 422–426. https://doi.org/10.1109/CISP.2008.424

Vilarinho, C., Tavares, J. P., & Rossetti, R. J. F. (2017). Intelligent Traffic Lights: Green Time Period Negotiaton. *Transportation Research Procedia*, *22*(2016), 325–334. https://doi.org/10.1016/j.trpro.2017.03.039

Zhang, G., Avery, R. P., & Wang, Y. (2007). Video-based vehicle detection and classification system for real-time traffic data collection using uncalibrated video cameras. *Transportation Research Record*, (1993), 138–147. https://doi.org/10.3141/1993-19

Corresponding author:
David Švorc, tel.:+420720230366, e-mail: svorcd@tf.czu.cz

ABRASION RESISTANCE TEST OF THE OK 84.58 WELD DEPOSIT AND HARDOX 450 MATERIAL

Monika Vargová, Miroslava Ťavodová

Department of Manufacturing Technology and Quality Management, Faculty of Technology, Technical University in Zvolen, Študentská 26, 960 01 Zvolen
e-mail: monika.vargova@tuzvo.sk, tavodova@tuzvo.sk

The article presents abrasion resistance study results of a modified snow ploughshare materials. The material HARDOX 450 was chosen as the etalon sample. Snow ploughshare ranking blade is made from HARDOX 450. Weld deposit OK 84.58 was chosen as a reference sample. Weld deposit was applied to a part of the discarded snow ploughshare. The test was performed according to the Russian standard GOST 23.208-79. Subsequently the relative abrasion resistance Ψ_{abr} and the hardness coefficients K_T were calculated. Based on this test, we can state that the sample with the OK 84.58 weld deposit achieved 24% better resistance to abrasive wear, compared to the sample made from HARDOX 450 material.

Key words: abrasive wear, abrasion resistance test, ploughshare, HARDOX

INTRODUCTION

The most common undesirable phenomenon in industry is the process of gradually losing material from the surface of a material called wear.

The most dominant type of wear is abrasive wear, that is responsible up to 50% of failures. Wear is caused by shocks and abrasion of hard abrasive particles, and it is a major problem in forestry (Singh *et al.,* 2020 a; Zdravecká *et al.,* 2014; Vencl *et al.,* 2010).

Snow ploughshares are exposed to unfavourable working conditions in the process of their work, especially abrasive wear, because they work in a heterogeneous environment. This causes technical and economic problems. For this reason, it is necessary to look for ways to increase their service life and examine their resistance to abrasive wear.

MATERIAL AND METHODS

The snow ploughshare was modified by hard surfacing the OK 84.58 electrode. We compared the abrasion resistance of the OK 84.58 weld with the abrasion resistance of the HARDOX 450 material. Test was performed in the laboratories of the Technical Faculty at Czech University of Life Sciences in Prague.

Test of resistance to abrasive wear was performed according to the Russian standard GOST 23.208-79. Electro corundum with a grain size of 16-P with a relative moisture content of at most 0.15% was used as abrasive material. Its hardness corresponds to the 9th degree according to the Mohs scale. Abrasive material corresponding to the material used during operation, but with a grain size up to 1.0mm can be used.

Each test sample (etalon, reference sample) is weighed and placed in the test device before the test. Subsequently, the abrasive supply is started, and the rubber disc is pressed against the test sample. After completion of set track, the sample is taken and weighed again. The arithmetic mean is calculated from the determined weight losses of the individual measurements of the etalon and the reference sample.

The relative resistance to abrasive wear is calculated from equation 1:

$$\Psi_{abr} = \frac{W_{hE}}{W_{hV}}\ [-] \tag{1}$$

where: W_{hE} – weight loss of the etalon sample [g]

W_{hR} – weight loss of the reference sample [g]

Hardness coefficient K_T [-]:

$$K_T = \frac{H}{H_a}\ [-] \tag{2}$$

where: H – Hardness of the etalon material, respectively reference material [HRC],

H_a – Hardness of the abrasive solid [HRC].

The etalon and reference samples were prepared according to the standard by abrasive water jet cutting (AWJM) technology, machined by milling and grinded with magnetic surface grinder to achieve accurate dimensions and surface roughness. OTTAWA SiO_2 silica sand with a grain size of 0.1-0.3 mm was used as abrasive solid. The hardness corresponds to the 7th degree of hardness of minerals according to Mohs scale, which corresponds to the Vickers 500 HV and Rockwell 54 HRC hardness.

RESULTS

The abrasion resistance test was firstly performed on an etalon sample. Secondly, it was performed on a reference sample with a weld deposit OK 84.58. After each cycle, samples were weighed 3 times and the average weights were written in a table to determine the weight loss. The weights and weight losses result for HARDOX 450, and weld deposit OK 84.58 are in Tab. 1.

Table 1 Abrasion resistance test result

Track R [m]	**Average weight [g]**		**Weight loss [g]**	
	HARDOX 450	**OK 84.58**	**HARDOX 450**	**OK 84.58**
0	35.3851	35.2833		
153,6	35.3718	35.2771	0.0133	0.0062
307,2	35.3610	35.2696	0.0108	0.0075
460,8	35.3519	35.2618	0.0091	0.0078
614,4	35.3442	35.2556	0.0077	0.0062
768,0	35.3376	35.2478	0.0066	0.0078
921,6	35.3307	34.9071	0.0069	0.3407
1 075,2	35.3226	35.2334	0.0081	-0.3263
1 228,8	35.3150	35.2264	0.0076	0.0070
1 382,4	35.3083	35.2214	0.0067	0.0050
1 536,0	35.3015	35.2152	0.0068	0.0062
1 689,6	35.2943	35.2099	0.0072	0.0053
Average weight loss[4] W_{hi}			**0.0082**	**0.0066**

From the weight losses W_{hE} a W_{hV}, the relative abrasion resistance $\Psi_h = 1.24$ was calculated according to equation 1.1.

Based on the abrasive wear resistance test, we can state that the sample with the OK 84.58 weld deposit achieved 24% better resistance to abrasive wear, compared to the sample made from HARDOX 450.

CONCLUSION

Snow ploughshares are very important in terms of maintaining the passability of forest roads in winter. These roads are used to make forests accessible for heavy machinery for timber harvesting. As the ranking blades are exposed to high wear during their operation, especially abrasive wear, and their replacement is relatively economically demanding, it is necessary to look for ways to increase their service life and examine their resistance to abrasive wear.

ACKNOWLEDGMENT

The article was supported by the APVV-16-0194 "Research on Impact of Innovation in Production Processes on the Life of Tooling and Components of Forest Mechanisms."

LITERATURE

FINDIK, F. Latest progress on tribological properties of industrial materials. *Materials & Design* 57, pp. 218-244. DOI:10.1016/j.matdes.2013.12.028

GOST 23.208-79 Ensuring of wear resistance of products. Wear resistance testing of materials by friction against loosely fixed abrasive particles. [online]. [cit. 20-05-2021]. Dostupné na: http://docs.cntd.ru/document/gost-23-208-79

SINGH, J., CHATHA, S.S., SIDHU, B.S. 2020a. Abrasive wear behavior of newly developed weld overlaid tillage tools in laboratory and in actual field conditions. *Journal of Manufacturing Processes* 55, pp. 143-152. DOI:10.1016/j.jmapro.2020.03.040

VENCL, A., MANIC, N., POPOVIC, V., MRDAK, M. 2010. Possibility of the abrasive wear resistance determination with scratch tester. *Tribology Letters* 37. pp. 591-604, DOI:10.1007/s11249-009-9556-x

ZDRAVECKÁ, E., TKÁČOVÁ, J., ONDÁČ, M. 2014. Effect of microstructure factors on abrasion resistance of high-strength steels. *Research in Agricultural Engineering* 60, pp. 115-120. ISSN 1212-9151

Corresponding author:
Ing. Monika Vargová, +421948906093, monika.vargova@is.tuzvo.sk

ISBN 978-80-228-3270-0